THE UNIVERSITY
of EDINBURGH

Thioredoxins enable selective and reversible redox signalling in plants

Jade R. Bleau

THE UNIVERSITY *of* EDINBURGH

Thesis submitted for the degree of

Doctor of Philosophy

The University of Edinburgh

School of Biological Sciences

2022

Abstract

Accumulation of reactive oxygen species (ROS) in eukaryotic cells is associated with several biological processes, including environmental stress responses. ROS levels are usually maintained at low levels by an extensive network of antioxidants, as dysregulation of ROS can cause severe cellular damage. However, ROS also play important signalling roles in large part through the oxidation of reactive cysteine residues in key regulatory proteins. These oxidative post-translational modifications (oxPTMs) are dynamic and diverse, generating a highly adaptable and signal-responsive proteome. While some oxPTMs are undesirable, the majority are reversible and thus, can be utilised as molecular signalling switches. Reversibility of oxPTMs can largely be attributed to a superfamily of oxidoreductases, known as Thioredoxins (TRXs). Plants contain a large number of diverse TRXs which are localised throughout the cell, with several sharing the same subcellular localisation. While TRXs are known to be involved in many biological processes, the extent to which they signal selectively rather than redundantly remains unclear. The work in this thesis explores the versatility and selectivity of TRX-mediated redox signalling in response to stress.

In *Arabidopsis,* the oxidoreductase, Nucleoredoxin1 (NRX1), protects the cell in ROS-rich environments by guarding antioxidant enzymes involved in H_2O_2 scavenging. However, little is known about the role NRX1 plays in curbing oxidative stress independent of antioxidant enzymes. Chapter 3 shows that NRX1 selectively rescues oxidative stress responses in antioxidant-deficient plants. While expression of NRX1 was unable to rescue *pad2* plants that are deficient in the antioxidant glutathione from oxidative cell death, it rescued catalase-deficient (*cat2*) plants from cell death induced by high light and the oxidative stressor methyl viologen (MV). The data in this chapter

suggests that NRX1 rescues catalase mutants from light-induced oxidative stress by partially restoring ROS-induced changes in gene expression back to near wild-type levels. Interestingly, NRX1 rescued expression of TRX*h*5, a stress-induced cytosolic TRX member with major roles in biotic and abiotic stress resistance. In Chapter 4 it is shown that selective rescue of stress responses extends to other members of the TRX-*h* family. TRX-*h* members showed a distinct separation in their ability to rescue differentially induced stress responses. While both *cat2* and *pad2* mutants are immune compromised, TRX-*h* members display strong preference for rescuing immunity only in *pad2* mutants. Additionally, different TRX-*h* members selectively rescued MV-induced cell death in either *pad2* or *cat2* mutants. Taken together, these results suggest that TRXs each have specific substrate repertoires that control different ROS signalling pathways in response to stress.

Whilst PTMs allow for increased regulation of proteins, there is still much to uncover about how PTMs themselves are regulated. Chapter 5 shows that NRX1 may control oxPTMs of accessory proteins of the ubiquitin-proteasome system (UPS). The UPS is a sophisticated pathway that coordinates the degradation of intracellular proteins by labelling unstable or damaged proteins with chains of the small post-translational modifier, ubiquitin, thereby targeting them for proteasomal degradation. The work in Chapter 5 reports that NRX1 maintains the activity of deubiquitinase (DUB) enzymes responsible for cleaving ubiquitin chains. It is shown that the DUB, UBP13, is subject to H_2O_2-induced oxidation, which inhibited its DUB activity. Furthermore, NRX1 physically interacted with UBP13 and acted as a molecular reductant to activate and maintain UBP13 activity. Preliminary findings indicate that NRX1 may regulate UBP13-mediated hormonal signalling, as JA hypersensitivity observed in transgenic plants overexpressing UBP13 was impaired in the absence of NRX1.

Overall, the work in this thesis demonstrates that TRX family members are highly selective regulators of diverse ROS signalling pathways, enabling plants to tailor their responses depending on the stresses they encounter. It further shows that cross-talk between different PTMs (*i.e.* oxPTMs and ubiquitin) enables precise regulation of the proteome during oxidative stress and hormonal signalling.

Lay summary

Plants are continuously faced with environmental stresses, such as drought, heat stress and pathogen infection. In order to combat these challenges, they need to be able to respond rapidly. Plants have evolved extensive molecular signalling networks that communicate throughout the plant, this enabling dynamic and efficient responses to unfavourable conditions. One of the ways plants can communicate signals within cells is via reactive molecules, such as hydrogen peroxide. Excessive accumulation of these molecules can severely disrupt processes in plant cells and may result in cell death if unregulated. However, plants have utilised these molecules as reversible signalling tools so that they can prioritise appropriate responses. In this thesis the model plant *Arabidopsis thaliana* is used to genetically manipulate plant responses to stress. The findings of this work uncover remarkable selectivity in how plants shape their responses to specific stresses they encounter and mechanisms behind key regulatory processes that could be transferred to crops for protection in the field.

Acknowledgements

First and foremost, I would like the thank my supervisor Prof. Steven Spoel for giving me the opportunity to undertake this PhD. You have been an excellent supervisor, offering continuous support and guidance throughout my PhD. You always manage to find the positives when I think the world is ending!

I would also like to thank my committee members Tony Ly and Naomi Nakayama for their help and advice.

Thank you to Sophie Kneeshaw for your previous work in the lab. Your thesis and lab books have been invaluable throughout my PhD.

A massive thank you to the Spoel, van Ooijen, and Orosa labs. You all provided the best lab environment, and I honestly couldn't have asked for a better lab to do my PhD in. I am so grateful to be able to have worked with such great scientists who I can also call my friends. A special thank you to Michael for always being there to answer my many questions and for your help while writing my thesis.

There are many friends who have been very supportive over the last few years, but I would like to especially thank Becky, Helen, and Holly. Thank you for all the walks, fancy coffees, cakes, and weird theatre pieces. But most of all, thank you for the endless fun and laughter. Also, thank you to Emmy, who was always at the other end of the phone. From undergrad all the way through to our PhDs you have always been there, and look at us now!

Importantly, I would like to thank my family and Phil for providing me with continuous love, support, and encouragement throughout my PhD. I could not have done this without you all. I would also like to thank my wonderful cat Basil for being an excellent writing partner.

Finally, thank you to Eastbio and the Biotechnology and Biological Sciences Research Council (BBSRC) for providing training and funding for my project.

There are many people who have helped me greatly throughout my PhD. I wish I could write something about you all, but that would make my acknowledgements as long as my thesis!

Declaration

I declare the thesis presented here is my own work unless stated otherwise* and has not been submitted in any form for any degree or professional qualification at University of Edinburgh or any other institute.

Jade R. Bleau

*Data presented in figure 4.11B and 4.17D was produced by Shi-Rui Ong under the supervision of Jade R. Bleau

Contents

List of figures

List of tables

List of abbreviations

$^1O_2$	Singlet oxygen
ABA	Abscisic acid
ACT2	Actin 2
AO	Ascorbate oxidase
APX	Ascorbate peroxidase
Asc	Ascorbate
Ca^{2+}	Calcium
CAT	Catalase
CDPK	Calcium-dependent protein kinases
CRK	Cysteine rich receptor-like kinase
Cys	Cysteine
DHA	Dehydroascrobate
DHAR	DHA reductase
DTT	Dithiothreitol
FTR	Ferredoxin-dependent thioredoxin reductase
GAPDH	Glyceraldehyde-3-Phosphate Dehydrogenase
GOX	Glycolate oxidase
GPX	Glutathione peroxidase
GR	Glutathione reductase
GRX	Glutaredoxin
GSH	Reduced glutathione
GSNO	S-nitrosoglutahione
GSNOR1	S-nitrosoglutahione reductase
GSSG	oxidise glutathione
GST	Glutathione S-transferase

H_2O_2	Hydrogen peroxide
IP	immunoprecipitation
JA	Jasmonic acid
MV	Methyl viologen
NADPH	Nicotinamide adenine dinucleotide phosphate
NEM	N-Ethylmaleimide
NO	Nitric oxide
NOS	Nitric oxide synthetase
nox1	nitric oxide overproducer 1
NPR1	NONEXPRESSOR OF PATHOGENESIS-RELATED GENES 1
NR	nitrate reductase
NRX	Nucleoredoxin
NTR	NADPH-dependent thioredoxin reductase
O_2^-	Superoxide
pad2	*phytoalexin-deficient 2*
PAMP	Pathogen-associated molecular pattern
PDI	protein disulphide isomerases
PMSF	Phenylmethylsulphonyl fluoride
PR1	PATHOGENESIS-RELATED GENES 1
PRX	Peroxidase
PSI/II	Photosystem I/II
Psm	*Pseudomonas syringae* pv. *maculicola* ES4326
PTI	PAMP-triggered immunity
PTM	Post-translational modification
qPCR	Quantitative real-time PCR

RBOH	Respiratory burst oxidative homologs
RNS	Reactive nitrogen species
ROS	Reactive oxygen species
SA	Salicylic acid
SAG13	SENESCENCE-ASSOCIATED GENE 13
SDS	sodium dodecyl sulphate
SH	Free cysteine thiol
SNO	*S*-nitrosylation/ *S*-nitrosothiol
SO_2H	*S*-sulphination
SO_3H	*S*-sulphonation
SOD	Superoxide dismutase
SOH	*S*-sulphenation
SS	Disulphide bridge
SSG	S-glutathionylation
TAT	TYROSINE AMINOTRANSFERASE
TLCK	Nα-Tosyl-L-lysine chloromethyl ketone hydrochloride
TPCK	N-p-Tosyl-L-phenylalanine chloromethyl ketone
TRX	Thioredoxin
Ub	Ubiquitin
UBQ5	Ubiquitin 5
UPS	Ubiquitin Proteasome System
vtc	*vitamin c*
YFP	Yellow fluorescent protein

Chapter 1

Introduction

Parts of this chapter have been published in:
Bleau, J. R. and Spoel, S. H. (2021) Selective redox signaling shapes plant – pathogen interactions *Plant Physiology* Volume 186, Issue 1, Pages 53–65

Plants are continuously under threat from a variety of different environmental stresses, meaning they must be able to respond dynamically to rapid changes in their environment. To combat this, plants have evolved extensive signalling networks in order to regulate physiological responses to environmental stresses, both biotic and abiotic. One such response is the use of molecules such as reactive oxygen and nitrogen species (ROS and RNS, respectively) as signalling tools. Accumulation of ROS and RNS perturbs the 'redox status' of the cell (Spoel and Loake, 2011; Torres et al., 2006), which can result in detrimental protein oxidation and cause severe cellular damage. Due to this, it was widely thought that ROS/RNS were toxic by-products of metabolism, whereas ROS/RNS scavenging antioxidant systems were solely responsible for keeping ROS/RNS at low levels (Noctor, 2006). However, it is now established that ROS/RNS and antioxidant enzymes are necessary signalling tools for intracellular and intercellular communication. Plants are able to utilise redox-based reversible modifications for signal transduction in response to many stimuli, enabling them to tailor their responses to combat specific stresses they may encounter.

1.1 ROS/RNS generation during stress responses

Diverse reactive oxygen and nitrogen species (ROS/RNS) can be produced throughout the cell, including singlet oxygen ($^1O_2$), superoxide (O_2^-), hydrogen peroxide (H_2O_2), hydroxyl radicals ($^{\bullet}OH$), nitric oxide (NO) and other NO derivatives. These molecules have distinct reactivities, different stabilities and are produced by different cellular compartments, thereby generating the potential for selective signalling. ROS/RNS act in cellular signalling or as long distance signalling molecules via interaction with hormones (Fichman and Mittler, 2020; Miller et al., 2009; Wang et al., 2014).

1.1.1 Apoplastic ROS Production

The apoplast is a major source of ROS. Environmental changes can trigger sequential bursts of ROS in the apoplast with key systemic signalling functions (Fichman and Mittler, 2020). Apoplast-generated ROS are largely produced by transmembrane localised nicotinamide adenine dinucleotide phosphate (NADPH) oxidases, known as Respiratory Burst Oxidase Homologs (RBOHs), in response to a wide range of stimuli (Miller et al., 2009). RBOHs transfer electrons from intracellular NADPH across the plasma membrane where they are coupled to molecular oxygen in the apoplast to produce O_2^- (Suzuki et al., 2011) (Fig. 1.1). O_2^- is short lived and rapidly converted to H_2O_2, either spontaneously or by superoxide dismutase (SOD), and enters the cell through plasma membrane channels. The *Arabidopsis* genome encodes for 10 RBOH genes, of which RBOHD and RBOHF are among the best studied. RBOHD and RBOHF are reported to be the main producers of ROS upon recognition of pathogen-associated molecular patterns (PAMPs) and both are also required for the initiation of programmed cell death upon intracellular detection of pathogen effectors (Torres et al., 2002). Additionally, both RBOHD and RBOHF have been shown to be responsible for H_2O_2 production when plants are under hypoxic conditions (Liu et al., 2017), and are also involved in hormonal signalling via abscisic acid (ABA)-induced H_2O_2 production required for stomatal closure (Kwak et al., 2003). Moreover, changes in apoplastic redox balance are a determinant of sensitivity to high-light induced photosynthesis inhibition (Karpinska et al., 2018). RBOHD is also responsible for the local induction of ROS and triggering of a systemic ROS wave during light stress, as *rbohD* knockout mutants were unable to induce long-distance signalling (Fichman et al., 2021).

In addition to NADPH oxidases, apoplastic ROS can also be induced by peroxidases (PRXs). In addition to eliminating ROS during their peroxidative cycle, class III PRXs are able to generate ROS during their oxidative and hydroxylic cycles (Shigeto and Tsutsumi, 2016), and are involved in development as well as biotic and abiotic stresses (Kidwai et al., 2020). They have been reported to display cell wall crosslinking activity and are responsible for generating a highly toxic environment upon pathogen infection (Bindschedler et al., 2006; Delannoy et al., 2003). Indeed *Arabidopsis* PRX33 and PRX34 are important in the activation of PAMP-triggered immunity, as knockdown mutant cell cultures show severely reduced H_2O_2 levels in response to PAMP treatments and a decrease in expression of PAMP-induced defence-related proteins (O'Brien et al., 2012).

In addition to ROS production in response to stress, buffering of the apoplast to sustain ROS levels is of importance and can be attributed to oxidases, including ascorbate oxidase (AO). AO reduces apoplastic amounts of the antioxidant ascorbate, thus generating an environment in which apoplastic ROS can be sustained (Foyer et al., 2019). AO deficiency results in perturbation of auxin-stimulated shoot growth, enhanced mitogen-activated protein kinase (MAPK) activity and increased susceptibility to *Pseudomonas syringae* (Pignocchi et al., 2006). How the ROS-related activities of RBOH, PRX and AO enzymes are balanced remains unknown, but their interplay likely generates specific ROS signatures depending on the stress encountered.

1.1.2 Organellar ROS production

While the apoplast is a major generator of ROS during stress responses, stress-induced ROS production in organelles is also important in coordinating ROS

signatures throughout the cell (Fig 1.1). Chloroplasts are a source of ROS through the electron transport chain, while NO is produced through the thylakoid-associated nitrite reductase pathway or via an NO-synthase-like enzyme (Astier et al., 2018; Lu and Yao, 2018). Photosystem I of the photosynthetic transport chain continuously produces O_2^-, which is swiftly converted to H_2O_2 and O_2 by SOD, while $^1O_2$ is produced by photosystem II. $^1O_2$ is uniquely produced in the chloroplast in response to light and is a major source of ROS during photo-oxidative damage (Triantaphylidès et al., 2008). The *fluorescent* (*flu*) and *chlorina1* (*chl1*) mutants specifically accumulate $^1O_2$ and display enhanced cell death in response to photo-oxidative stress (op den Camp et al., 2003; Ramel et al., 2012). Induction of light stress using the *flu* mutant showed that $^1O_2$ is able to act as a signal to trigger cell death during photo-oxidative stress via the plastid-localised proteins EXECUTER1 and EXECUTER2, with *flu/ex1* double knockout mutants exhibiting compromised *flu*-associated cell death (Lee et al., 2007; Wagner et al., 2004; Wang et al., 2016). Furthermore, while the importance of apoplastic ROS production during biotic stress is well described, the importance of chloroplasts in pathogen-induced ROS production and downstream immune signalling has only recently emerged. Indeed, PAMP perception leads to a second burst of ROS generated by the chloroplast that occurs after apoplastic ROS production (de Torres Zabala et al., 2015). Moreover, compared to the wild-type strain, infection with a disabled *P. syringae* strain, deficient in delivering pathogen effectors into host cells, resulted in chloroplastic ROS production, suggesting pathogens actively block formation of ROS in the chloroplast. As opposed to the wild-type pathogen, the disabled strain is largely non-infectious, further suggesting that chloroplastic ROS contributes to immunity. In accordance, it was also observed that inhibition of H_2O_2 production via photosystem II with 3-(3,4-dichlorophenyl)-1,1-dimethylurea (DCMU), abolished ROS production and promoted virulence of this disabled pathogen (de Torres Zabala et al., 2015).

As chloroplasts and mitochondria have important roles in regulating localised cell death and nuclear gene expression via retrograde signalling (Cui et al., 2019; De Clercq et al., 2013; Straus et al., 2010; Zurbriggen et al., 2009), it is likely that the specific organelle generated ROS signal is perceived throughout the cell. In addition to the chloroplast, organellar ROS is generated in peroxisomes largely via the oxidation of glycolate by glycolate oxidase (GOX), and the mitochondria via the mitochondrial electron transport chain (Fig 1.1) (Foyer and Noctor, 2009). Peroxisomes and mitochondria make direct contact with chloroplasts upon exposure to light, and were found to change from a spherical to elliptical shape to increase surface area interaction (Oikawa et al., 2015) . This was not observed when PSII was inhibited, suggesting that ROS produced in the chloroplast are transmitted to different organelles (Oikawa et al., 2015). Similarly, chloroplasts either congregate around the nucleus or send out dynamic extensions along microtubules called stromules that physically connect to the nucleus (Caplan et al., 2015; Kumar et al., 2018). Interestingly, exogenous application of H_2O_2 but not of NO or O_2^-, mimicked pathogen-induced stromule formation, suggesting that this process is coordinated by specific ROS. Moreover, treatment with the NADPH-oxidase inhibitor diphenyleneiodonium (DPI), or the ROS scavengers dimethylthiourea (DMTU) and Tiron, resulted in a drastic reduction in the percentage of nuclei surrounded by chloroplasts (Ding et al., 2019). These findings suggest that H_2O_2 produced in the apoplast by NADPH oxidases signals to chloroplasts prior to the chloroplastic ROS burst. The use of genetically encoded biosensors can also be used to measure dynamic changes in the redox state of the cell. For example, GFP modified with an artificial disulphide bridge to make it redox sensitive (roGFP) has been fused to human glutaredoxin (GRX) or the glutathione peroxidase-like enzyme oxidant receptor peroxidase 1 (Orp1) from *Sacchromyces cerevisiae* to enable measurement of cellular glutathione redox

potential and endogenous H_2O_2, respectively (Gutscher et al., 2008; Marty et al., 2009; Nietzel et al., 2019). The detection of oxidation and reduction of roGFP at different wavelength allows for quantification of the redox state of the cell. Most recently, Grx1-roGFP2 and roGFP2-Orp1 have been used to show that methyl viologen (MV)-induced chloroplastic ROS generation led to rapid oxidation initially in the chloroplast and subsequently in the cytosol and mitochondria (Ugalde et al., 2021)

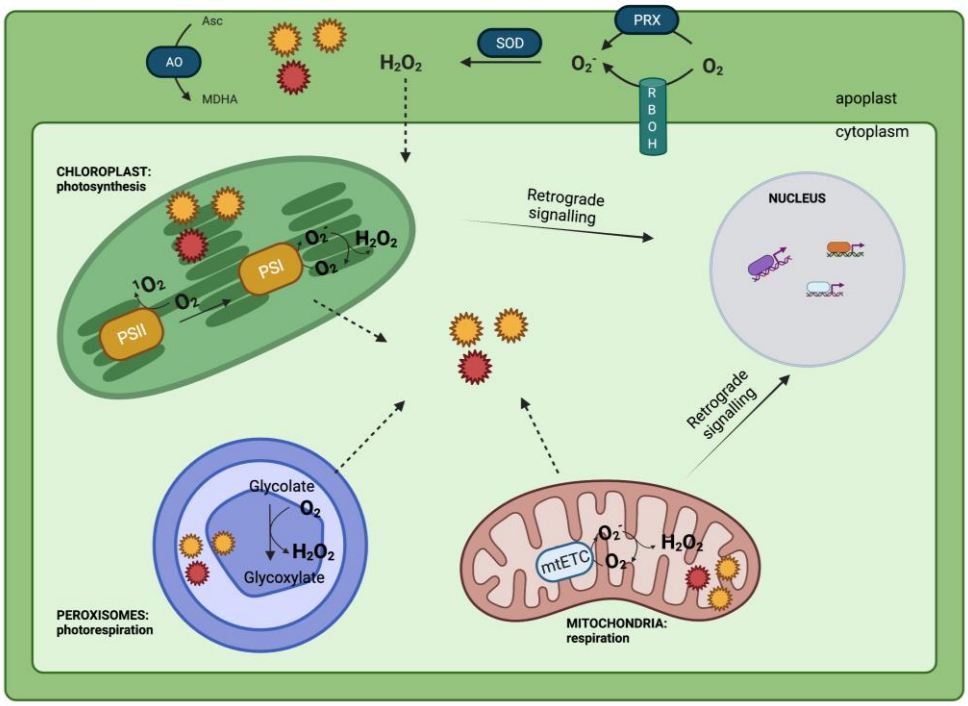

Figure 1. 1 Main sites of ROS production during stress

ROS generation via the reduction of molecular oxygen occurs at several subcellular and extracellular sites. ROS generation can be perceived throughout the cell and integrated into signalling pathways to the nucleus. AO, ascorbate oxidase; SOD, superoxide dismutase; PRX, peroxidase; RBOH, respiratory burst oxidative homolog; PSI/II, photosystem I/II; mtETC, mitochondrial electron transport chain; O_2^-, superoxide, H_2O_2, hydrogen peroxide; $^1O_2$, singlet oxygen. Created with Biorender.com

1.1.3 Stress-induced production of nitric oxide

In animals, NO is one of the main RNS and is synthesised by dedicated nitric oxide synthetases (NOS). NO is formed by the NADPH-dependent oxidation of L-arginine

to NO and citrulline. However, a bona fide NOS has not yet been identified in higher plants. Instead, in plants NO is synthesised through nitrite reductase and NOS-like activity (Astier et al., 2018). One of the main sources of NO during the immune response is via nitrate reductases (NRs). The NR-deficient mutant *nia1 nia2* in *Arabidopsis* provided insight into the importance of NO in response to pathogen infection. Lower levels of endogenous NO in *nia1 nia2* mutants have been linked to regulation of oligogalacturonide-triggered immunity, elicitor-triggered immunity, and resistance to both the necrotrophic fungus *Botrytis cinerea* and cucumber mosaic virus (CMV) (Jian et al., 2015; Rasul et al., 2012). In addition, NO feedback regulates the nitrogen assimilation pathway, thereby controlling its own production (Frungillo et al., 2014) . Pathogen infection leads not only to the accumulation of free NO but also of the NO derivative *S*-nitrosoglutathione (GSNO). Both of these RNS play key roles in immunity as their respective overaccumulation in *NO Overexpressing 1* (*nox1*) and *GSNO Reductase 1* (*gsnor1*) mutants results in enhanced disease susceptibility (Feechan et al., 2005; Kneeshaw et al., 2014). While free NO● radicals are highly reactive and short-lived, GSNO is more stable and is thought to function as a cellular reservoir for NO bioactivity. The difference between these molecules in terms of molecular structure and mode of reactivity with Cys residues to form *S*-nitrosothiols (SNO), suggest that they could have distinct roles in cell signalling. In accordance, upon pathogen infection *gsnor1 nox1* double mutants displayed an increase in total cellular SNO upon pathogen perception and enhanced disease susceptibility compared to either of the single mutants (Yun et al., 2016). Moreover, overexpression of the GSNO scavenger enzyme *GSNOR1* rescued disease resistance in *gsnor1* but not in *nox1* mutants (Yun et al., 2016). These findings provide genetic evidence that RNS have distinct and selective signalling roles in plant immunity.

1.2 Oxidative post-translational modifications

Stress-induced ROS/RNS alter the redox state of the cell, largely due the change in the oxidative state of small redox couples, such as oxidised versus reduced glutathione (Spoel and Loake, 2011). These redox couples buffer changes in cellular redox levels, resulting in an electron flow from molecules with a lower reduction potential, such as NAD(P)H, to molecules with higher reduction potentials, including glutathione and ascorbate (Spoel and Loake, 2011). Such changes can be sensed directly by signalling proteins that contain rare reactive cysteine residues that switch between oxidised and reduced states, known as 'redox sensors', which enable them to dynamically respond to the cellular redox environment. This is perhaps best illustrated by the immune transcription coactivator NPR1 (Non-Expressor of Pathogenesis Related Genes 1). Remarkably, NPR1 resides in the cytoplasm as a disulphide-linked oligomer. Upon infection, an increasingly reduced cellular environment results in release of NPR1 monomer by either spontaneous reduction of disulphides or their cleavage by specific oxidoreductases (Mou et al., 2003; Tada et al., 2008). The NPR1 monomer then translocates into the nucleus where it orchestrates transcriptional reprogramming to prioritise immunity over other cellular processes (Kinkema et al., 2000; Wang et al., 2006).

ROS/RNS can also directly oxidise reactive Cys residues of signalling proteins (Waszczak et al., 2015). This results in oxidative post-translational modifications (oxPTMs) of a diverse nature and varying levels of oxidation, including protein *S*-nitrosylation (–SNO), disulphides (S–S), *S*-glutathionylation (–SSG), S-sulphenylation (–SOH), *S*-sulphination ($–SO_2H$), and *S*-sulphonation ($–SO_3H$) (Fig. 1.2). Except for *S*-sulphonation, all other oxPTMs are reversible either through small molecule- or

enzymatic reduction (Spadaro et al., 2010). Reversible oxPTMs can also occur on methionine, another sulphur containing amino acid. Unlike Cys oxidation, which is pH-dependent and requires its thiols to be ionised for oxidation to occur, methionine oxidation to methionine sulfoxide occurs over a broad pH range (Kim et al., 2014; Levine et al., 2000; Peskin and Winterbourn, 2001). Thus, oxPTMs ensure ROS/RNS signatures are translated into dynamic molecular processes.

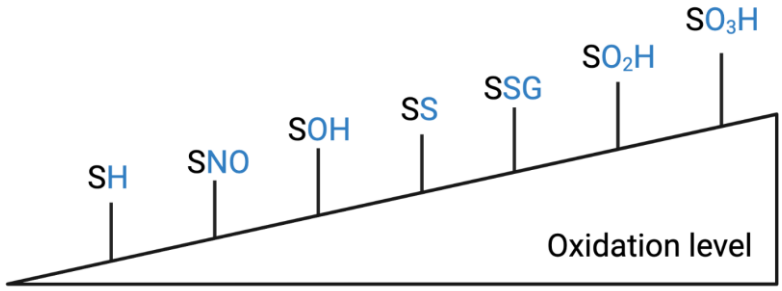

Figure 1. 2 Redox-based cysteine modifications

Free cysteine thiols (SH) can be further oxidised by *S*-nitrosylation (SNO), *S*-sulphenation (SOH), *S*- thiolation (SS), *S*-glutathionylation (SSG), *S*-sulphination (SO_2H) and *S*-sulphonation (SO_3H). With the exception of *S*-sulphonation, all modifications are reversible. Adapted from Spadaro et al. (2010). Created with Biorender.com

How the versatility of oxPTMs increases the number of ways a protein can be regulated is highlighted by the oxidation of the highly conserved metabolic enzyme, glyceraldehyde-3-phosphate dehydrogenase (GAPDH). GAPDH is *S*-nitrosylated in rice upon increasing NO levels and in *Arabidopsis* upon treatment with GSNO (Lin et al., 2012; Lindermayr et al., 2005), and H_2O_2-induced sulphenation, results in the inhibition of its activity (Hancock et al., 2005; Zaffagnini et al., 2013). Furthermore, under oxidative conditions induced by either H_2O_2 or GSNO, GAPDH displays

enhanced localisation to the nucleus, which is not observed when its catalytic Cys residue is mutated (Schneider et al., 2018), indicating that oxidation of GAPDH influences its cellular localisation. This demonstrates that diverse oxPTMs on a single protein can lead to various functional outcomes.

OxPTMs are important in regulating cellular processes, from perception to signal transduction. Recent work demonstrated that oxPTMs underpin perception of apoplastic H_2O_2 at the cell surface. A forward genetic screen based on imaging H_2O_2-induced calcium fluxes identified the plasma membrane-localised leucine-rich repeat receptor kinase HPCA1 (Hydrogen-Peroxide-induced Ca^{2+} increases) (Wu et al., 2020) . HPCA1 contains extracellular Cys residues that are oxidised upon exposure to H_2O_2, leading to its activation by autophosphorylation and downstream induction of calcium channels and stomatal closure. Additionally, early oxPTMs that function upstream of RBOHD-mediated ROS production may control downstream redox signalling mechanisms. Calcium (Ca^{2+})-dependent protein kinases (CDPKs) and Receptor-like kinases (RLKs) regulate RBOHD-mediated ROS production (Dubiella et al., 2013; Kimura et al., 2020, 2017); however it has been suggested that CDPKs and RLKs themselves may be redox regulated. The cysteine-rich receptor kinase (CRK) subfamily of RLKs contain a high number of conserved Cys residues, suggesting that CRKs may be targets of redox regulation. In accordance, Lee et al. (2017) showed that overexpression of CRK36 enhanced the cell death response and increased stomatal immunity, as well as resistance to hemibiotrophic and necrotrophic pathogens, while overexpression of Cys mutants abolished responses. Furthermore, the authors showed that CRK36 interacted with the receptor-like cytoplasmic kinase, BIK1, which is responsible for activating RBOHD upon PAMP-perception (Kadota et al., 2014) , suggesting that early redox modifications of CRKs can control downstream ROS production.

Increasing evidence has shown there is cross-talk between ROS and NO to tightly control redox signalling responses, including programmed cell death (Astier et al., 2018). Following infection with an avirulent strain of *P. syringae,* treatment with the NO donors GSNO or CysNO substantial decreased NADPH oxidase activity, indicating that that NO negatively regulates NADPH-mediated ROS production upon pathogen infection (Yun et al., 2011). Further analysis showed that RBOHD is *S*-nitrosylated at Cys890 and its mutation enhanced RBOHD activity in response to pathogen infection, further showing that ROS and NO signalling are interlinked.

1.3 Reversible oxidative signalling

The transient and reversible nature of oxPTMs greatly increases the potential of the proteome to rapidly adjust in the face of dynamic environmental changes. However, the wide variety of oxPTMs, their relatively spontaneous formation by cellular ROS/RNS, and their ability to change protein function or activity raises the question; how are these modifications tightly controlled to enable cell signalling and prevent protein hyperoxidation? Firstly, the chemistry of each ROS/RNS and the accessibility of their Cys targets play an important role. Protein conformation will selectively exclude access for some ROS/RNS but not others, while residues surrounding the oxPTM can stabilise or destabilise the oxidative group, thereby determining oxPTM turnover times. Secondly, the spatial and temporal production of ROS can selectively expose Cys residues to ROS/RNS. As described above, the activities of enzymes such as NADPH oxidases are indeed tightly controlled by numerous post-translational modifications to ensure temporal production. Thirdly, cellular scavenging via antioxidant systems also determines the effects of ROS/RNS on Cys residues.

1.4.1 Antioxidants

Regulation of ROS homeostasis in plant cells is orchestrated by an extensive network of antioxidants, both enzymatic and non-enzymatic. Non-enzymatic antioxidants include ascorbate, glutathione, carotenoids, α-tocopherol and polyphenols. They can directly scavenge ROS and function as cofactors for enzymatic antioxidants (Sharma et al., 2012). Of the non-enzymatic antioxidants, ascorbate and glutathione are the most abundant throughout the cell and show great versatility in ROS scavenging, as they are capable of detoxifying H_2O_2, O_2^-, $^1O_2$, and OH● (Foyer and Noctor, 2011). Glutathione can also act as an electron donor to render NO more stable by forming bioactive S-nitrosoglutathione (GSNO), and can also protect proteins from irreversible oxidation via *S*-glutathionylation (*i.e.* addition of glutathione to Cys residues in proteins). Glutathione has a high redox potential and is a particularly important redox buffer, with increasing intracellular ROS levels driving the accumulation of glutathione (Mhamdi et al., 2010a; Queval et al., 2011, 2007). Furthermore, glutathione can also determine the spatio-temporal effects of ROS/RNS in plant cells. A recent study demonstrated that the glutathione antioxidant system determines the cytosolic effects of the apoplastic ROS burst induced by pathogen perception. In absence of cytosolic glutathione reductase (GR1), the enzyme responsible for converting glutathione back to a reduced state, cytosolic H_2O_2 levels increased earlier and were of higher amplitude, indicating that in wild-type plants (reduced) glutathione effectively scavenged H_2O_2 (Nietzel et al., 2019), thereby likely defining the spatiotemporal dynamics of ROS-mediated oxPTMs.

In addition to small molecule antioxidants, ROS can be directly scavenged enzymatically (Fig. 1.3), predominantly by peroxidases. While O_2^- can be converted to H_2O_2 either spontaneously or by SOD, the catalytic activities of peroxidases are

important for the full detoxification of ROS. The presence of antioxidant enzymes, including ascorbate peroxidase (APX), peroxiredoxins (PRX) and glutathione peroxidases (GPX), have been shown to play roles in a variety of abiotic and biotic stresses (Ahmad et al., 2010; Choi et al., 2007; Daudi et al., 2012; Survila et al., 2016; Yuan et al., 2017). Catalase (CAT) enzymes are particularly important in scavenging peroxisomal H_2O_2 (Mhamdi et al., 2010b). The absence of CATs results in a clear disruption of the cellular redox state, indicated by the change in glutathione status (Chaouch et al., 2010; Mhamdi et al., 2010a; Queval et al., 2007). Perturbations of the transcriptome in response to many abiotic and biotic stress are similar to those observed in *cat2* knockout mutants (Mhamdi et al., 2010b), highlighting its importance in redox signalling. The ectopic expression of antioxidant enzymes in crops, such as catalase, enhances stress tolerance in crops (Liu et al., 2021), which provides potential biotechnological advancements to utilise antioxidants to enable tolerance to stressful conditions in the field.

Antioxidant enzymes are also important players in regulating hormonal signalling. Silencing of *GPX3* in *Arabidopsis* resulted in increased H_2O_2 production upon ABA treatment, and impaired stomatal closure (Miao et al., 2006). Consequently, this resulted in a reduced tolerance to drought. In addition, antioxidants control hormonal signalling during biotic stress. Silencing of the thylakoid-localised H_2O_2 scavenging enzyme, tAPX, resulted in the activation of defence-related genes, including *ICS1* which is responsible for SA biosynthesis and downstream expression of *Pathogenesis-Related* (*PR*) genes (Maruta et al., 2012) and CAT2. Thus, regulation by ROS scavenging enzymes may be a critical link between ROS and hormone signalling. The potential of ROS/RNS scavenging enzymes to shape the oxidative proteome is also clearly illustrated by the GSNO scavenger GSNOR1. In absence of functional GSNOR1, cellular levels of GSNO and consequently, protein *S*-

nitrosylation markedly increase, particularly upon pathogen infection, which leads to disease susceptibility (Feechan et al., 2005; Yun et al., 2011).

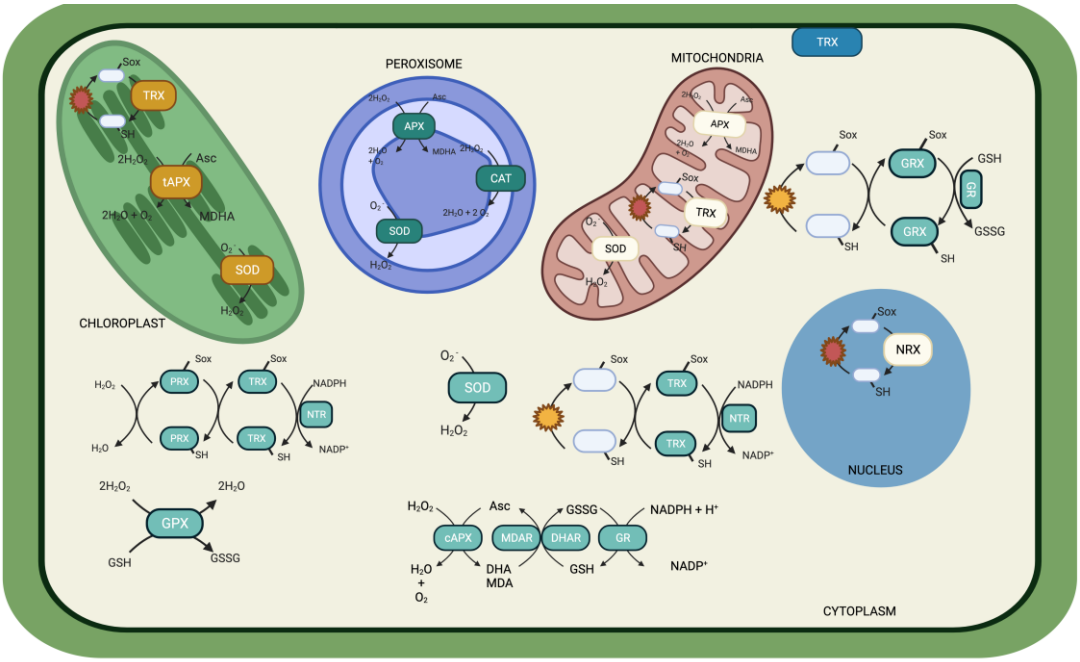

Figure 1. 3 Plant antioxidant systems

Examples of known antioxidants and TRXs and their subcellular locations. ROS/RNS are produced in different subcellular locations, as are the antioxidant enzymes and oxidoreductases responsible for maintaining cellular redox homeostasis and reversal of oxidative protein modifications. Different cellular localisation is indicative of selectivity and specificity in redox signalling. RBOH; Respiratory Burst Oxidative Homologs, SOD; Superoxide Dismutase, AO; PRX; Peroxiredoxin, TRX; Thioredoxin, NTR; NADPH-dependent TRX reductase, APX; Ascorbate Peroxidase, thylakoid (tAPX) and cytosolic (cAPX), Asc; Ascorbate, MDA; Monodehydroascorbate, MDAR; MDA reductase, DHA; dehydroascorbate, DHAR; DHA reductase, GRX; Glutaredoxin, GR; Glutathione Reductase, NRX; Nucleoredoxin CAT; catalase, GPX; Glutathione Peroxidase. Created with BioRender.com

1.4.2 Thioredoxins

While scavenging enzymes are important in directly regulating ROS/RNS levels, another group of enzymes, known as oxidoreductases or redoxins, are responsible

for maintaining cell signalling via the direct reversal of ROS/RNS-induced oxPTMs. These enzymes belong to the superfamily of Thioredoxins (TRXs) that are emerging as central players in selective redox signalling. This superfamily consists of conventional TRXs, Glutaredoxins (GRXs), Nucleoredoxins (NRXs) and protein disulphide isomerases (PDIs) (Marchal et al., 2014; Meyer et al., 2008). Conventional TRXs are characterised by a 'TRX-like' fold and the conserved active site sequence WC(G/P)PC (Meyer et al., 2008). The conserved proline is important for determining the reducing power of TRXs, whilst the tryptophan residue is important for maintaining thermodynamic stability (Collet and Messens, 2010). One of the key functions of conventional TRX enzymes is to reduce disulphide bonds in target proteins, a process that requires both active site Cys residues. Disulphide bridges are reduced by a dithiol mechanism (Fig. 1.4). Here, the first active-site Cys of TRX attacks the substrate's disulphide bond and generates a covalent mixed-disulphide bond between the TRX active site and the substrate. Next, the second active-site Cys resolves the mixed disulphide, thereby releasing the reduced target protein, while rendering the TRX active-site Cys residues oxidised as a disulphide bridge (Fig. 1.4). TRX activity is recycled by cytosolic NADPH-dependent thioredoxin reductases (NTR) or chloroplastic Ferredoxin-dependent thioredoxin reductases (FTR) that reduce oxidised TRXs by donating electrons to NADPH (Meyer et al., 2012; Fig 1.4). Over time it has become clear that in addition to disulphides, TRXs can reduce multiple oxidised Cys forms, including *S*-nitrosothiols and sulphenic acids (Benhar et al., 2008; Kneeshaw et al., 2014; Tarrago et al., 2010).

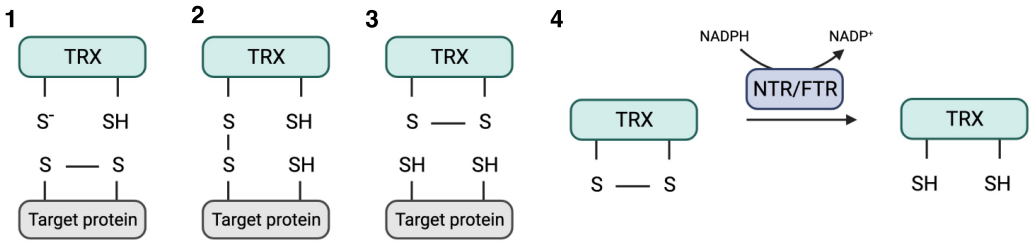

Figure 1. 4 Mechanism of Thioredoxin disulphide reduction

1) TRX encounters its oxidised target **2)** The first active site thiol reduces the first thiol of the target protein, creating a mixed disulphide between the TRX and the target. **3)** The second active site thiol resolves the mixed disulphide, releasing a reduced target protein an oxidised TRX. **4)** The TRX is fully reduce by an NADPH-dependent thioredoxin reductase (NTR). Created with Biorender.com

Plants have evolved different types of TRXs that are localised to specific subcellular locations to combat different causes of oxidative stress (Fig 1.3) (Belin et al., 2015; Gelhaye et al., 2005). For example, the chloroplast contains more than half of TRXs found in plant cells, but different sub-families play different roles. While the *f*- and majority of *m*-type TRXs in the chloroplast regulate photosynthetic activity by maintaining the activity of enzymes during carbon metabolism (Collin et al., 2003; Okegawa and Motohashi, 2015; Yoshida et al., 2015), the *y*-, and other *m*-type TRXs are important in regulating stress responses (Laugier et al., 2013; Rey et al., 2013).

The mechanisms of action of TRXs range from exhibiting direct anti-microbial activity to reversing oxPTMs to either enable signalling or to protect critical proteins from the damaging effects of oxidation. With regard to the former, OsTRXm and the TRX-like protein OsTDX from rice (*Oryza sativa*) were found to display anti-microbial activity (Park et al., 2019a, 2019b). OsTRXm was identified as a novel anti-fungal protein, inhibiting the growth of several fungi, including the maize pathogen *Fusarium moniliforme* (Park et al., 2019b). Although TRX*h*5 is not secreted and thus not considered to be a natural antifungal protein, recombinant TRX*h*5 from *Arabidopsis*

was found to display antifungal properties. Interestingly, when the yeast *Candida albicans* was treated with *At*TRX*h*5, it exhibited an increase in ROS generation, suggesting that TRX*h*5 inhibited fungal growth by eliciting ROS production (Park et al., 2017). The identification of antifungal properties associated with TRX*h*5 suggests that there is scope for using its redox properties as a biotechnological crop improvement strategy.

TRXs have emerged as major regulators of signalling, perhaps best illustrated by the roles of TRX*h*5 and closely related TRX*h*3 in plant immune signalling (Kneeshaw et al., 2014; Laloi et al., 2004; Tada et al., 2008). Specifically, these TRXs regulate the conformational state and thus activity of the NPR1 immune transcriptional activator. As described in section 1.2, in resting cells NPR1 exists in an oligomeric form in the cytoplasm bound together by disulphide bridges (Mou et al., 2003). Upon pathogen-induced SA accumulation, TRX*h*3/*h*5 facilitate NPR1 disulphide reduction and associated monomerisation (Tada et al., 2008). Moreover, TRX*h*5 directly denitrosylates NPR1, which prevents the formation of further disulphide bridges (Kneeshaw et al., 2014; Tada et al., 2008). Consequently, TRX*h*5 plays a critical role in NPR1 homeostasis and NPR1-dependent transcriptional reprogramming.

Furthermore, TRXs have been shown to exhibit protective roles. It is well known that in plant and algal species, TRXs function to protect the activities of peroxiredoxins (Broin et al., 2002; Broin and Rey, 2003; Rey et al., 2005). More recently, a substrate-trapping approach identified several H_2O_2-scavenging enzymes as targets of the nuclear and cytosolic oxidoreductase Nucleoredoxin 1 (NRX1), highlighting a role for TRX family members in enabling antioxidant enzymes to function in ROS-rich environments (Kneeshaw et al., 2017).

1.5 Aims and objectives

The effects of oxidative modifications on the localisation, function and activity of proteins are continuously emerging. However, to fully understand how oxPTMs can be used as selective molecular signalling switches, the extent of specificity within redox signalling networks must be studied. The importance of the TRX family in metabolism and stress signalling has been clearly demonstrated, but the extent of their selectivity remains to be unravelled. Therefore, the overarching aim of this thesis is to explore the versatility and selectivity of TRX members in regulating redox-mediated signalling during plant stress responses.

1.5.1 Thesis objectives

1) Determine if and how NRX1 is able to restore redox homeostasis in the absence of key antioxidants, catalase or glutathione

While the TRX family member NRX1 has been implicated in the protection of antioxidant enzymes during immune signalling (Kneeshaw et al., 2017), it remains unclear if it has additional roles in redox signalling. One of the aims of this thesis is to determine if and how NRX1 can restore redox homeostasis in the absence of key antioxidant enzymes, which is explored in Chapter 3. Furthermore, TRX enzymes are known to regulate stress-induced transcriptional reprogramming (Kneeshaw, 2016; Kneeshaw et al., 2014; Tada et al., 2008), so this thesis aims to establish the role of NRX1 in countering ROS-induced transcriptome changes in response to photo-oxidative stress is also investigated.

2) Determine the selectivity of TRX *h* family in regulating oxidative signalling in catalase- or glutathione-deficient plants

Because TRXs exhibit preferences for targets despite sharing the same subcellular location, and display selective activity in immune signalling (Kneeshaw et

al., 2014; Yoshida et al., 2015), Chapter 4 assesses which TRX-*h* family members selectively rescue plant phenotypes caused by excessive oxidative signalling. The findings from Chapters 3 and 4 indicate that each TRX family member has specific roles in countering different oxidative signalling pathways. These data indicate that the combined selective activities of TRXs enable plant cells to utilise ROS as specific signalling cues.

3) Determine the role of NRX1 in the interplay between oxidation and ubiquitination

PTMs enable dynamic regulation of the proteome, and the interplay of PTMs drastically enhances the cell's ability to fine-tune responses to external and internal cues. Given the structural and enzymatic roles of Cys in cellular signalling, oxPTMs have the potential to cross talk with other PTMs. Previous work identified accessory proteins of the ubiquitin proteasome system (UPS) as targets of NRX1 (Kneeshaw et al., 2017), suggesting that NRX1 might play a role in the regulation of proteasome-mediated protein degradation. Chapter 5 investigates if NRX1 is responsible for reversing the oxidative inhibition of deubiquitinase enzymes and how this affects downstream hormonal signalling. The presented findings indicate that NRX1 is a critical regulator of deubiquitinase enzyme activity, thereby controlling signalling by the plant developmental and stress hormone, jasmonic acid (JA).

Taken together, this thesis sheds new light on the selective and reversible nature of redox signalling in plants by uncovering the specific roles of TRX family members. Redox signalling is widespread across cellular processes, suggesting that it can be exploited to enhance responses to different stimuli. However, as the components of redox signalling are so interconnected with many redundancies, it has proven difficult to understand the selective signalling roles they may be involved in. The findings of this thesis show that redox signalling can be manipulated to generate

specific phenotypes, which could prove to be a useful tool in utilising redox signalling in plant biotechnology.

Chapter 2

Methods

2.1. Plant growth conditions

All *Arabidopsis* plant materials used were in the Col-0 ecotype. The *cat2-1, cat2-2,* and *nrx1-1* mutants are all SALK T-DNA insertion lines (Table 2.1). The *pad2-1* mutant is a point mutation previously described (Glazebrook and Ausubel, 1994). Plants were grown at 22°C on a 16hr light/ 8hr dark photoperiod at 65% humidity at 100 µmol m^{-2} s^{-1}. During light stress experiments, plants were moved to 600 µmol m^{-2} s^{-1} for 3 days.

Table 2. 1 T-DNA insertion SALK lines

Gene	Allele	SALK line
CAT2	*cat2-1*	SALK_076998
	cat2-2	SALK_057998
NRX1	*nrx1-1*	SALK_113401

2.2. Generation of plasmids and plant transformation

Thioredoxin *h* members (*TRXh1, 2, 3, 4, and 5*) and *UBP13* were cloned into pENTR™/D-TOPO (Invitrogen) by Lucas Frungillo and Michael Skelly, respectively, according to the manufacturer's instructions. Constructs were then recombined into their respective Gateway compatible destination vectors using Gateway™ LR Clonase™ II Enzyme (Invitrogen) according to the manufacturer's instructions (Table 2.2). The UBP13 active site mutant, *UBP13 (C207S),* was generated using site-directed mutagenesis by Michael Skelly using the Agilent Quick-Change Lightening kit (Table 2.3).

Constructs for plant transformation were introduced into *Agrobacterium tumefaciens* strain GV3101 (pMP90) using a freeze-thaw method (Weigel and

Glazebrook, 2002). *Arabidopsis* plants were transformed by floral dip (Weigel and Glazebrook, 2002) and transgenic plants were selected in subsequent generations by spraying with 120 µg/ml glufosinate ammonium.

Table 2. 2 Genes and corresponding vectors used

Gene name	Destination vector	N-terminal tag
TRXh1	pEarleyGate 202	Flag
TRXh2	pEarleyGate 202	Flag
TRXh3	pEarleyGate 202	Flag
TRXh4	pEarleyGate 202	Flag
TRXh5	pEarleyGate 202	Flag
UBP13	pEarleyGate 203	Myc
	pDest17	GST
	pUBQ10::YFP	YFP
UBP13 (C207S)	pEarleyGate 203	Myc
	pDest17	GST
	pUBQ10::YFP	YFP

Table 2. 3 Site-mutagenesis primers used for the UBP13 active site mutant (C207S)

UBP13 (C207S)	**F** CCAAGGTGCTACCTCTTACATGAATTCTC	Michael Skelly, Spoel lab
	R GAGAATTCATGTAAGAGGTAGCACCTTGG	

2.3 RNA extraction

For total RNA extraction, leaves were ground in liquid nitrogen and homogenised with 0.5 ml RNA extraction buffer (100mM LiCl, 100 mM Tris pH 8.0, 10mM EDTA, 1 % SDS) and 0.5 ml phenol:chloroform:isoamylalcohol (25:24:1), and centrifuged for 5 minutes at 4°C at 13,000rpm. The aqueous phase was transferred to a new tube, mixed with chloroform:isoamylalcohol (24:1), and centrifuged as described previously; then this step was repeated. The aqueous layer was added to 1/3 volumes of 8M LiCl and incubated overnight at 4°C. The following day, samples

were centrifuged for 20 minutes at 4°C at 13,000rpm to form a pellet. The pellet was washed with ice-cold (-20°C) 70% ethanol and incubated with 400 µl ddH_2O for 30 mins on ice. The pellets were resuspended and precipitated with 40 µl 3M NaAC (pH 5.2) and 1 ml ice cold (-20°C) 96% ethanol for at least 1 hour at -20°C. Samples were again centrifuged for 20 minutes at 4°C at 13,000rpm to form a pellet. The pellet was washed with ice-cold (-20°C) 70% ethanol and resuspended in 50 µl ddH_2O before quantification with the Nanodrop spectrophotometer (Thermo Scientific).

2.4 cDNA synthesis and qPCR

After RNA quantification samples were diluted to equivalent concentrations and 1.5 µg mRNA was reverse transcribed into cDNA using oligodT primer and SuperScript Reverse Transcriptase II (Invitrogen) according to the manufacturer's instructions. qPCR was conducted using 20-fold diluted cDNA using Power SYBR green (Life Technologies) and 0.5 µM gene-specific primers (Table 2.4) using the 2-step program on a StepOne Plus Real Time PCR system (Life Technologies).

Table 2. 4 Primers used for qPCR

Gene	Sequence 5'-3'	Reference
HSP17.6	**F** GGAGAAAGAAGATAAGAATGACACG	Queval et al. 2007
	R TCAACACACCATTCTCCATCG	
GPX6	**F** GATGTTAACGGTGACAAAGCTG	Queval et al. 2007
	R TTGGTGCGAAACGATCG	
GSTF8	**F** CGAAGGTAAGCTCCAGAAAGTC	Queval et al. 2007
	R AGAGTCAAAGAGCACCTTGGAG	
PR1	**F** CTAAGGGTTCACAACCAGGC	Kneeshaw et al. 2017
	R AAGGCCCACCAGAGTGTATG	
UBP13	**F** AGACGAGGAGATGCTTGTTCCG	Vanhaeren et al. 2020
	R AGCAGGATCAGTTTGGGCAACTTC	
VSP2	**F** TGCCAAAGGACTTGCCCTAAA	Lucas Frungillo, Spoel lab
	R GGTCGGTCTTCTCTGTTCCGT	
PDF1.2	**F** ACCCTTATCTTCGCTGCTCTTG	Michael Skelly, Spoel lab
	R TCCTTCAAGGTTAATGCACTGATTC	
LOX2	**F** AATGAGCCTGTTATCAATGC	Michael Skelly, Spoel lab
	R CATACTTAACAACACCAGCTCC	
SAG13	**F** AGGAAAACTCAACATCCTCGTC	Jeong et al. 2017
	R GCTGACTCGAGATTTGTAGCC	
TAT	**F** TGGCTCTAGGGGCAGAGAAT	Jeong et al. 2017
	R CCTTGGAGATGGCATGACGA	
UBQ5	**F** CCAAGCCGAAGAAGATCAAG	Kneeshaw et al. 2017
	R ACTCCTTCCTCAAACGCTGA	
ACT2	**F** AGTGGTCGTACAACCGGTATTGT	Jeong et al. 2017
	R GATGGCATGAGGAAGAGAGAAAC	

2.5 RNAseq

RNA extraction was performed as described in section 2.3, the integrity of RNA confirmed using a Bioanalyser (Agilent 2100), and submitted to Beijing Genomics Institute (Hong Kong, China) for RNA sequencing and bioinformatic analysis. The RNA-Seq workflow in the Strand NGS software was used to quantify transcripts. The RNA-seq reads were aligned to the *Arabidopsis thaliana* TAIR10 genome using Bowtie. TopHat identified potential exon-exon splice junctions of the initial alignment. Raw counts were normalised using DESeq with baseline transformation to the median of all samples. Data were then expressed as normalised

signal values (i.e., log2[RPKM] where RPKM is read count per kilobase of exon model per million reads) for all statistical tests and plotting.

2.6 Disease assays

Pseudomonas syringae pv. *maculicola* strain ES4326 (*Psm* ES4326) was cultured overnight in an LB liquid culture containing 50 µg/ml streptomycin and 10mM $MgSO_4$ at 28°C. The next day a subculture was made and incubated at 28°C until the OD_{600} reached 0.6. The culture was centrifuged at 2,000*g* for 5 minutes and diluted to OD_{600} = 0.002, corresponding to $2X10^6$ cfu/ml, in 10 mM $MgSO_4$ for inoculation. Two leaves per plant were infiltrated on 3-4 week old plants. To measure bacterial growth leaves were harvested 3 days post infiltration (dpi) and leaf discs were cut from infected leaves and ground in 10 mM $MgSO_4$. Serial dilutions were made and then spread on LB agar plates containing 50 µg/ml streptomycin, 10 mM $MgSO_4$ and 50 µM cycloheximide and incubated at room temperature for 2 days. Colonies were counted and bacterial growth was expressed as cfu/cm^2 of leaf tissue. Experiments were conducted with 8 replicates and an ANOVA followed by a Tukey post-hoc test was conducted to analyse statistical differences.

2.7 Methyl Viologen treatments and electrolyte leakage assays

Four-week old plants were infiltrated with 10 µM methyl viologen (MV) (Sigma). Ten leaf discs (5 mm diameter) per genotype were taken 1 hour after infiltration and washed 3 times in H_2O before being placed in a 50 ml Falcon tube containing 10ml H_2O. Samples were put under light and electrolyte leakage was measured using an ion conductivity meter at indicated time points over a period of 24 hours. After the final time point leaf discs and the water they were incubated in were transferred into glass tubes and boiled for 10 minutes. Tubes were left to cool to room

temperature before total electrolyte readings were taken. All samples were performed in triplicate.

2.8 Transient expression in *Nicotiana benthamiana*

Constructs containing *35S::Flag-NRX1* and *35S::Myc-UBP13* were introduced into *Agrobacterium tumefaciens* (strain GV3101) by transformation as described in section 2.2 and cultured overnight in LB media containing rifampicin (25 µg/ml), gentamycin (50 µg/ml) and kanamycin (50 µg/ml). The following day cultures were centrifuged at 4,000 rpm for 10 minutes. Pellets were resuspended in 10mM $MgCl_2$ and centrifuged again for 10 minutes at 4,000 rpm. Pellets were resuspended in 10ml of 10mM $MgCl_2$ containing 10 µl/L of benzylaminopurine (BAP) and diluted until the indicated OD_{600}. The two cultures were combined and incubated at room temperature for 2 hours. 3-4 week old *Nicotiana benthamiana* plants were infiltrated with the *Agrobacterium* solution before leaf tissue was harvested 3 dpi and stored at -80°C until use.

2.9 Co-immunoprecipitation assays

Leaf tissue was extracted in fixation buffer (diluted H_{25}EN buffer (25mM Hepes, 1mM EDTA, 0.1mM neocuproine), 2.5% SDS, 25 mM NEM and protease inhibitor cocktail) and incubated at 50°C for 20 minutes with frequent vortexing. Samples were centrifuged at 14,000*g* for 20 minutes at room temperature and acetone precipitated at -20°C for 20 minutes. Pellets were collected by centrifuging at 14,000*g* for 10 minutes at 4°C. The supernatant was discarded, and pellets were washed in ice cold 70% acetone and centrifuged as mentioned above. Pellets were resuspended in diluted H_{25}EN buffer containing 0.5% SDS. Inputs were taken and the remaining samples mixed with 4.5 ml Neutralisation buffer (diluted H_{25}EN buffer containing 0.5%

Triton X-100 and 150 mM NaCl). Diluted samples were incubated with rotation at 4°C with 40 µl anti-Flag M2 affinity resin (Sigma) prewashed with elution buffer (0.1M glycine, pH 3.5) and diluted with 0.5ml neutralisation buffer for 3 hours. Samples were washed a total of five times with 1ml neutralisation buffer and centrifuged for 1 minute at 4,000 rpm at 4°C. After the final wash the supernatant was removed before addition of 2X SDS sample buffer containing 200mM DTT. Samples were then heated at 95°C for 1 minute and loaded on SDS-PAGE gels for western blotting.

2.10 Mixed-disulphide assay

To assess mixed disulphides between NRX1 and targets, protein was extracted in HEN buffer (100 mM Hepes (pH 7.7), 1 mM EDTA, and 0.1mM neocuproine), 2.5% SDS and 25 mM NEM. Samples were then incubated at 50°C for 20 minutes with frequent vortexing. Samples were centrifuged at 14,000*g* for 20 minutes at room temperature. Samples were prepared for nonreducing (no DTT) or reducing (50mM DTT) SDS-PAGE gel. Western blots were probed with an antibody against NRX1.

2.10 Recombinant protein purification

2.10.1 GST-UBP13 and GST-UBP13 (C207S)

Recombinant GST-UBP13 and GST-UBP13 (C207S) constructs in the pDEST17 vector were grown in BL21 (DE3) cells and grown overnight at 37°C in LB with 100 µg/ul ampicillin. The next day, cultures were subcultured and grown until they reached OD_{600} = 0.6-0.8. Protein expression was induced with 0.1mM Isopropyl-B-D-Thiogalactopyranoside (IPTG) overnight at 26°C. Cells were collected by centrifugation at 6,500rpm for 15 minutes. Cells were resuspended and lysed in buffer containing 1X Bugbuster (Novagen), phosphate buffered saline (PBS), 1 µl/ml benzonase nuclease and protease inhibitor cocktail (PIC; 50 mg/ml TPCK, 50 mg/ml

TLCK, and 0.6 mM PMSF). Extracts were then incubated with rotation for 1 hour at room temperature and centrifuged for 20 minutes at 4°C at 13,000rpm. The supernatant was collected and syringe filtered before incubating with Glutathione Sepharose 4B beads (GE Healthcare), pre-washed with PBS, overnight with rotation at 4°C. The following day, beads were collected by gravity flow and washed 3 times with PBS before proteins were eluted in 1 ml Tris (pH 8.0) and 10 mM reduced glutathione. Samples were then dialysed against appropriate buffers using Slide-A-Lyzer cassettes (Thermo Scientific).

2.10.2 His-NRX1 and His-NRX1 (C55,58,375,378S)

Recombinant His-NRX1 and His-NRX1 (C55,58,375,378S) in the pET28a vector (Kneeshaw et al., 2017) were grown in BL21 (DE3) cells overnight at 37°C in LB with 50 µg/µl Kanamycin, subcultured and grown until they reached OD_{600} = 0.6-0.8 and induced with 1 mM IPTG and grown for a further 5 hours at 37°C. Cells were collected by centrifugation at 6,500rpm for 15 minutes. Cells were resuspended and lysed in buffer containing 1X Bugbuster (Novagen), 50 mM potassium phosphate (pH 7.4), 10 mM imidazole, 1 µl/ml benzonase nuclease, 10 mM β-mercaptoethanol and PIC. Extracts were incubated with rotation at room temperature for 30 minutes and then centrifuged at 13,000rpm for 20 minutes at 4°C. The supernatant was syringe filtered and purified on HisPur Cobalt Resin (Pierce) by gravity flow. Columns were washed 3 times with wash buffer (50 mM potassium phosphate pH 7.4, 300mM NaCl, 10mM imidazole and PIC), before eluting in 1 ml of 50 mM potassium phosphate 7.4, 300mM NaCl and 500 mM imidazole. Samples were then dialysed against appropriate buffers using Slide-A-Lyzer cassettes (Thermo Scientific).

Protein concentrations were determined against a bovine serum albumin (BSA) standard curve using Bio-rad Protein Assay according to the manufacturer's instructions.

2.11 Reductive switch

Frozen leaf tissue was ground in liquid nitrogen and homogenised with 4 times volumes (1 ml per 1 g tissue) Fixation buffer (HEN buffer (100mM Hepes, 1mM EDTA, 0.1mM neocuproine), 25mM NEM, 2.5% SDS) with PIC. Samples were centrifuged for 20 minutes at 13,000 rpm at 4°C. The supernatant was then incubated on a thermomixer at ~800 rpm at 50°C for 20 minutes before adding 2 times the volume of the supernatant of ice-cold (-20°C) acetone and incubating at -20°C for 20 minutes. Samples were centrifuged for 5 minutes at 13,000 rpm 4°C and the pellet was washed 3 times with ice-cold (-20°C) 70% acetone. Samples were resuspended in 490 µl HEN buffer containing 1% SDS before adding either 10 µl 100 mM DTT (final concentration 2mM) or ddH_2O and incubated with rotation at room temperature for 10 minutes. Samples were then acetone precipitated as previously described. After precipitation, pellets were resuspended in 450 µl HEN buffer containing 1% SDS, and 50 µl of 4mM EZ-linked Biotin-HPDP (Thermo Fisher, 21341) was added to each sample before incubation with rotation in the dark at room temperature for 1 hour. Samples were then acetone precipitated once more as previously described. Pellets were resuspended in 100 µl HEN buffer containing 1% SDS and 10 µl was taken for total protein detection. The remaining samples were then diluted 10-fold with neutralisation buffer (H_{25}EN (25mM Hepes, 1mM EDTA, 0.1mM neocuproine), 0.5% Triton X-100, 100mM NaCl) and incubated with 10 µl streptavidin beads pre-equilibrated with neutralisation buffer, and incubated overnight with rotation at 4°C. The following day, samples were centrifuged for 1 minute at 5,000rpm at 4°C followed by 1 minute on

ice. Samples were then washed 5 times in wash buffer (H_{25}EN, 0.5% Triton-X 100, 600mM NaCl) and eluted in H_{25}EN with 1% β-mercaptoethanol for 30 minutes with shaking at room temperature. Finally, samples were analysed by SDS-PAGE and western blotting.

2.12 *in vitro* Deubiquitination assays

2.12.1 Western blotting

20 nM GST-UBP13 or GST-UBP13 (C207S) were incubated with DUB buffer (50 mM Tris pH7.4m 5mM $MgCl_2$) with or without 1 mM DTT, 400 nM ubiquitin chains (R&D systems) and incubated at 30°C for the indicated period of time. Samples were then incubated with SDS sample buffer containing 50 mM DTT and heated at 70°C for 20 minutes before analysis by SDS-PAGE and western blotting.

2.12.2 Ub-AFC assays

The activity of the indicated DUBs was determined by measuring the increase in fluorescence upon cleavage of ubiquitin-AFC (Ub-AFC, R&D systems). 20nM purified DUBs were mixed with DUB buffer with or without either 1mM DTT or 2 μM His-tagged NRX1/NRX1 (C55,58,375,378S). 0.5 μM Ub-AFC was added immediately before beginning the fluorescence measurements. Reactions were conducted in 100 μl volumes in triplicate on a black opaque 96-well plate. The fluorescence intensity was measured using a Tecan Infinite M200 PRO plate reader with excitation and emission wavelengths at 400nm and 505nm, respectively. Measurements were taken every 10 seconds for 5 minutes at 30°C.

2.13 SDS-PAGE and Western blotting

Protein samples were added to appropriate volumes of 4X SDS-PAGE sample buffer to give a final concentration of 50 mM Tris-HCl pH 6.8, 2% SDS, 0.02% bromophenol blue and 10% glycerol with or without 50 mM dithiothreitol (DTT). Samples were

heated at 70°C for 15-20 minutes before centrifugation at 13,000rpm for 1 minute and separating by SDS-PAGE using gels of appropriate polyacrylamide percentage. For Instant Blue staining, gels were washed in H_2O before incubating with Instant Blue for 30 mins.

For western blot analysis, proteins were first transferred from gels to nitrocellulose membranes at 4°C either at 20V overnight or 90V for 1-2 hours. Membranes were then stained with Ponceau S solution (0.1% (w/v) Ponceau S, 5% acetic acid) for 30 seconds and then rinsed with ddH_2O. They were de- stained in PBS-T (PBS, 0.1% Tween20) and incubated with shaking for 1 hour in blocking buffer (PBS- T, 5% dried skimmed milk). Primary antibodies were incubated for 1-4 hours at room temperature or overnight at 4°C. Blots were washed three times with blocking buffer and then incubated with the appropriate secondary horseradish peroxidase (HRP)-linked antibodies for 1 hour at room temperature. After washing a further three times with blocking buffer and once with PBS-T, SuperSignal West Pico/Dura Chemiluminescent Substrate (Thermo Scientific) was added to the blot to detect bands by exposure using a Licor Odyssey® XF. Table 2.5 lists the antibodies used, their manufacturers and their relevant HRP-linked secondary antibody.

Table 2. 5 Antibodies used for western blotting

Primary antibody (concentration used)	**Manufacture (Catalogue no.)**	**HRP-linked Secondary antibody* (concentration used)**
anti-Flag (1:3000)	Sigma (F3165)	Mouse (1:2000)
anti-Myc (1:1000)	Invitrogen (9E10)	Mouse (1:2000)
anti-GFP (1:2000)	Roche (11814460001)	Mouse (1:2000)
anti-GST (1:5000)	Sigma Aldrich (SAB4200237)	Mouse (1:2000)
anti-His (1:5000)	Cell Signalling (2365)	Mouse (1:2000)
anti-NRX1 (1:10000)	ProteinTech (Custom-generated against full length recombinant His_6-NRX1, Kneeshaw et al 2017)	Rabbit (1:2000)

*All secondary antibodies are from Cell Signalling Technology
Anti-mouse (7076)
Anti-rabbit (7074)

Chapter 3

Nucleoredoxin selectively regulates cellular pathways that protect plant cells from oxidative stress

3.1 Background

Plant cells undergo oxidative stress in response to several stimuli resulting in a rapid accumulation of ROS and RNS. This can cause severe perturbation of cellular function via the oxidation of reactive cysteine residues. Whilst ROS/RNS pose a threat, they can also be utilised as signalling tools. Therefore, ROS/RNS homeostasis needs to be controlled to allow cellular signalling while minimising damage. To protect against oxidative damage and maintain redox signalling, organisms have evolved extensive networks of antioxidant molecules and enzymes, many of which are subject to redox modification themselves. Indeed, in the fungus *Neurospora crassa*, the H_2O_2 scavenger, catalase (CAT), is modified by singlet oxygen, but the presence of a reducing agent inhibits this modification (Lledías et al., 1998). Furthermore, an increase in oxidation by hydrogen sulphide (H_2S) resulted in a decrease of CAT activity in *Arabidopsis* (Corpas et al., 2019). However, oxidative modifications of antioxidant enzymes do not always result in their inhibition. In response to biotic and abiotic stresses, ascorbate peroxidase (APX) is positively regulated by *S*-sulphenation, and both positively and negatively regulated by *S*-nitrosylation (Begara-Morales et al., 2014a; de Pinto et al., 2013; Kaur et al., 2021; Yang et al., 2015). Many antioxidants rely on thiol-based mechanisms as reducing agents to maintain activity. The oxidoreductases superfamily of Thioredoxins (TRXs) are key players in reversible oxidative signalling and in preventing undesired cysteine modifications to maintain and protect cellular signalling.

TRXs are a superfamily of redox enzymes made up of protein disulphide isomerases (PDIs), conventional thioredoxins (TRXs), glutaredoxins (GRXs) and nucleoredoxins (NRXs), and are found in almost all cellular compartments. One of the key functions of conventional TRX enzymes is to reduce disulphide bonds in target

proteins, but over the last several years it has become clear that TRXs also target other oxidised Cys forms, including *S*-nitrosothiols and sulphenic acids, via either heterolytic or homolytic cleavage reactions (Benhar et al., 2008; Kneeshaw et al., 2014; Tarrago et al., 2010).

Interestingly, stress inducible Nucleoredoxin 1 (NRX1) in *Arabidopsis* has been shown to play a key role in the protection of antioxidant enzymes. NRXs have been identified in both plants and animals, but are absent in yeast (Lechward et al., 2006). In *Arabidopsis,* two NRX proteins have been characterised, NRX1 and NRX2. Both are found in the nucleus and cytoplasm, with NRX1 showing higher reductase activity than NRX2 (Marchal et al., 2014). Unlike conventional TRXs, NRXs have multiple active sites (Marchal et al., 2014). NRX1 contains three active sites, two of which contain the characteristic TRX active site sequence and are required for disulphide reductase activity *in vitro* (Kang et al., 2020; Kneeshaw et al., 2017; Marchal et al., 2014), while the third active site contains an atypical active site sequence (SYRKC; Marchal et al., 2014). As mutation of the two conventional active sties abolished NRX1 reductase activity *in vitro* (Kneeshaw et al., 2017), the third active site is not thought to be required for NRX1 disulphide reductase activity.

In *Arabidopsis,* NRX1 protects cells by guarding antioxidant enzymes. Kneeshaw et al. (2017) showed that NRX1 enables antioxidant enzymes to function in hostile, oxidative environments. Substrate-capture coupled to mass spectrometry identified several proteins that are members of the H_2O_2 scavenging pathway as targets of NRX1. These included APX and all three members of the CAT family in *Arabidopsis*. The authors went on to show that there is an increase in CAT oxidation in *nrx1* knockout mutants, which correlated with a reduction in CAT activity. Furthermore, recombinant NRX1 was able to rescue CAT activity in *nrx1* cell extracts.

While CATs are haem-containing enzymes and were previously thought to not require a reducing agent (Gill and Tuteja, 2010), this study indicates that CATs and probably other antioxidant enzymes, indeed require the reducing activity of NRX1 to maintain function under oxidative conditions. This highlights the cooperation between the TRX family and antioxidants; however, the extent of this cooperation remains unknown.

The above findings pose an important question: is NRX1-mediated protection of cells against oxidative stress to maintain signalling specific to protection of catalases? Due to redundancy within and between the GRX and TRX systems (Reichheld et al., 2009), knockout mutants often do not reveal the individual contributions of TRX family members, thereby preventing delineation of the individual functions of TRX enzymes and their substrate selectivity. One method of studying TRX substrate selectivity is by overexpressing each member of the family in redox-perturbed mutants. This has uncovered the specificity of the well-studied TRX*h*5 in rescuing immune responses in different NO accumulating backgrounds (Kneeshaw et al., 2014) and is therefore a useful tool for unravelling the functions of TRXs.

In this chapter, a similar genetic approach is used to show a new role of NRX1 in selectively protecting plants against oxidative stress in absence of major cellular H_2O_2 detoxification systems. Furthermore, using transcriptome analyses it is shown that in the absence of ROS-scavenging CAT activity, NRX1 partially counteracted ROS-induced transcriptional reprogramming in response to photo-oxidative stress.

3.2 Results

3.2.1 NRX1 does not rescue the immune-deficient phenotypes of ROS accumulating mutants

NRX1 is a pathogen-inducible oxidoreductase that was found to protect antioxidant enzymes during the immune response (Kneeshaw et al., 2017). To explore if NRX1 plays roles beyond protecting antioxidant enzymes, we investigated if NRX1 restores the immune-deficient phenotypes of antioxidant mutants that overaccumulate ROS. First, we utilised *cat2* mutants to explore if in the absence of CAT2 activity, NRX1 provides additional protection from high ROS. Similar to *nrx1* mutants, catalase mutants have been reported to display enhanced resistance to *Pseudomonas syringae* (Chaouch et al., 2010; Kneeshaw et al., 2017). In contrast to the literature, however, in our hands *cat2* mutants showed increased susceptibility to *Pseudomonas syringae* pv. *maculicola* (*Psm*) ES4326. This could be due to differences in light intensity compared to previous studies. For example, Chaouch et al. and Yuan et al. (2017) grew plants under 150 µmol $m^{-2}s^{-1}$ and 200 µmol $m^{-2}s^{-1}$, respectively, whereas here plants where grown under 100 µmol $m^{-2}s^{-1}$. As higher light intensities are known to cause cell death lesions in *cat2* mutants as described previously (Chaouch et al, 2010) and later in this chapter, this could have a negative effect on bacterial growth in the plants, possibly resulting in the enhanced resistance observed. Nevertheless, under the conditions tested in this thesis immunity against *Psm* was not restored in these mutants by constitutive expression of Flag-tagged NRX1 (Fig. 3.1A and 3.2A), suggesting that NRX1's role in protection from pathogen-induced ROS may be predominantly dependent on its role in maintaining CAT activity.

Next, we tested the *pad2* mutant that accumulates ROS due to highly reduced cellular levels of the tripeptide antioxidant glutathione (GSH). Consequently, *pad2* mutants are constantly in a heightened state of oxidation (Dubreuil-Maurizi et al.,

2011). SA accumulation is impaired in *pad2* plants, in part due to their inability to induce expression of the SA biosynthesis enzyme *ISOCHORISMATE SYNTHETASE1* (*ICS1*), resulting in increased susceptibility to pathogen infection (Dubreuil-Maurizi et al., 2011). As NRX1-mediated responses in immunity are also SA-dependent (Kneeshaw et al., 2017), the ability of NRX1 to restore immunity was tested in *pad2* mutants. As reported previously (Dubreuil-Maurizi et al., 2011), *pad2* plants showed enhanced susceptibility to *Psm* in comparison to wild-type (Fig. 3.2B) and this was unaffected by introduction of the *35S::Flag-NRX1* transgene (Fig. 3.1B and 3.2B). Taken together, these results indicate that NRX1 overexpression is unable to restore immunity in ROS-accumulating mutants.

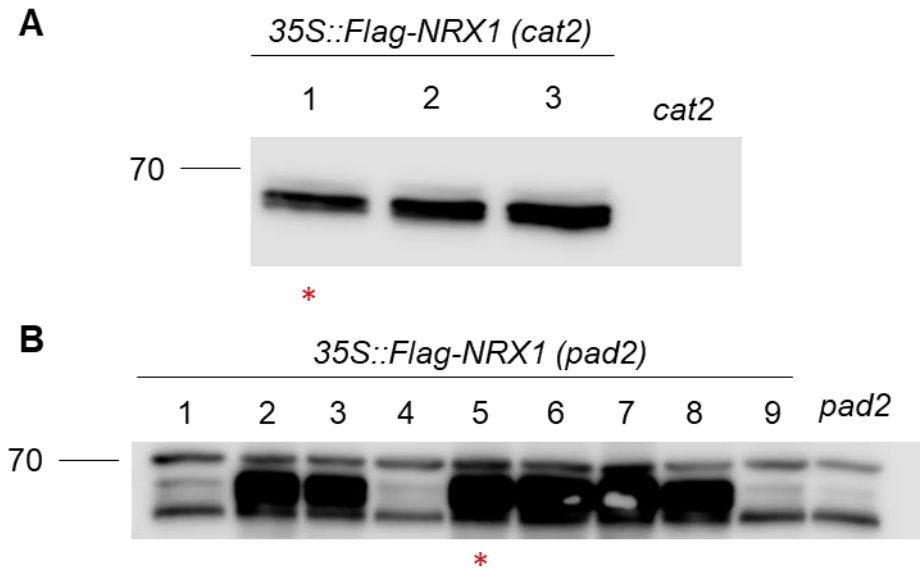

Figure 3. 1 Western blot of *35S::Flag-NRX1* in *cat2* and *pad2* mutants

Mutant *cat2* **(A)** and *pad2* **(B)** plants were transformed with Flag-tagged NRX1 driven by the constitutive 35S promoter (*35S::Flag-NRX1*). Expression of Flag-NRX1 was detected with an antibody against Flag Lines generated by Sophie Kneeshaw. Asterisks indicates lines used. Markers indicate kDa

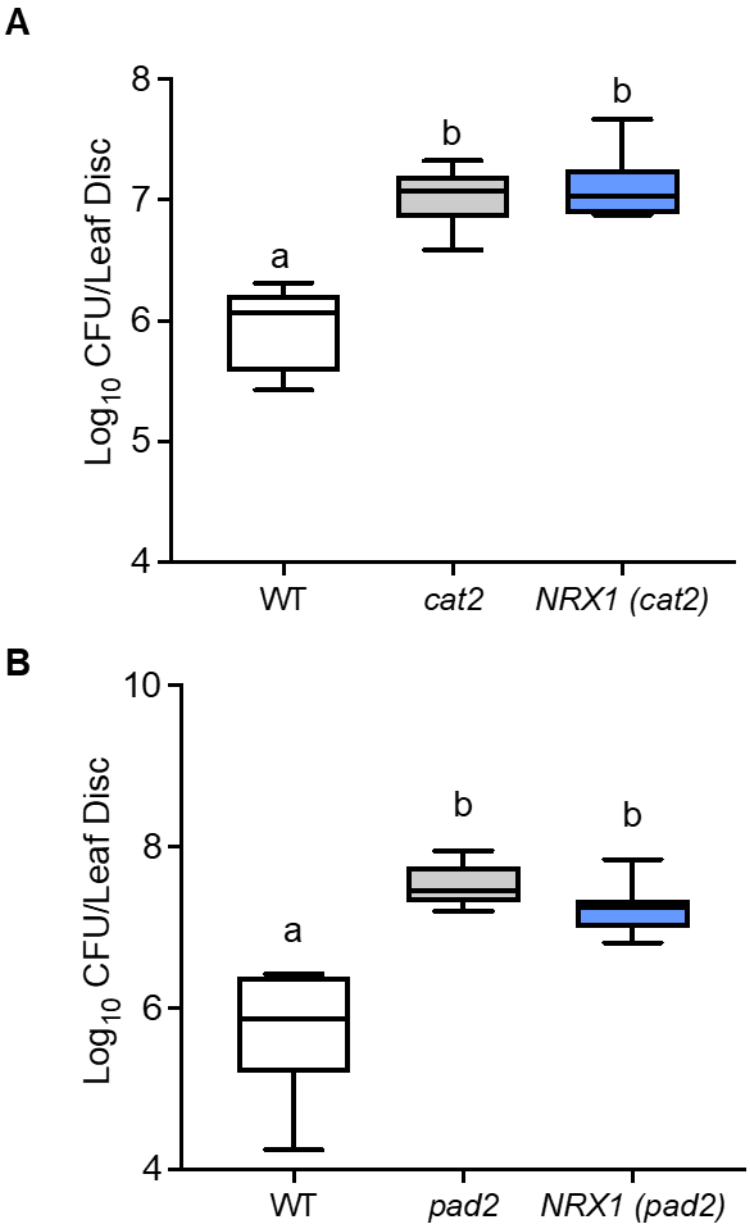

Figure 3. 2 NRX1 does not rescue the immune phenotype in *cat2* or *pad2* mutants

Plants were infiltrated with the bacterial pathogen *Pseudomonas syringae* pv. *maculicola* (*Psm*) ES4326 (OD_{600} = 0.002) and bacterial growth was analysed 3 days post infection. Different letters indicate $P < 0.05$ after analysis with ANOVA, n=8. CFU, Colony Forming Units *35S::Flag-NRX1 (pad2)* (B) assay was conducted by Shi Rui Ong

3.2.2 NRX1 selectively rescues electrolyte leakage in antioxidant-deficient plants

The identification of CATs and other antioxidant enzymes as targets of NRX1 indicates that NRX1 plays a key role in maintaining antioxidant-mediated signalling upon ROS accumulation.. Indeed, *nrx1* mutants show an increase in methyl viologen (MV)-induced electrolyte leakage increased levels in total glutathione compared to wild-type, similar to that of *cat2* mutants (Kneeshaw et al., 2017). This prompted us to investigate the ability of NRX1 to MV-induced oxidative stress in antioxidant-deficient plants. Wild-type, *cat2* and *35S::Flag-NRX1 (cat2)* plants were infiltrated with the ROS-generating chemical, MV, and ion leakage resulting from cell injury was measured over 24 hours. As expected, *cat2* plants displayed enhanced electrolyte leakage compared to wild-type (Fig. 3.3A). Intriguingly, overexpression of NRX1 in *cat2* plants was able to rescue electrolyte leakage back to wild-type levels (Fig. 3.3B), suggesting that to protect against oxidative stress, NRX1 not only protect CATs, but also utilises alternative mechanisms.

To determine if the ability of NRX1 to rescue electrolyte leakage is a general response, the capacity of NRX1 to rescue MV-induced electrolyte leakage when expressed in *pad2* was also tested. As with *cat2*, MV-treated *pad2* plants exhibited an increase in electrolyte leakage compared to wild-type plants (Fig. 3.3B). Surprisingly, *35S::Flag-NRX1* in *pad2* was unable to rescue electrolyte leakage back to wild-type levels (Fig. 3.3B). This indicates that NRX1 displays selectivity in its ability to protect cells against MV-inducedoxidative stress.

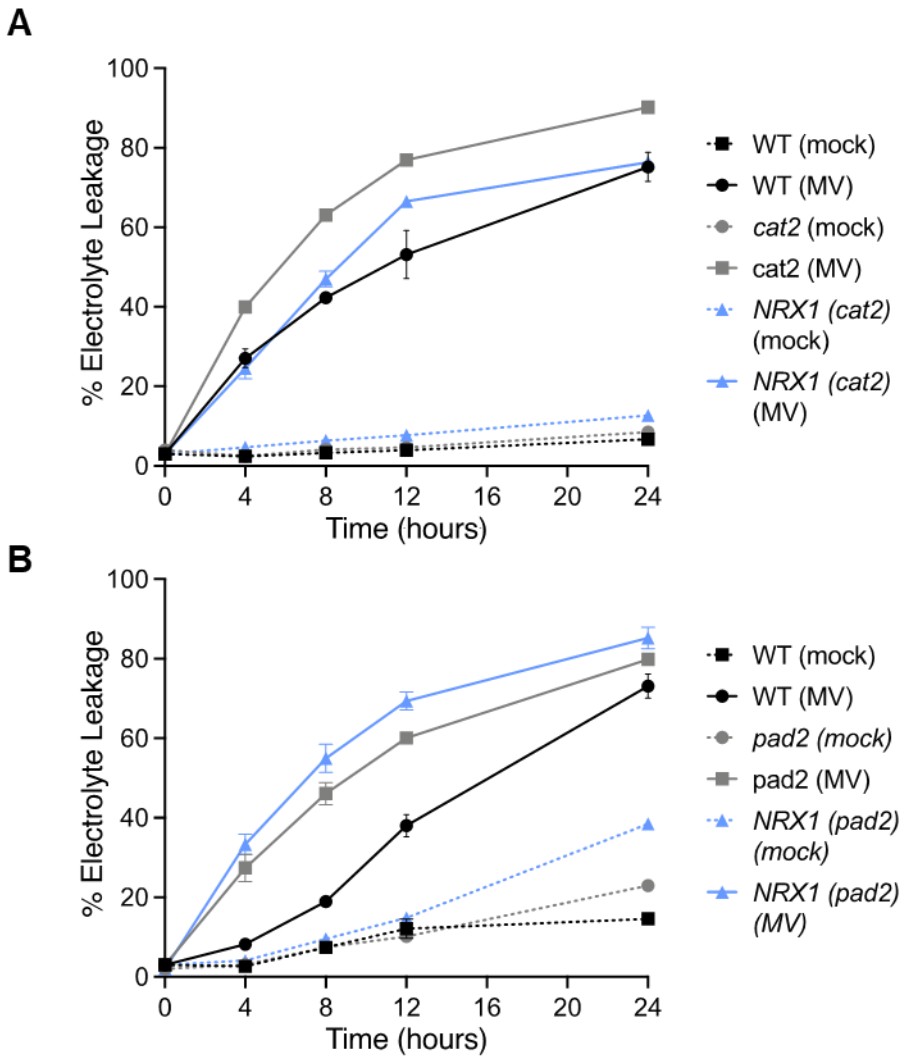

Figure 3. 3 NRX1 selectively restores enhanced cell death in *cat2*, but not *pad2* mutants

Leaves of Col-0, *cat2* and *35S::Flag-NRX1 (cat2)* **(A)** and Col-0, *pad2* and *35S::Flag-NRX1 (pad2)* **(B)** plants were infiltrated with 10μM of the oxidative stressor Methyl viologen (MV) or water (mock). Electrolyte leakage was measured over a period of 24 hours at indicated timepoints and are presented as a percentage of the total electrolyte leakage measured after boiling leaves. Error bars indicate standard error of the mean (n=3)

Upon pathogen infection, there is an increase in mixed disulphides between NRX1 and its substrates (Kneeshaw et al., 2017). Like pathogen infection, compared to mock-treated plants, MV treatment increased mixed disulphides between NRX1 and its substrates, indicating that NRX1 oxidoreductase activity is enhanced in

response to MV-induced ROS accumulation (Fig. 3.4). Intriguingly, compared to mock-treated wild-type, mock-treated *cat2* mutants displayed an increase in mixed disulphides, suggesting that NRX1 oxidoreductase activity is enhanced in *cat2* mutants. However, unlike wild-type plants, the amount of mixed disulphides between NRX1 and its targets did not appear to increase upon MV treatment, although the pattern of mixed disulphide formation did change (Fig. 3.4). These data suggest that in *cat2* mutants, the heightened state of oxidation in a resting state modifies NRX1 substrates, in turn amplifying its oxidoreductase activity. Furthermore, the change in the pattern of mixed disulphides suggests that upon oxidative stress the repertoire of NRX1 substrates is altered, indicating changes in oxidative signalling.

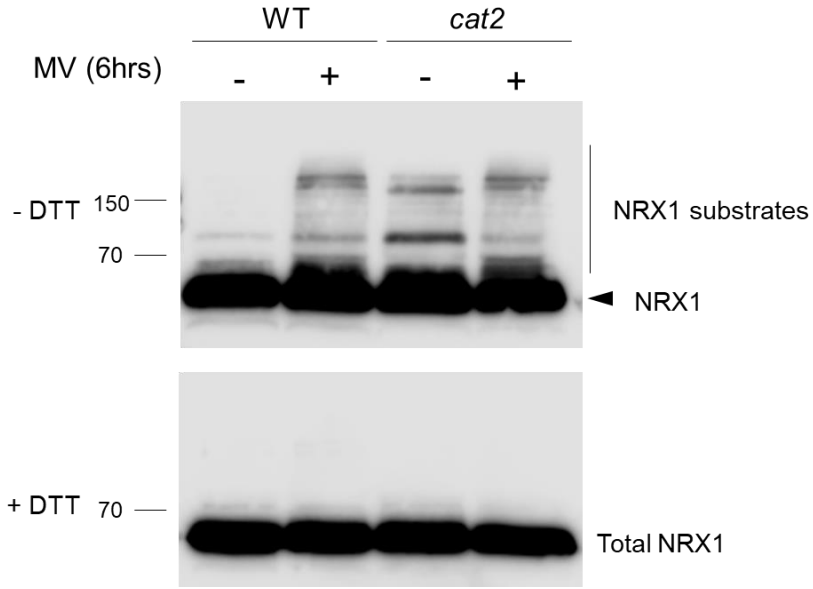

Figure 3. 4 Mixed disulphides between NRX1 and target substrates

Col-0 and *cat2* plants were infiltrated with 10 µM methyl viologen. Total protein was denatured with SDS and alkylated with NEM to capture mixed disulphide intermediates between NRX1 and its substrates. Samples were separated by SDS/PAGE with or without DTT to visualise total NRX1 and mixed disulphides between NRX1 and its substrates, respectively. Protein was detected by Western blot against NRX1.

3.2.3 NRX1 rescues light-induced oxidative stress in catalase mutants

Based on the finding that overexpression of NRX1 can rescue the enhanced MV-induced electrolyte leakage phenotype of *cat2* mutants, further study of the role of NRX1 in antioxidant-deficient plants focused on *35S::Flag-NRX1* in the *cat2* background. As MV causes an accumulation of O_2^-, by redirecting electrons from photosystem I to O_2 (Scarpeci et al., 2008), it acts as a useful mimic for photo-oxidative stress in photosynthetic organisms. Therefore, the role of NRX1 in response to light stress was assessed. To determine if NRX1 could rescue the macroscopic cell death lesions observed in *cat2* mutants during photo-oxidative stress (Vandenabeele et al., 2004), wild-type, *cat2*, and *35S:: Flag-NRX1 (cat2)* plants were placed in higher light conditions (200 µmol $m^{-2}s^{-1}$) for 5 days. As previously reported, wild-type plants showed no cell-death lesions, but did display brown-purple colouration on the abaxial side of the leaf (data not shown), an indication of anthocyanin accumulation (Vandenabeele et al., 2004). As expected, photo-oxidative stress resulted in extensive cell death lesioning in *cat2* mutants (Mhamdi et al., 2010b; Vandenabeele et al., 2004). However, expression of *Flag-NRX1* in *cat2* mutants substantially reduced the cell death phenotype (Fig. 3.5A), indicating that NRX1 is able to rescue photo-oxidative stress in CAT-deficient plants.

Previous research into *cat2* oxidative stress responses reported induction of H_2O_2-responsive marker genes (Queval et al., 2007). Expression of H_2O_2-responsive genes was tested in wild-type, *cat2* and *35S::Flag-NRX1 (cat2)* plants. Induction of these genes was indeed higher in *cat2* mutants compared to wild-type plants, but expression of *Flag-NRX1* was able to reduce their expression levels back to wild-type levels (Queval et al., 2007; Fig 3.5B). Together, these data show that expression of NRX1 can prevent oxidative stress in *cat2* mutants.

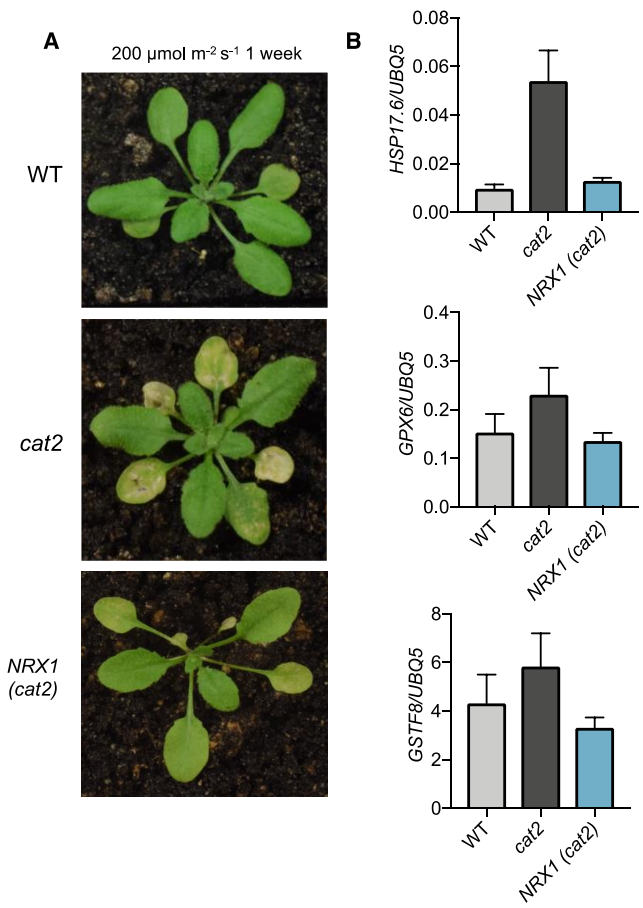

Figure 3. 5 NRX1 rescues light-induced cell death responses in *cat2* mutants

(A) Col-0, *cat2,* and *35S::Flag-NRX1 (cat2)* were grown at 100 µmol m^{-2} s^{-1} for 3 weeks and then moved to 200 µmol m^{-2} s^{-1} for 1 week. **(B)** Analysis of oxidative stress marker genes in Col-0, *cat2,* and *35S::Flag-NRX1 (cat2)* plants grown in conditions described in **(A)**
Error bars represent SEM of 3 technical replicates from a pool of 12 leaves from individual plants

3.2.4. NRX1 rescues oxidative stress in catalase mutants via partial rescue of ROS-induced changes in gene expression

So how does NRX1 maintain oxidative signalling in *cat2* mutants? Previous research has shown that light stress can induce dramatic transcriptomic changes in plants (Crisp et al., 2017; Huang et al., 2019; Zandalinas et al., 2019). Thus, RNA-

seq was conducted to determine if NRX1 was able to rescue ROS-induced changes in gene expression between *cat2* and wild-type plants. Comparisons of genes up- or down-regulated between *cat2* and wild-type plants under light stress showed a remarkable differential expression of genes, with over 2000 genes showing a fold-change of at least 2 (Fig. 3.6A). Expression of *Flag-NRX1* in the *cat2* background resulted in the differential expression (FC ≥ 2) of 272 genes compared to *cat2* mutants, however these were also differentially expressed compared to wild-type plants, revealing that no genes had their expression fully restored to wild-type levels (Fig. 3.6A). However, 182 genes in total were identified as being partially rescued by NRX1 in the *cat2* mutant background (Fig. 3.6B,C, Table S1). To validate the rescued genes were indeed induced by high light, the list of partial rescues by NRX1 was compared with the published high-light RNA-seq from Zandalinas et al. (2019), which identified a core set of high light-induced genes in locally stressed and distally untreated leaves. This comparison showed that ~34% of the genes partially rescued by NRX1 overlapped with locally stressed leaves, while ~40% overlapped with systemic leaves (Fig. 3.7, Tables S2 and S3). Comparisons were also made for genes that remained unchanged between wild-type and *cat2* mutant plants, but were differentially expressed between *cat2* and *35S::Flag NRX1* in *cat2* and wild-type and *35S::Flag NRX1* in *cat2* (FC ≥ 2) (Fig S1, Table S4). Of these genes, ~25% of DEGs between *cat2* and *35S::Flag NRX1* in *cat2* overlapped with the locally and systemically induced genes in Zandalinas et al. (Fig. S2,Tables S5 and S6). Significance of the overlap between the partially rescued genes identified and the light-induced genes in Zandalinas et al. was tested using a Fisher's exact test. The overlap between the genes was not significant, which indicates that the genes identified in this chapter as partial rescues are not necessarily a specific response to photo-oxidative stress.

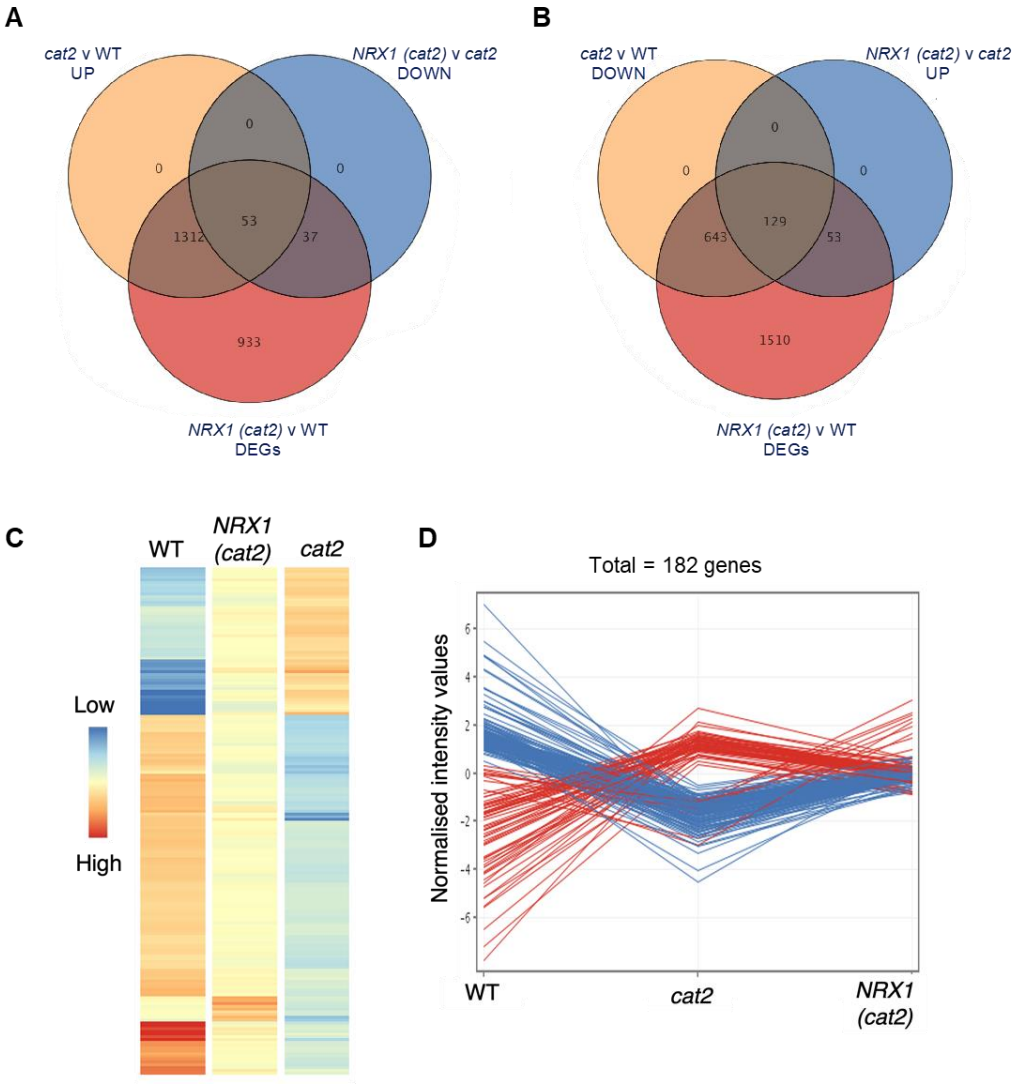

Figure 3. 6 NRX1 partially rescues oxidative stress in *cat2* mutants by partial rescue of ROS-induced changes in gene expression

(A) Comparisons of up-regulated genes in *cat2* mutants vs wild-type (WT) with down-regulated genes in *35S::Flag-NRX1 (cat2)* and all differentially expressed genes (DEGs) of *35S::Flag-NRX1 (cat2)* and WT plants following RNA-seq on plants placed under light-stress conditions for 3 days (FC >2, $p < 0.05$) **(B)** Comparisons of down-regulated genes in *cat2* mutants vs wild-type (WT) with up-regulated genes in *35S::Flag-NRX1 (cat2)* and all differentially expressed genes (DEGs) of *35S::Flag-NRX1 (cat2)* and WT plants following RNA-seq on plants placed under light-stress conditions for 3 days (FC >2, $p < 0.05$)

(C) Heatmap and **(D)** profile plot showing the combined (53 +129) partial rescue of gene expression in response to light-stress treatment described in **(A)**

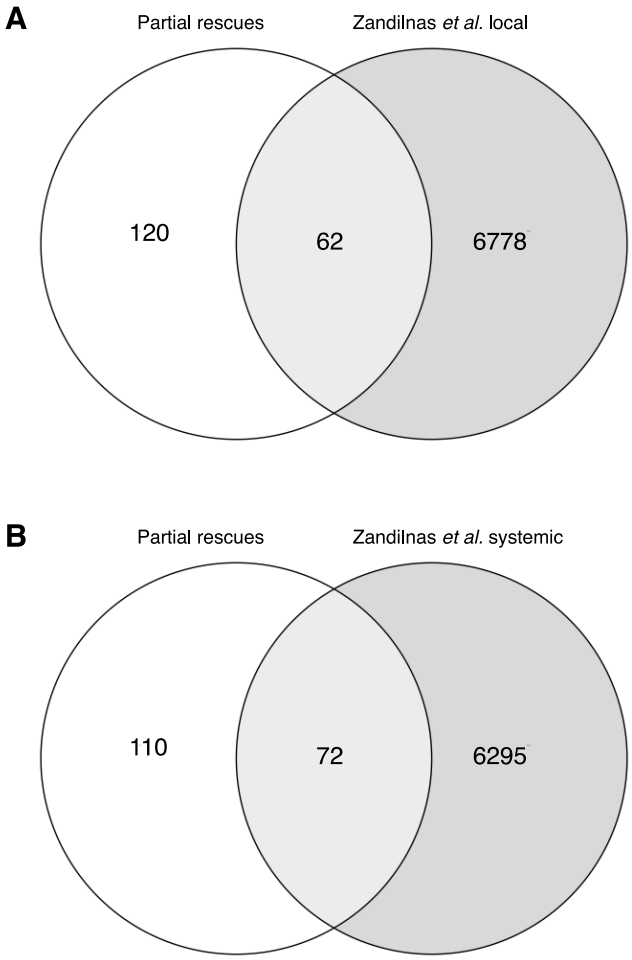

Figure 3. 7 Partial rescues identified correspond to published RNA-seq datasets of plants in 'high light' conditions

Comparisons were made between genes identified as partially rescued by NRX1 (Fig. 3.6) and genes that were differentially expressed in response to local light stress **(A)** and systemic stress in untreated leaves **(B)** from Zandalinas et al. (2019)

Using BarToronto and PANTHER software, Gene Ontology (GO) analysis was conducted to determine the molecular function of genes partially rescued by NRX1. The category containing the highest number of genes using BarToronto software was 'other enzyme activity' (data not shown). Similarly, using PANTHER software, the category containing the highest number of genes was 'catalytic activity' (Fig. 3.8A). GO analysis was also conducted on the genes only differentially expressed in *NRX1 (cat2)* plants (Fig. S2), but no significant GO terms were identified (data not shown).

As the PANTHER software allows for a more detailed look at subcategories, further GO analysis was conducted using this software. Within the ‘catalytic activity’ group, there was a large number of genes in the subgroups ‘oxidoreductase activity’, ‘transferase activity’, ‘hydrolase activity’ and ‘catalytic activity, acting on a protein’ (Fig 3.8B). Within these sub-categories, many redox-related genes families commonly appeared, including for example cysteine-rich receptor kinases, glutathione S-transferases, and oxidoreductases such as peroxiredoxins and the stress inducible TRX*h5*.

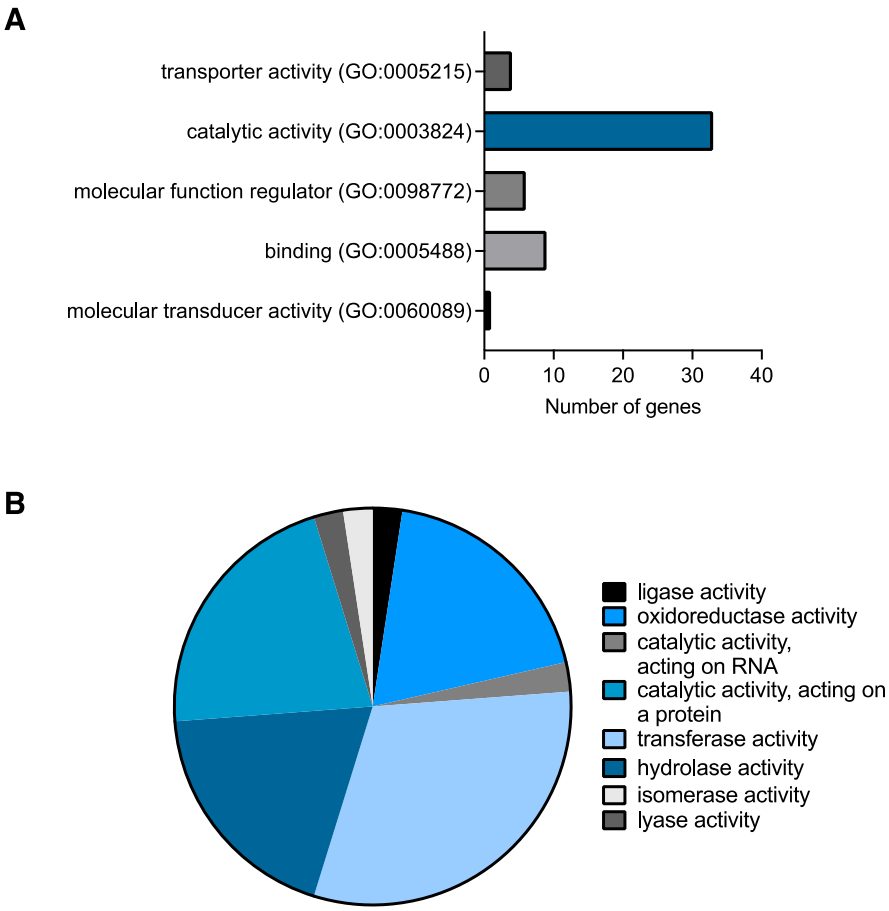

Figure 3. 8 Gene Ontology of partially rescued genes(A) GO term analysis for molecular function of partial rescues was performed using PANTHER (pantherdb.org) **(B)** Subcategory of the highest molecular function GO term 'catalytic activity' identified in **(A)**

Several transcription factor (TF) families are known to be redox regulated (Dietz, 2014), therefore it is possible that NRX1 may regulate ROS-induced transcriptional changes by maintaining the activity of TFs under oxidative conditions. The genes identified as partial rescues were assessed for significantly enriched binding factors using Plant Regulomics (Ran et al., 2019). This showed that the highest number of genes bind WRKY55, but in general genes were found to predominantly bind members of the NAC family of TFs (Fig. 3.9). Members of the WRKY and NAC TF families are regulated by oxidative species (Doll et al., 2020;

Jiang et al., 2020, 2017; Kneeshaw, 2016) and although the enriched TFs found are not amongst the partially rescued genes, other members of the WRKY and NAC TF families were also families identified as partial rescues (Table S1), indicating that in response to photo-oxidative stress NRX1 regulates TF activity both directly (*i.e.* by interacting with TFs) and indirectly (*i.e.* by inducing their expression via other TFs). Interestingly, WRKYs can induce the expression of TRX*h*5 during oxidative stress (Laloi et al., 2004) and TRX*h*5 was identified as a partial rescue by expression of *NRX1* in *cat2* mutants under photo-oxidative stress (Fig. 3.10), which implies NRX1 may recruit the activity of other TRXs via the regulation of TFs to help maintain redox homeostasis upon oxidative stress.

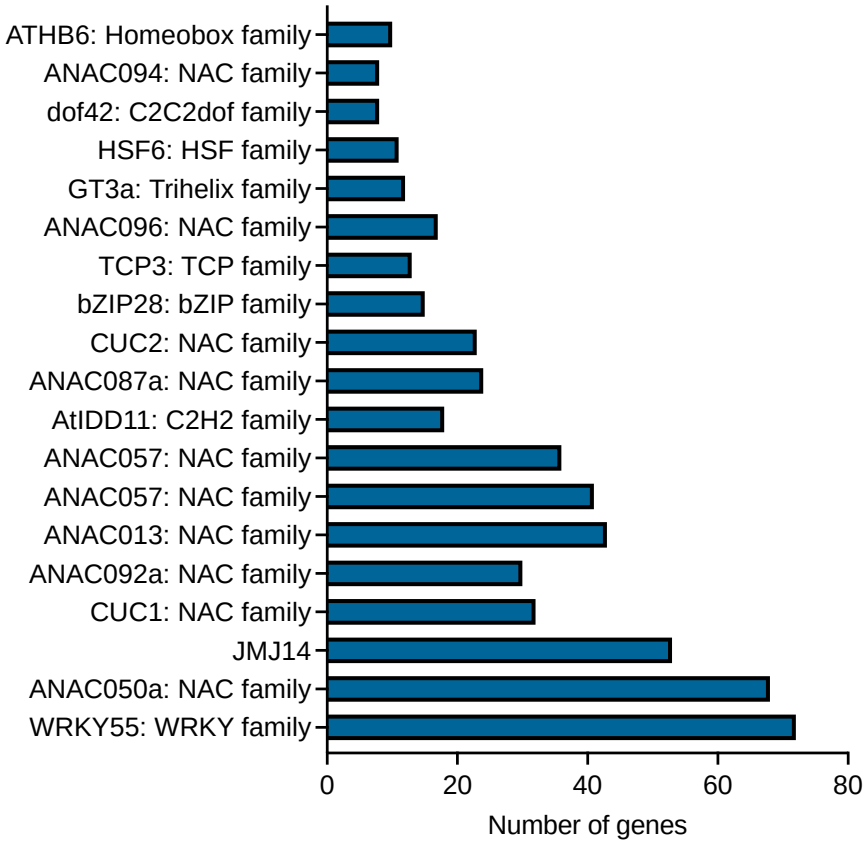

Figure 3. 9 Promoter analysis of rescued genes

Enrichment for transcription factor binding was analysed for the 182 genes identified as 'partial rescues' using Plant Regulomics (Ran et al. (2019)). Transcription factors shown are significantly enriched ($P < 0.05$).

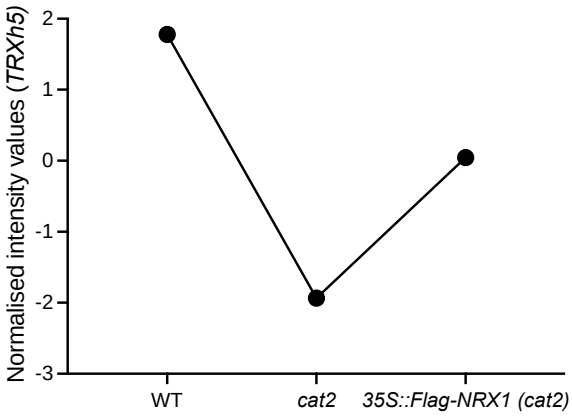

Figure 3. 10 Overexpression of *NRX1* in *cat2* mutants partially restores the expression of *TRXh5* during photo-oxidative stress

Expression profile of *TRXh5* in wild-type, *cat2*, and *35S::Flag-NRX1* plants following following RNA-seq on plants placed under light-stress conditions for 3 days.

3.3 Discussion

Redox signalling is crucial to many cellular processes. The different types and sources of ROS production provide different ROS signatures within the cell which may impact specific downstream signalling pathways. This chapter aimed to identify selectivity in the role of NRX1 in protecting oxidative signalling and the mechanism that enables this protection.

NRX1 was unable to rescue the immune phenotype of *pad2* mutants deficient in glutathione (Fig. 3.2B). GSH is one of the main antioxidants in the activation of defence genes and is involved in SA-mediated responses during immune signalling. SA responses in *pad2* mutants are blocked upon pathogen infection, due to the inability to induce expression of the SA biosynthesis enzyme *ICS1* (Dubreuil-Maurizi et al., 2011). As NRX1-mediated responses also appear to be SA-dependent, with

the *nrx1* autoimmune phenotype abolished in the *nrx1 ics1* double mutant (Kneeshaw et al., 2017), it could be suggested that NRX1 responses during pathogen infection are also impaired in the *pad2* mutant and therefore unable to restore immunity back to wild-type levels.

NRX1 was also unable to rescue electrolyte leakage in *pad2* mutants induced by treatment with MV (Fig. 3.3B). There are several possible explanations as to why this may be the case. Firstly, *nrx1* mutants exhibit elevated levels of total GSH compared to wild-type plants (Kneeshaw et al., 2017). Therefore, it could be suggested that the ability of NRX1 to protect cells against oxidative stress is at least in part GSH-dependent. This is supported by the identification of members of the Glutathione S-transferase (GST) family, *GSTU3* and *GSTU11*, as partially rescued genes in the RNA-seq conducted in this chapter (Table S1). This could suggest that in the absence of GSH, NRX1 is unable to rescue oxidative signalling. Furthermore, in the glutathione-ascorbate pathway, the GSH/glutathione reductase (GR) system is required for the reduction of dehydroascorbate reductase (DHAR), which was also found to be a target of NRX1 (Foyer and Noctor, 2011; Kneeshaw et al., 2017). Therefore, in the absence of GSH, NRX1 may fail to provide the reducing power required to facilitate the activity of other targets in this pathway. The TRX system can act as a backup for the GSH system (Marty et al., 2009; Meyer et al., 2012, 2008; Tan et al., 2010). However, based on the large number of TRX members in *Arabidopsis*, it is likely that only specific TRXs are able to perform this role, a notion explored further in Chapter 4.

Similar to *pad2,* NRX1 was unable to rescue the immune response in *cat2* mutants (Fig. 3.2A). The role of NRX1 in rescuing the immune response in different ROS accumulating mutants was initially tested as CAT2 was identified as a substrate of NRX1 in response to pathogen infection (Kneeshaw et al., 2017). This suggests

that the role of NRX1 in the immune system is likely dependent on its ability to maintain CAT activity. Yuan et al. (2017) reported that CAT2 is an SA-binding protein and may function as an SA receptor, whereby SA inhibited its H_2O_2 scavenging activity. Decreased activity of SA-bound CAT2 and associated increases in H_2O_2 levels inhibited auxin and jasmonic acid (JA) biosynthesis enzymes, thus alleviating the negative effects of these hormones on SA-mediated resistance to biotrophic pathogens. Interestingly, *nrx1* mutants constitutively express SA-responsive genes (Kneeshaw et al., 2017) and exhibit an impaired response to JA (discussed further in Chapter 5). Therefore, in wild-type plants, NRX1 may act antagonistically in response to SA-mediated inhibition of CAT2 activity by maintaining some level of CAT2 antioxidant activity, which would limit increases in H_2O_2 concentrations. Consequently, in *cat2* mutants, NRX1 cannot maintain CAT2 activity, allowing accumulation of SA-induced H_2O_2.

Whilst overexpression of NRX1 was unable to restore immunity in *cat2* and *pad2*, it was able to rescue the electrolyte leakage phenotype of *cat2* mutants (Fig 3.3A), which suggests that accumulation of ROS in *cat2* mutants may oxidise proteins that are substrates of NRX1. Indeed, NRX1 formed more mixed disulphide bonds with substrates in the *cat2* mutant compared to WT (Fig 3.4). In addition to CAT2, NRX1 was reported to interact with APX1 and a DHAR (Kneeshaw et al., 2017). There is certain extent of redundancy amongst peroxidases, for example APX activity increases in the absence of CAT2 (Mhamdi et al., 2010a). Therefore, it is plausible that in absence of CAT2, overexpression of NRX1 enables it to promote the activities of these alternative antioxidant enzymes.

The rescue of the electrolyte leakage phenotype in *cat2* but not *pad2* mutants shows that NRX1 is able to selectively rescue oxidative signalling not only in different ROS accumulating backgrounds, but also between different stresses that cause

oxidative stress. This supports the hypothesis that different sources of ROS may have specific targets, which in turn are guarded by specific oxidoreductases. This is in accordance with previous work showing that during the immune response, TRX*h*5 selectively rescues compromised immunity in *nox1* mutants that accumulate free NO, but not in *gsnor1* mutants that accumulate GSNO. This was found to be due to its selective de-nitrosylation of protein-SNOs (Kneeshaw et al., 2014).

Intriguingly, NRX1 overexpression appears to rescue photo-oxidative stress exhibited in *cat2* mutants via rescue of ROS-induced transcriptional changes (Fig. 3.5). While the electron flow during photosynthesis is considered the main source of ROS during light stress, studies have shown that H_2O_2 exits the chloroplast during light stress (Mubarakshina et al., 2010). In addition to retrograde signalling from plastids to the nucleus, chloroplast-derived H_2O_2 is important for intracellular signalling (Cui et al., 2019; Exposito-Rodriguez et al., 2017). Indeed, the genetically encoded biosensors Grx1-roGFP2 and roGFP2-Orp1 that measure the cellular glutathione redox potential and endogenous H_2O_2, respectively, were used to demonstrate that MV-induced chloroplastic ROS generation, which led to subsequent oxidation in the cytosol and mitochondria (Ugalde et al., 2021). Therefore, downstream oxidation could affect cytosolic and nuclear targets of NRX1, thereby recruiting its activity during photo-oxidative stress. Interestingly, many of the partial rescued genes encode for 'redox-related' enzymes, including GSTs, methionine sulfoxide reductases and TRX*h*5 (Table S1). This indicates that NRX1 may promote the expression of genes encoding for antioxidant enzymes to protect against undesired redox modifications and maintain general redox homeostasis during light stress. Engineering the Grx1-roGFP2 and roGFP2-Orp1 sensors into *cat2* and *35S::Flag-NRX1 (cat2)* would be an interesting method to determine if NRX1 is able to rescue altered cellular oxidation induced by light in *cat2* mutants.

As there was not a 'low-light' control, the partially rescued genes were compared to the Zandalinas et al (2019) study as the authors tested the induction of genes in response to high light. Whilst some of the partially rescued genes overlapped, the overlap was not statistically significant. Although this indicates that the partially rescued genes are not specific to photo-oxidative stress, there are differences between the conditions tested in this chapter and the Zandalias study which could explain the non-significant overlap. For example, Zandalinas et al. looked at initial induction up to 8 minutes and used a higher light intensity (1000 µmol $m^{-2}s^{-1}$) than tested in this chapter, so the two datasets are not entirely comparable. To confirm that the DEGs and partially rescued genes are indeed light-responsive, ideally the RNAseq should be repeated with a lower light intensity condition. Nevertheless, the partially rescued genes still show that overexpression of NRX1 in the *cat2* mutant is able to partially rescue a subset of genes that are altered between wild-type plants and the redox-sensitive mutant *cat2*.

Upon analysis of promoter regions of rescued genes identified by RNA-seq, different TF families were identified (Fig. 3.9). Many TFs in different organisms are known to be redox controlled during development and stress responses, with several TFs and transcription activators being regulated by the TRX family (Dietz, 2014; Kneeshaw, 2016; Li et al., 2009; Tada et al., 2008). WRKY55 showed binding enrichment for the highest number of partially rescued genes (Fig. 3.9). WRKY55 has been implicated in regulating the biosynthesis of ROS during leaf senescence (Wang et al., 2020) and recently an integrated gene regulatory network identified WRKY55 as a novel TF that may have a function in oxidative signalling (De Clercq et al., 2021). Interestingly, expression of WRKY55 is elevated in response to light stress and is NO- and GSNO-responsive (Begara-Morales et al., 2014b; Imran et al., 2018; Zandalinas et al., 2019). Several members of the WRKY family are SNO targets, with *S*-

nitrosylation affecting their DNA binding ability (Kneeshaw, 2016). TRX*h*5 has been shown to denitrosylate WRKY TFs, consequently reversing the effects of *S*-nitrosylation on WRKY binding affinity (Kneeshaw, 2016). NRX1 also exhibits denitrosylation activity (Capilla Mata-Perez, Lucas Frungillo et al., unpublished), which suggests that NRX1 could potentially target WRKY55 during photo-oxidative stress. Additionally, 10 members of the NAC transcription factor family were identified (Fig. 3.9). The NAC TF family is one of the largest in Arabidopsis and several, including ANAC013 and ANAC092 have been identified with roles in ROS signalling (Balazadeh et al., 2010; De Clercq et al., 2013). For example, ANAC013 was found to be involved in mitochondrial retrograde signalling and tolerance to oxidative stress, which is of importance during photo-oxidative stress conditions. Both ANAC013 and ANAC092 are also differentially regulated during light stress (Huang et al., 2019; Zandalinas et al., 2019) and could therefore also be plausible targets of NRX1 during photo-oxidative stress. Thus, NRX1 may promote tolerance to photo-oxidative stress by ensuring TF activities are maintained in a ROS-rich environment, in turn maintaining oxidative signalling.

Interestingly, *TRXh5* was also identified as a partially rescued gene (Fig. 3.10 and Table S1) and can be induced by identified WRKY TFs. NTRs are largely responsible for the full reduction of conventional TRXs, however the rescue of TRX*h*5 expression in this chapter suggests that some TRXs may also regulate each other's activities, e.g. NRX1 maintains TRX*h*5 activity or *vice versa*. Indeed, Kneeshaw (2016) reported that NRX1 and TRX*h*5 exhibit mixed disulphide interactions, suggesting reciprocal reduction activities. As no other conventional TRXs were identified as rescues, this further suggests that only specific TRXs are involved in protection against oxidative stress in CAT-deficient plants. Although this chapter provides new insight into TRX specificity, the extent of redundancy and/or specificity

across the TRX family remains largely unknown and will be explored further in chapter 4.

Chapter 4

Uncovering selectivity of Thioredoxin enzymes in regulating plant stress responses

4.1 Background

Reactive thiol groups of cysteine residues can undergo a range of oxidative modifications. These modifications can be rendered into specific protein functions, which in turn dictate downstream cellular signalling. Many ROS/RNS-induced Cys modifications, such as those caused by H_2O_2, O_2^-, and NO, are reversible and substrate specific, enabling an abundance of redox-mediated signalling pathways from just a few molecules (D'Autréaux and Toledano, 2007; Umbreen et al., 2018). The reversible nature of these modifications adds an additional layer of regulation to redox-mediated signalling. Reversibility is enabled by the action of (oxido)reductases, particularly the Thioredoxin family.

Compared to other eukaryotes, plant genomes encode for a large number of TRXs, with over 40 TRX/TRX-like enzymes characterised in *Arabidopsis* (Meyer et al., 2012, 2008). As there are so many TRXs found in plants, it has been postulated for some time that TRXs have specific substrate repertoires (Bleau and Spoel, 2021; Mata-Pérez and Spoel, 2019), adding to the complexity of the 'redox code'. This is particularly intriguing for TRXs that share the same subcellular location, such as the *h*-type family of conventional TRXs, which are localised to the cytosol or mitochondria (Gelhaye et al., 2004). The *Arabidopsis* TRX-*h* family is made up of 8 members, which are further divided into 3 subgroups (Gelhaye et al., 2004). Many of the TRX *h* members, particularly in subgroup 1, are found in the cytosol (Gelhaye et al., 2004), suggesting they may each have separate specific functions. Indeed, this has been reported for TRX*h*5. Overexpression of *Arabidopsis* TRX*h*5 in two different protein–SNO accumulating mutant backgrounds, *gsnor1* and *nox1*, that overaccumulate GSNO and free NO, respectively, showed that in response to *P. syringae* infection, TRX*h*5 selectively rescued immune deficiencies in *nox1* but not *gsnor1* (Kneeshaw

et al., 2014). Even though TRX*h*5 localised to similar subcellular locations in both mutants, it only decreased protein–SNO concentrations in *nox1* mutants, indicating TRX*h*5 selectively denitrosylated protein-SNO. These findings suggest that TRX*h*5 can distinguish between protein–SNO derived from free NO as opposed to GSNO.

So, does the selectivity of TRX*h*5 extend to other TRX-*h* members? In this chapter the ability and selectivity TRX-*h* members in rescuing oxidative stress and the immune response in different ROS-accumulating mutants was surveyed. The ability of TRXs to reverse phenotypes of *cat2* and *pad2* mutants showed remarkable selectivity not only between mutants, but also in response to different stresses. This shows the vast potential of specific roles TRXs play in stress signalling cascades.

4.2 Results

4.2.1 TRX*h*1 may function as a backup for glutathione during immunity

TRX*h*1 is a conventional TRX that is part of Subgroup 1 of the *h* family (Gelhaye et al., 2004). TRX*h*1 displays reductase activity *in vitro* and has shown selectivity in its interaction with substrates in different subcellular locations (Henne et al., 2015; Huang et al., 2018). However, little is known about potential functional roles of TRX*h*1 in stress responses. Mutant *cat2* and *pad2* plants were transformed with *35S::Flag-TRXh1* (Fig. 4.1) and infected with *Psm* to determine if TRX*h*1 could restore immunity. TRX*h*1 was unable to restore immunity in *cat2* mutants but was able to rescue immunity back to wild-type levels in *pad2* (Fig. 4.2). This suggests that TRX*h*1 selectively restores immunity by acting as a back-up system for glutathione.

Additionally, the ability of TRX*h*1 to rescue MV-induced electrolyte leakage was also tested. Leaves of wild-type, *cat2, pad2* and *35S::Flag-TRXh1* expressed in

both mutants were infiltrated with 10 μM MV and electrolyte leakage was measured over 24 hours. As described in Chapter 3, both *cat2* and *pad2* exhibited enhanced electrolyte leakage compared to wild-type plants after MV treatment, but the expression of *35S::Flag-TRXh1* in both mutants was unable to rescue this phenotype (Fig 4.3). This indicates that TRX*h*1 does not play an obvious role in MV-induced oxidative stress in ROS accumulating mutants.

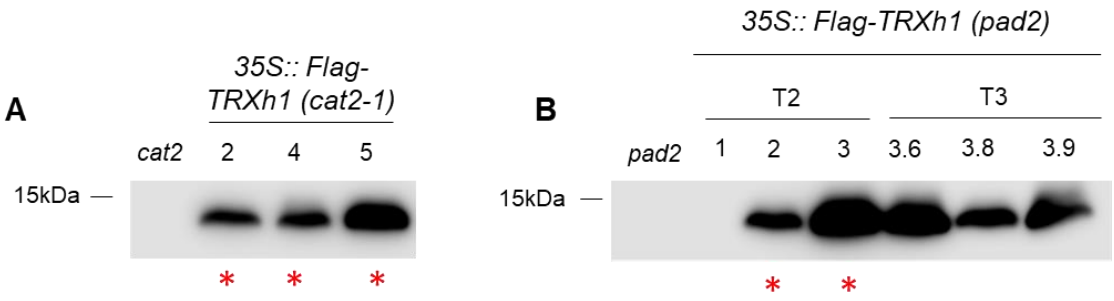

Figure 4. 1 Western blot of *35S:Flag-TRXh1* expressed in *cat2* and *pad2* mutants

Mutant *cat2* **(A)** and *pad2* **(B)** plants were transformed with Flag-tagged TRX*h*1 driven by the constitutive 35S promoter (*35S::Flag-TRXh1*). Expression of Flag-TRXh1 was detected with an antibody against the Flag tag. Asterisks indicates lines used.

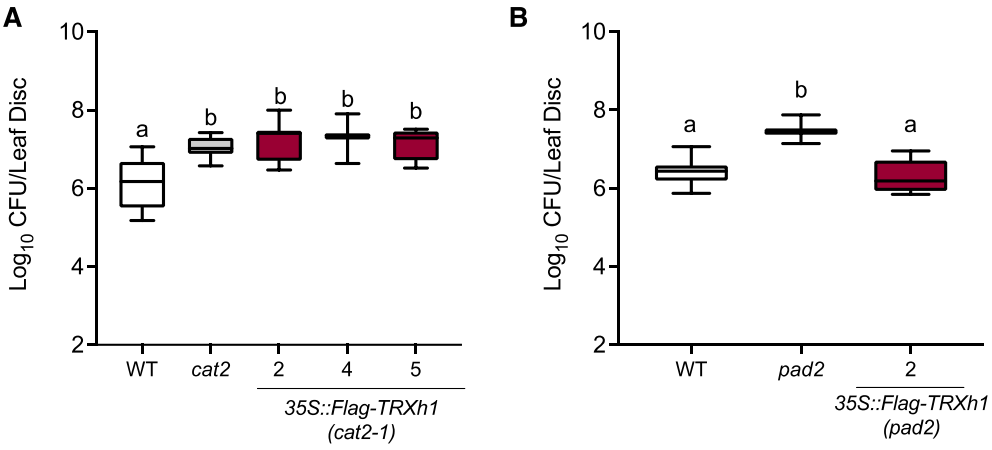

Figure 4. 2 TRXh1 selectively rescues the immune phenotype in *pad2* mutants but not *cat2* mutants

Plants were infected with *Psm* ES4326 (OD_{600} = 0.002) and pathogen grown was assessed after 3 days. Different letters indicate statistical significance (ANOVA, Tukey p <0.05) CFU, colony forming units (n=8).

A second independent line for *35S::Flag-TRXh1 (pad2)* can be found in the appendix (Fig S3)

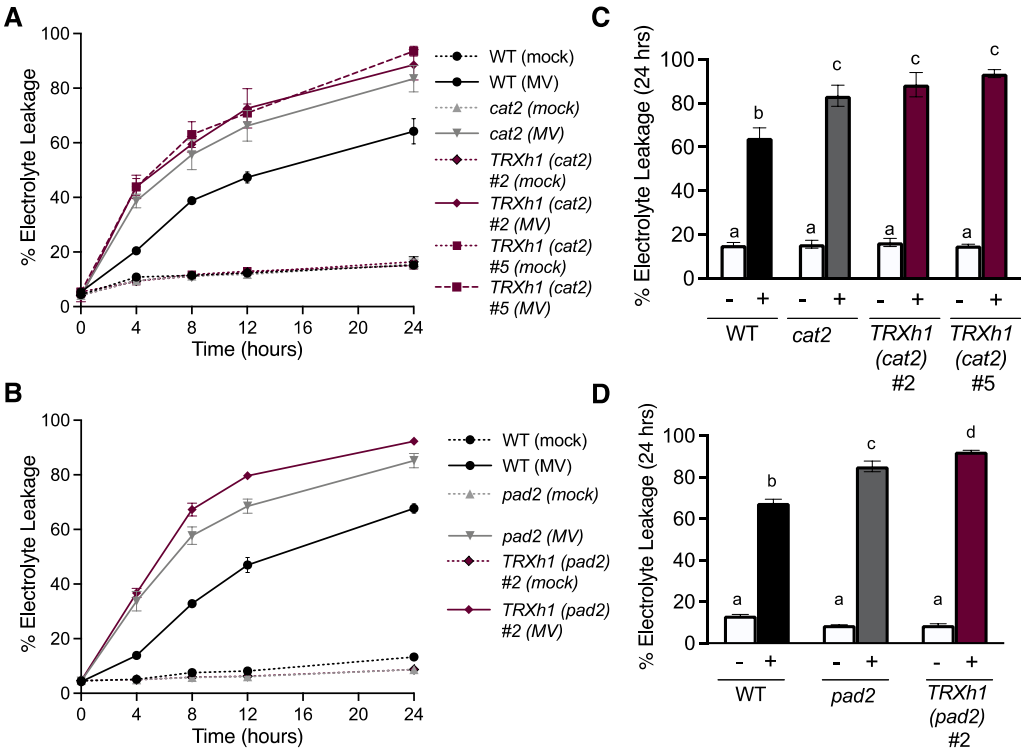

Figure 4. 3 TRXh1 is unable to rescue enhanced electrolyte leakage in *cat2* and *pad2* mutants

Plants were infiltrated with 10μM of the oxidative stressor methyl viologen (MV) or water (mock). Electrolyte leakage was measured at indicated timepoints over a period of 24 hours and are presented as a percentage of the total electrolytes. Error bars indicate standard error (n=3).

(A) and **(B)** Electrolyte leakage over 24 hours. **(C)** and **(D)** 24 hour time point only Different letters indicate statistical significance (ANOVA, Tukey p <0.05). A second independent line for *35S::Flag-TRXh1 (pad2)* can be found in the appendix (Fig S3)

4.2.2 TRX*h*2 acts selectively depending on the type of stress

TRX*h*2 is a conventional TRX that is part of Subgroup 2 of the *h* family, characterised by an N-terminal protein extension (Gelhaye et al., 2004) and a glycine as the second amino acid that is predicted to be myristolated (Traverso et al., 2013). It has been found to localise to the mitochondria, endoplasmic reticulum and cytoplasm (Meng et al., 2010; Traverso et al., 2013) and plays a role in the regulation of mitochondrial photorespiratory metabolism (da Fonseca-Pereira et al., 2020; Daloso et al., 2015). Expression of *TRXh2* reportedly responds to very few stresses and hormonal treatments, with the exception of *Hyaloperonospora parasitica* infection (Belin et al., 2015), and it is not known how TRX*h*2 acts in the absence of key antioxidants. Expression of *35S::Flag-TRXh2* in *cat2* and *pad2* mutants (Fig. 4.4) showed selectivity in rescuing the immune response. *35S::Flag-TRXh2* was unable to restore the immune response in *cat2* mutants, whereas it was able to restore immunity back to wild-type levels in *pad2* mutants (Fig. 4.5). In contrast, when treated with MV and assessed for the electrolyte leakage response, TRX*h*2 was able to partially prevent electrolyte leakage in *cat2* mutants similar to NRX1 (chapter 3), but was unable to rescue electrolyte leakage when expressed in *pad2* mutants (Fig. 4.6). Thus, it can be concluded that TRX*h*2 acts selectively depending on the source of ROS accumulation and possibly type of ROS encountered.

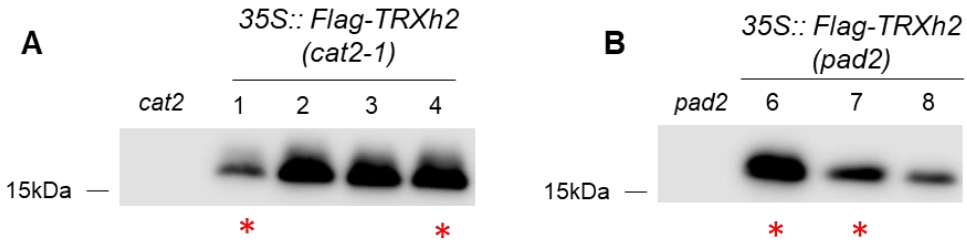

Figure 4. 4 Western blot of *35S:Flag-TRXh2* expressed in *cat2* and *pad2* mutants

Mutant *cat2* **(A)** and *pad2* **(B)** plants were transformed with Flag-tagged TRX*h*2 driven by the constitutive 35S promoter (*35S::Flag-TRXh2*). Expression of Flag-TRXh2 was detected with an antibody against the Flag tag. Asterisks indicates lines used.

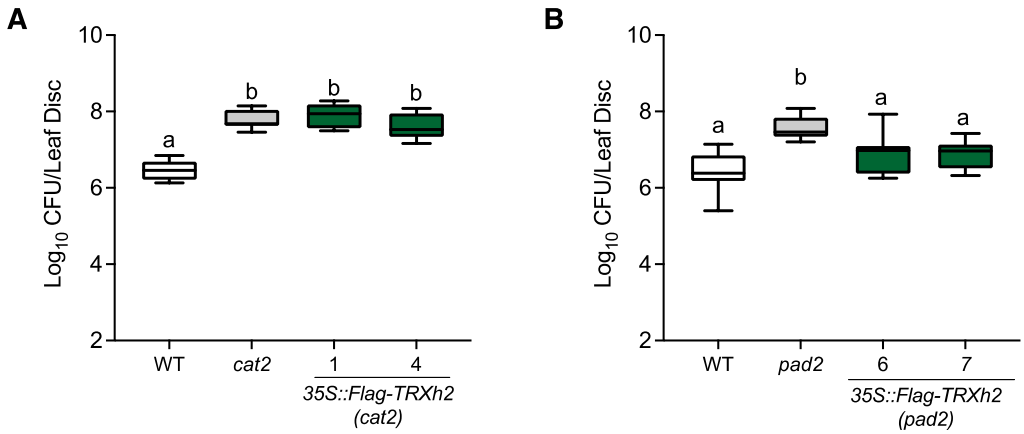

Figure 4. 5 TRXh2 selectively rescues the immune phenotype *pad2* mutants but not in *cat2* mutants

Plants were infected with *Psm* ES4326 (OD_{600} = 0.002) and pathogen grown was assessed after 3 days. Different letters indicate statistical significance (ANOVA, Tukey p <0.05) CFU, colony forming units (n=8).

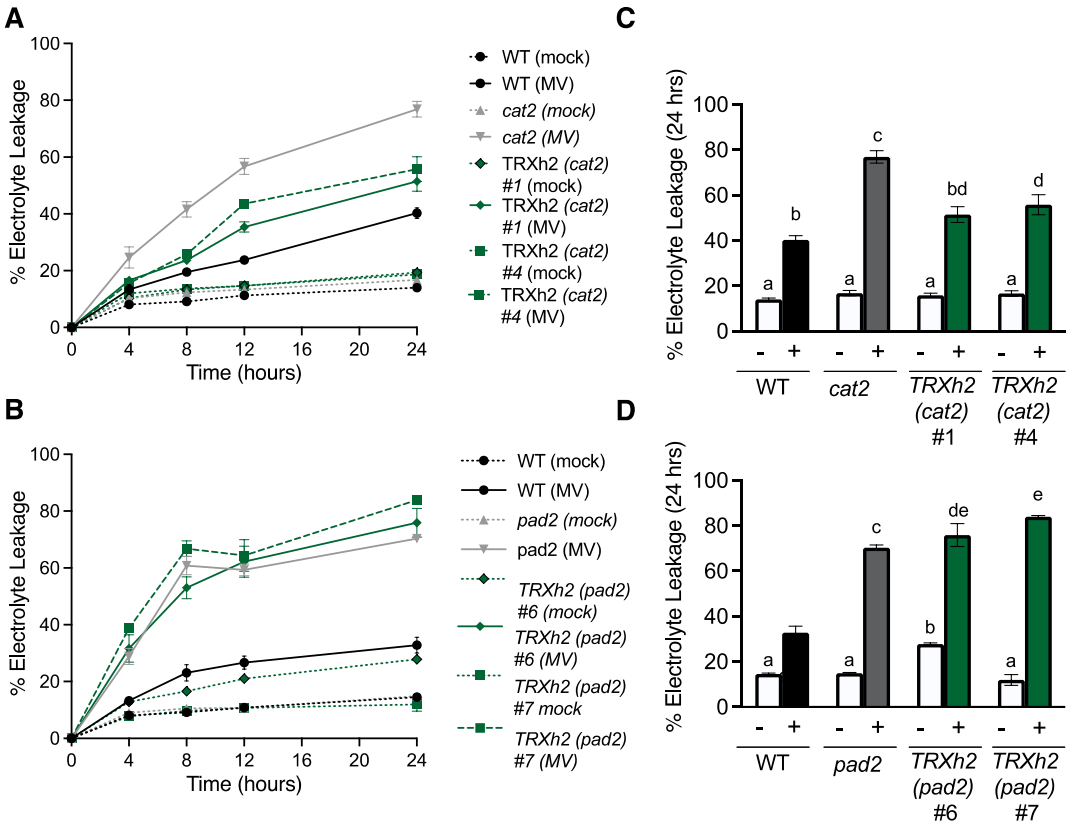

Figure 4. 6 TRXh2 selectively rescues enhanced electrolyte leakage in *cat2* mutants, but not in *pad2* mutants

Plants were infiltrated with 10μM of the oxidative stressor methyl viologen (MV) or water (mock). Electrolyte leakage was measured at indicated timepoints over a period of 24 hours and are presented as a percentage of the total electrolytes. Error bars indicate standard error (n=3).

(A) and **(B)** Electrolyte leakage over 24 hours. **(C)** and **(D)** 24 hour time point only Different letters indicate statistical significance (ANOVA, Tukey p <0.05).

4.2.3 Like TRX*h*1, TRX*h*3 restores the immune phenotype specifically in absence of glutathione

TRX*h*3 is also in subgroup 1 of the TRX-*h* family and is one of the best studied cytosolic TRX family members (Gelhaye et al., 2004). It displays constitutive expression and plays an important role in plant immunity by reducing the disulphide bonds of NPR1, leading to its monomerisation and translocation to the nucleus for immune signalling (Tada et al., 2008). TRX*h*3 is also able to reduce oxidised glutathione (GSSG) back to the reduced form (GSH) in the absence of glutathione reductase (Marty et al., 2009). However, it is not known if it can act as a backup for the GSH system in the absence of GSH itself. Mutant *cat2* and *pad2* plants were transformed with *35S::Flag-TRXh3* (Fig. 4.7) and infected with *Psm* to determine if TRX*h*3 could restore immunity. Infection with *Psm* was unable to restore immunity in *cat2* mutants but was able to rescue immunity in *pad2* mutants (Fig. 4.8). This indicates that TRX*h*3 selectively restores the susceptible immune phenotype of back to wild-type levels by acting as a back-up system for glutathione.

Like TRX*h*1, MV-induced electrolyte leakage showed that TRX*h*3 was unable to rescue enhanced electrolyte leakage in either *cat2* or *pad2* mutants (Fig 4.9), indicating that TRX*h*3 acts as a selective back-up system during the immune response rather than a general stress response.

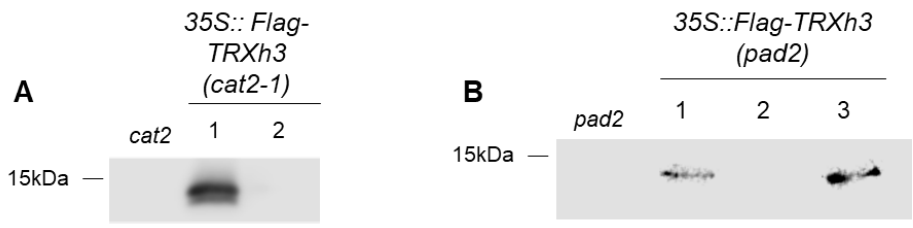

Figure 4. 7 Western blot of *35S::Flag-TRXh3* expressed in *cat2* and *pad2* mutants

Mutant *cat2* **(A)** and *pad2* **(B)** plants were transformed with Flag-tagged TRX*h*3 driven by the constitutive 35S promoter (*35S::Flag-TRXh3*). Expression of Flag-TRXh3 was detected with an antibody against the Flag tag. Expression of a second independent line for *35S::Flag-TRXh3 (cat2)* can be found in the appendix.

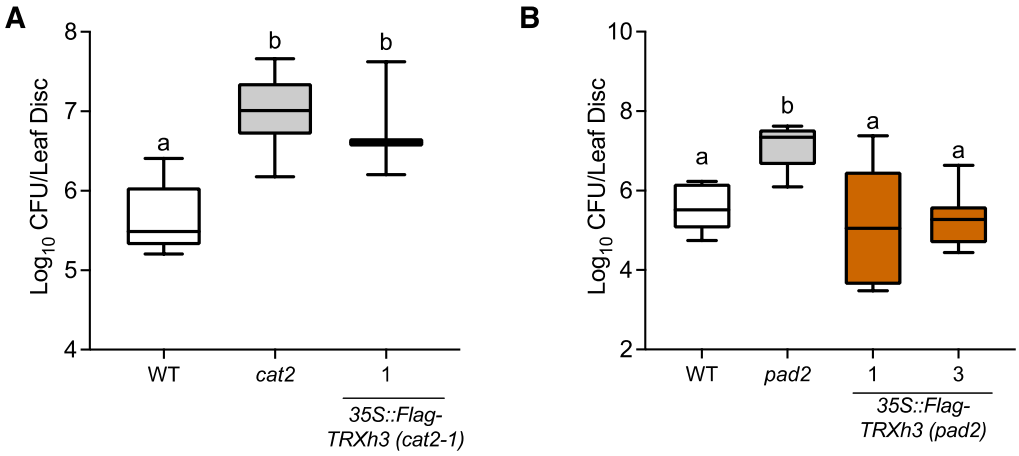

Figure 4. 8 TRXh3 selectively rescues the immune phenotype in *pad2*, but not *cat2*

Plants were infected with *Psm* ES4326 (OD_{600} = 0.002) and pathogen grown was assessed after 3 days. Different letters indicate statistical significance (ANOVA, Tukey p <0.05) CFU, colony forming units (n=8). A second independent line for *35S::Flag-TRXh3 (cat2)* can be found in the appendix

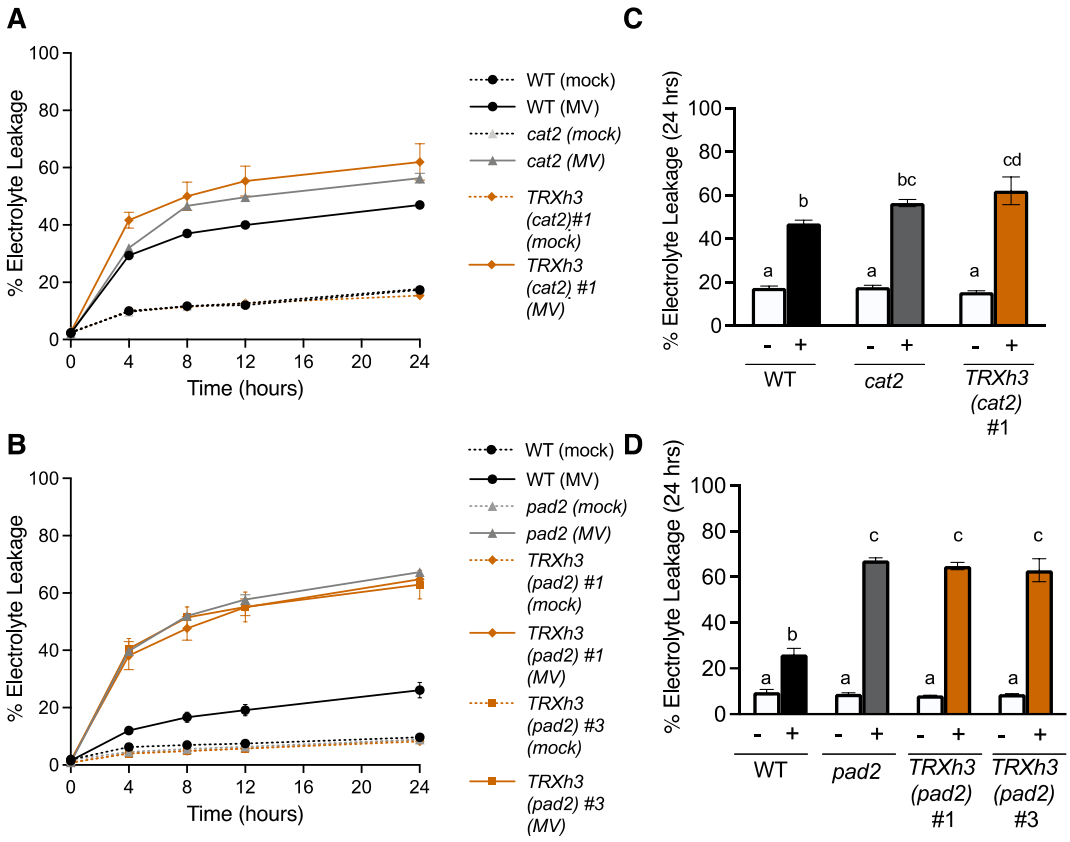

Figure 4. 9 TRXh3 does not rescue enhanced cell death in *cat2* or *pad2* mutants

Plants were infiltrated with 10μM of the oxidative stressor methyl viologen (MV) or water (mock). Electrolyte leakage was measured at indicated timepoints over a period of 24 hours and are presented as a percentage of the total electrolytes. Error bars indicate standard error (n=3).

(A) and **(B)** Electrolyte leakage over 24 hours. **(C)** and **(D)** 24 hour time point only. Different letters indicate statistical significance (ANOVA, Tukey p <0.05). A second independent line for *35S::Flag-TRXh3 (cat2)* can be found in the appendix

4.2.4 TRX*h*4 also acts selectively depending on the type of oxidative stress and source

TRX*h*4 is the third member of subgroup 1 (Gelhaye et al., 2004). Not much is known about TRX*h*4, but it may play a role in the cell cycle (Menges et al., 2002). To determine any roles of TRX*h*4 in rescuing stress responses in ROS-accumulating mutants, *35S::Flag-TRXh4* was transformed into *cat2* and *pad2* mutants (Fig 4.10). To assess the ability of TRX*h*4 to restore immune phenotypes, wild-type, *cat2, pad2* and *35S::Flag-TRXh4* expressed in both mutants were infected with *Psm* and bacterial growth was assessed. Both *cat2* and *pad2* showed an increase in susceptibility to *Psm* compared to wild-type, but the expression of *35S::Flag-TRXh4* in these mutants was only able to consistently restore immunity in *pad2* plants, not in *cat2* plants (Figure 4.11).

In addition to immunity, the ability of TRX*h*4 to rescue MV-induced electrolyte leakage was tested. Although TRX*h*4 was unable to restore immunity in *cat2*, it was able to rescue MV-induced electrolyte leakage back to almost wild-type levels (Fig. 4.12A). *35S::Flag-TRXh4* in *pad2* showed inconclusive results in rescuing the electrolyte leakage phenotype, as two independent lines gave different results (i.e. one rescued and the other did not)(Fig. 4.12B), possibly due to differing transgene insertion sites in the genome. Because a third independent line was unavailable, it remains unclear if TRX*h*4 can restore MV-induced electrolyte leakage responses in *pad2* mutants. Nevertheless, the results of TRX*h*4 expressed in different ROS accumulating mutants indicate that TRX*h*4 does show selectivity in rescuing oxidative stress induced by different stresses.

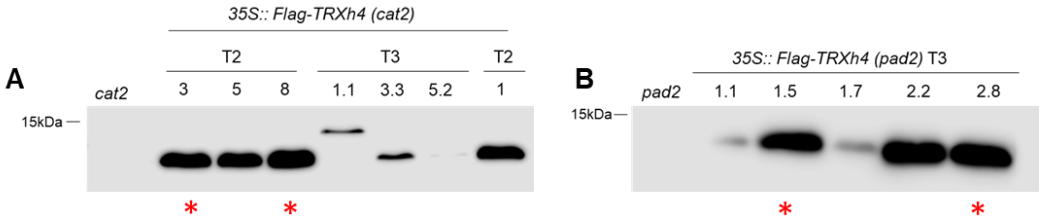

Figure 4. 10 Western blot of *35S::Flag-TRXh4* expressed in *cat2* and *pad2* mutants

Mutant *cat2* **(A)** and *pad2* **(B)** plants were transformed with Flag-tagged TRX*h*4 driven by the constitutive 35S promoter (*35S::Flag-TRXh4*). Expression of Flag-TRXh4 was detected with an antibody against the Flag tag.

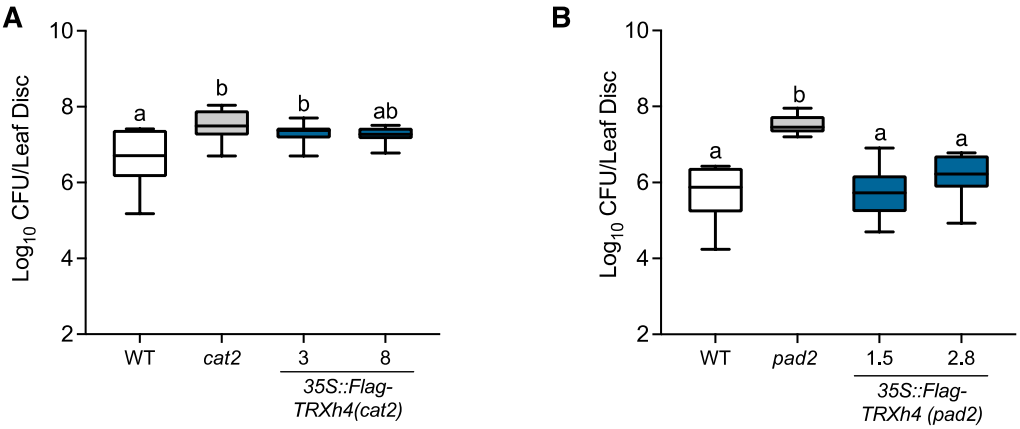

Figure 4. 11 TRXh4 selectively rescues the immune phenotype in *pad2*, but not *cat2*

Plants were infected with *Psm* ES4326 (OD_{600} = 0.002) and pathogen grown was assessed after 3 days. Different letters indicate statistical significance (ANOVA, Tukey p <0.05) CFU, colony forming units (n=8).

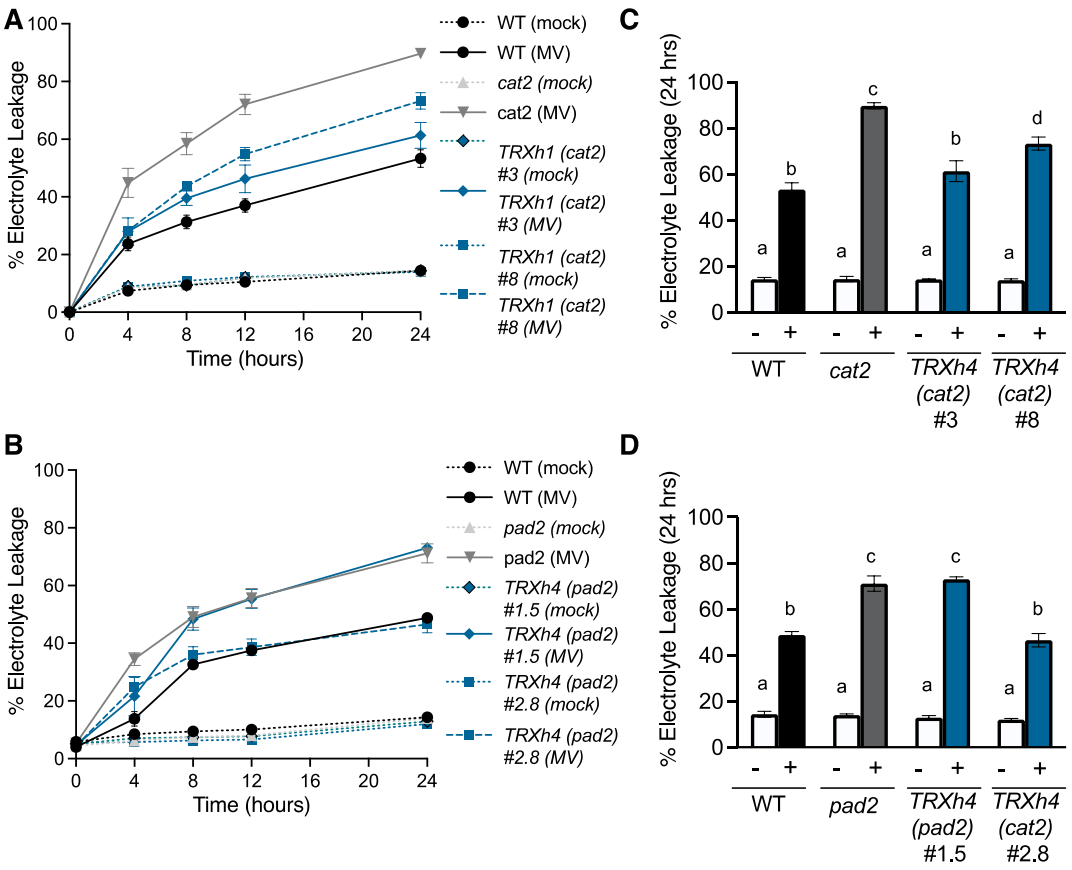

Figure 4. 12 TRXh4 selectively rescues enhanced electrolyte leakage in *cat2* and *pad2* mutants

Plants were infiltrated with 10μM of the oxidative stressor methyl viologen (MV) or water (mock). Electrolyte leakage was measured at indicated timepoints over a period of 24 hours and are presented as a percentage of the total electrolytes. Error bars indicate standard error (n=3).

(A) and **(B)** Electrolyte leakage over 24 hours. **(C)** and **(D)** 24 hour time point only. Different letters indicate statistical significance (ANOVA, Tukey p <0.05)

4.2.5 TRX*h*5 prevents oxidative cell death in absence of catalase

TRX*h*5 is the final member of the TRX-*h* subgroup 1 (Gelhaye et al., 2004) and is arguably one of the most well-studied TRX-*h* members. TRX*h*5 is highly pathogen-inducible and is required for the reduction of disulphide bonds within cytosolic NPR1 oligomers (Kneeshaw et al., 2014; Laloi et al., 2004; Tada et al., 2008). It also shows selective denitrosylation activity during the immune response, supporting the hypothesis that TRXs have distinct substrate repertoires (Kneeshaw et al., 2014). In addition to controlling stress responses, TRX*h*5 was shown to maintain growth and development via reduction of the transcription factor BRASSINAZOLE-RESISTANT1 (BZR1) (Tian et al., 2018). Moreover, TRX*h*5 was identified in chapter 3 of this thesis as a gene partially rescued by NRX1 overexpression in *cat2* mutants during light stress (Fig. 3.10, Table S1). This suggested that TRXs may regulate each other to protect cells against oxidative stress. Therefore, *35S::Flag-TRXh5* was expressed in *cat2* and *pad2* mutants (Fig. 4.13) to determine if TRX*h*5 restores tolerance to oxidative stress similar to NRX1. In contrast to the previous assays of this chapter, the *cat2* mutant suddenly displayed more resistance to *Psm* than wild-type, similar to previous reports (Chaouch et al., 2010; Yuan et al., 2017). As experiments with TRX*h*5 were interrupted for an extended period of time during the COVID-19 pandemic, it is possible that unknown parameters of the plant growth conditions changed in the meantime. Unfortunately, it was inconclusive if TRX*h*5 restored the immune phenotype of *cat2* back to wild-type levels, as one independent line (#1) appeared to restore immunity, while a second independent line (#3) did not (Fig. 4.14). Similarly, it was inconclusive if TRX*h*5 rescued immunity in the *pad2* mutants, with one independent line (#2) restoring resistance back to wild-type levels, whereas a second independent line (#4) tested did not (Fig. 4.14). Therefore, it remains unclear if TRX*h*5 restored immune phenotypes in *cat2* and *pad2* mutants.

By comparison, the ability of TRX*h*5 to rescue electrolyte leakage responses was very clear. After MV treatment, expression of *35S::Flag-TRXh5* was able to rescue electrolyte leakage to near wild-type levels in *cat2* mutants, but not in *pad2* mutants (Fig. 4.15). Together, these results demonstrate that like NRX1 (chapter 3), members of the TRX *h* family show selectivity in rescuing MV-induced phenotypes in ROS accumulating mutants.

Taken together, the phenotypic data presented here demonstrate that cytosolic TRX-*h* members show specificity in rescuing oxidative signalling responses, not only in different ROS accumulating mutants, but also dependent on different sources of stress (Table 4.1).

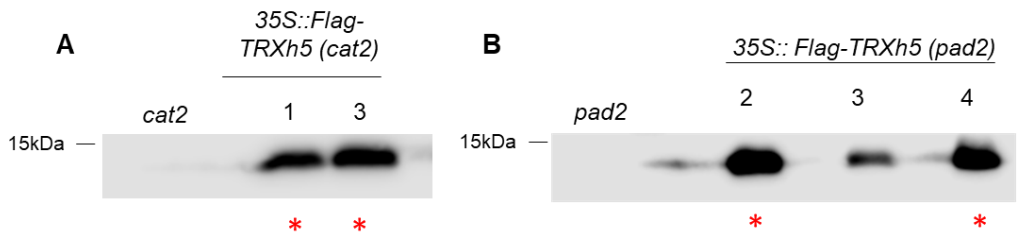

Figure 4. 13 Western blot of *35S::Flag-TRXh5* expressed in *cat2* and *pad2* mutants

Mutant *cat2* **(A)** and *pad2* **(B)** plants were transformed with Flag-tagged TRX*h*5 driven by the constitutive 35S promoter (*35S::Flag-TRXh5*). Expression of Flag-TRXh5 was detected with an antibody against the Flag tag.

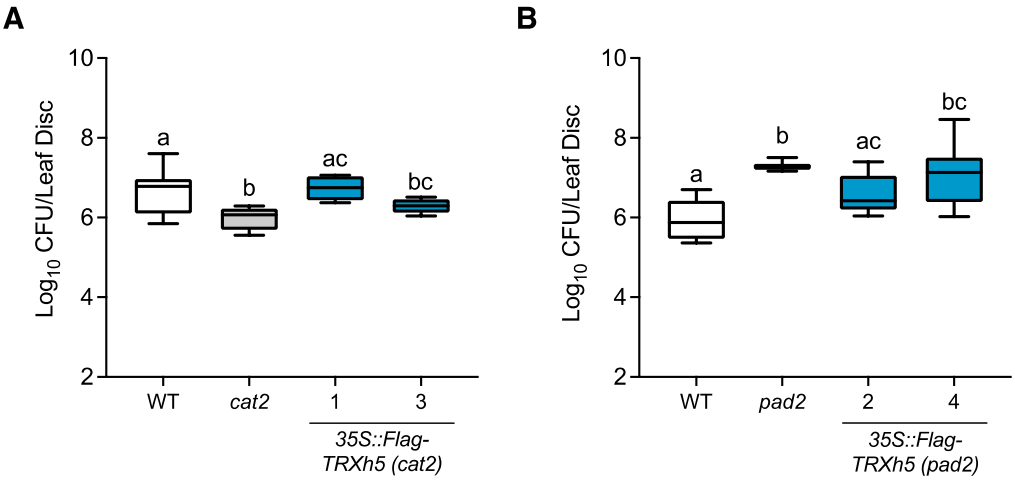

Figure 4. 14 It is inconclusive as to whether TRXh5 is able to rescue the immune phenotype of *cat2* or *pad2* mutants

Plants were infected with *Psm* ES4326 (OD_{600} = 0.002) and pathogen grown was assessed after 3 days. Different letters indicate statistical significance (ANOVA, Tukey p <0.05) CFU, colony forming units (n=8).

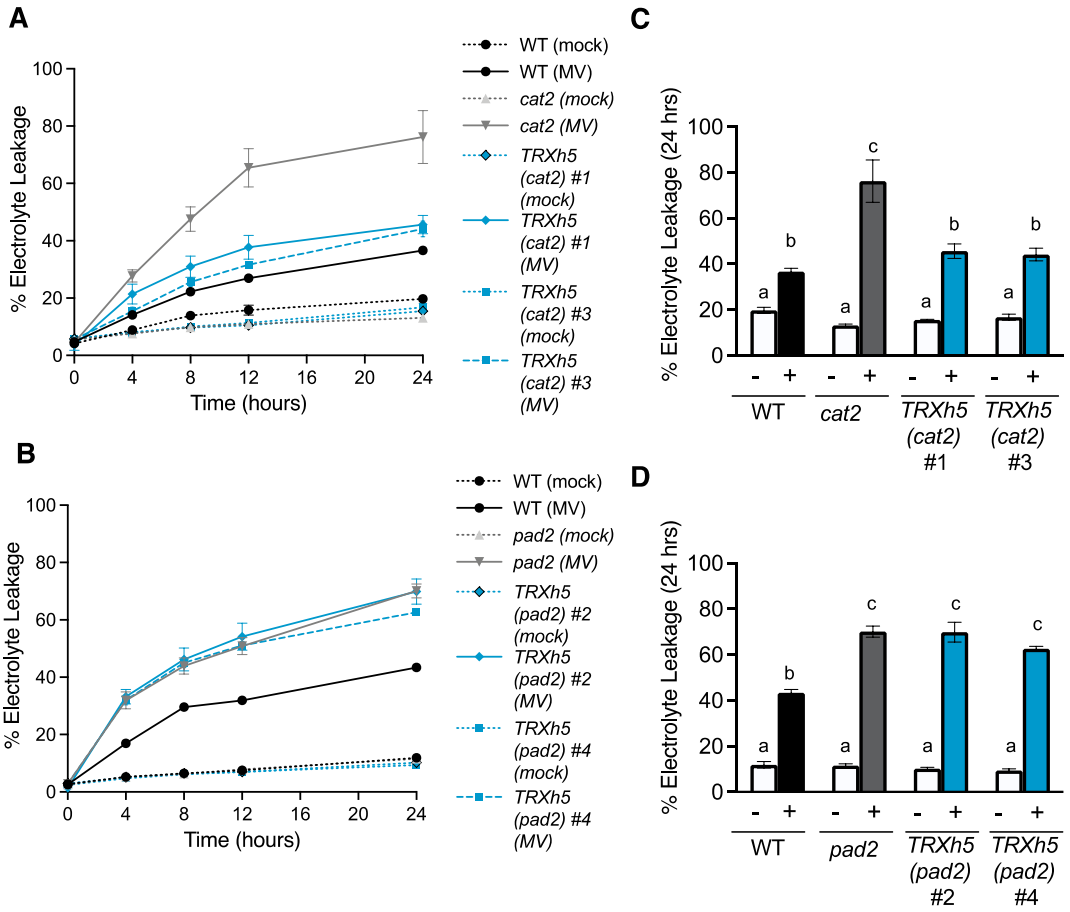

Figure 4. 15 TRXh5 selectively rescues enhanced electrolyte leakage in *cat2* but not *pad2* mutants

Plants were infiltrated with 10μM of the oxidative stressor methyl viologen (MV) or water (mock). Electrolyte leakage was measured at indicated timepoints over a period of 24 hours and are presented as a percentage of the total electrolytes. Error bars indicate standard error (n=3).

(A) and **(B)** Electrolyte leakage over 24 hours. **(C)** and **(D)** 24 hour time point only. Different letters indicate statistical significance (ANOVA, Tukey p <0.05)

.

Table 4. 1 Summary of 35S::Flag-TRXh phenotypes observed in cat2 and pad2 mutants

	cat2		*pad2*	
	Cell death	Immunity	Cell death	Immunity
TRXh1	No rescue	No rescue	No rescue	Rescue
TRXh2	Rescue	No rescue	No rescue	Rescue
TRXh3	No rescue	No rescue	No rescue	Rescue
TRXh4	Rescue	No rescue	Rescue?	Rescue
TRXh5	Rescue	Rescue?	No rescue	Rescue?

4.2.6 TRX*h* members use alternative mechanisms to rescue light-induced oxidative signalling

Based on the findings that like NRX1, TRX*h*2, *h*4, and *h*5 can also rescue MV-induced electrolyte leakage (Figs. 4.6, 4.12, 4.15), it was tested to see if they also rescue light stress in a similar manner to NRX1. Wild-type, *cat2* and the corresponding *35S::Flag-TRXh* plants were placed in high light conditions (500-600 µmol $m^{-2}s^{-1}$) for three days and the expression of H_2O_2-responsive markers *HSP17.6, GPX6,* and *GSTF8* (Queval et al., 2011) was tested. *35S::Flag-TRXh2* in *cat2* rescued the expression of *HSP17.6* and *GSTF8* (Fig. 4.16A), suggesting that TRX*h*4 might play a role in light stress responses. *35S::Flag-TRXh4* in *cat2* was unable to rescue any of the oxidative stress markers tested (Fig. 4.16B), suggesting that its rescue of phenotypes associated with chloroplast and mitochondrial ROS accumulation induced by MV might not be light-responsive. As expression of *TRXh5* was partially rescued by *35S::FLAG-NRX1* expression in *cat2* mutants (Chapter 3), it was hypothesised that it might play a role in protecting cells during photo-oxidative signalling. Indeed, *35S::Flag-TRXh5* in *cat2* showed a trend of partially rescuing the expression of *HSP17.6* and *GSTF8*, but not to the same extent as NRX1 (Fig. 4.16C and 3.5B),

suggesting that it might play a role during photo-oxidative signalling, but perhaps not to the same extent as NRX1 and TRX*h*2, or it may do so via alternative mechanisms.

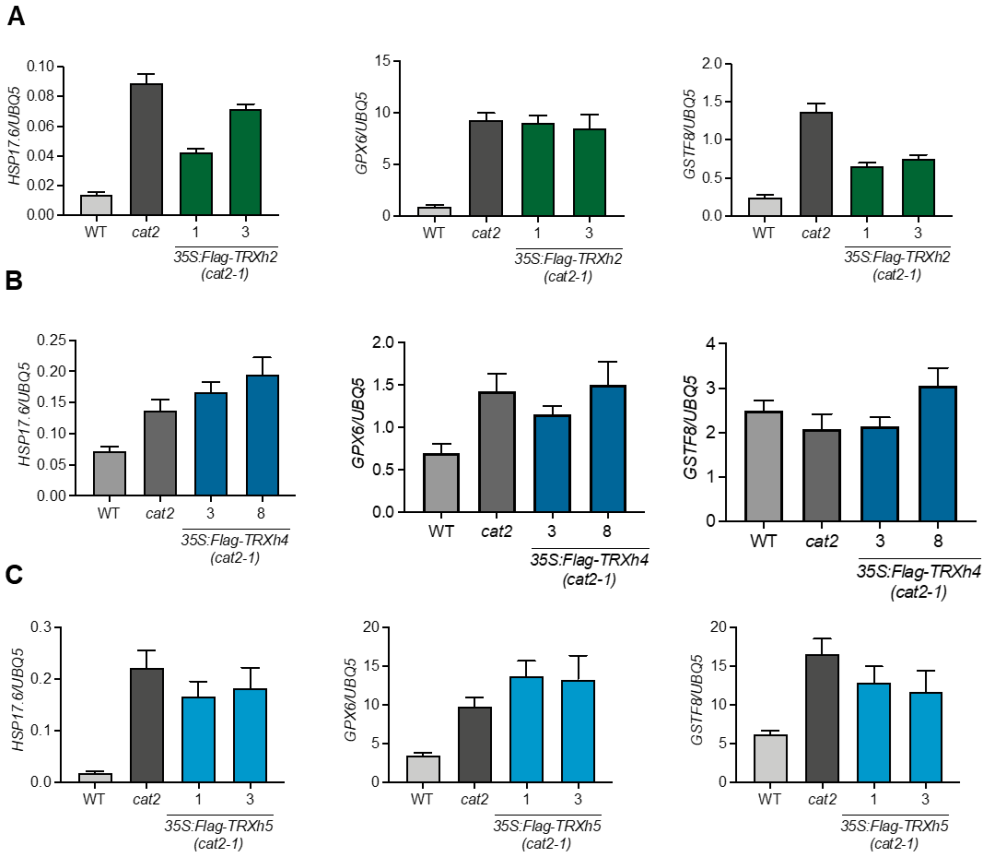

Figure 4. 16 High light induced expression of oxidative stress markers

Gene expression analysis of H_2O_2-responsive genes in Col-0, *cat2,* and **(A)** *35S::Flag-TRXh2,* **(B)** *35S::Flag-TRXh4,* and **(C)** *35S::Flag-TRXh5* expressed in *cat2* after high light treatment (500-600 µmol m^{-2} s^{-1}) for 3 days. Error bars represent SEM of three technical replicates from a pool of leaves from 12 individually treated leaves

4.2.7 TRX-*h* members may rescue immunity in *pad2* in both SA-dependent and SA-independent manners

The *pad2* mutant is deficient in SA signalling, causing increased susceptibility to pathogen infection (Dubreuil-Maurizi et al., 2011). In this chapter it was shown that all the TRX-*h* family members tested were likely able to restore immunity against *Psm* back to wild-type levels, but how they do this remains unclear. To assess if TRX-*h* members that rescue the immune phenotype can restore SA-induced defence gene expression, expression of the marker gene *PR1* was analysed. Wild-type, *pad2* and the corresponding *35S::Flag-TRXh* were infected with *Psm* and tissue was collected at 24 hours post infection. As expected, *pad2* mutants displayed a much lower induction of *PR1* expression than wild-type plants (Fig. 4.17). Interestingly, only TRX*h*4 was able to fully restore induction of *PR1* gene expression (Fig. 4.17D), whereas expression of TRX*h*1, *h*2, *h*3, or *h*5 did not alter compromised *PR1* expression (Fig. 4.17). Consistent with the notion that TRX-*h* members act selectively, these data suggest that while the majority of TRX-*h* members tested restore immunity in *pad2* mutants, the mechanisms behind these rescues are likely specific to each member.

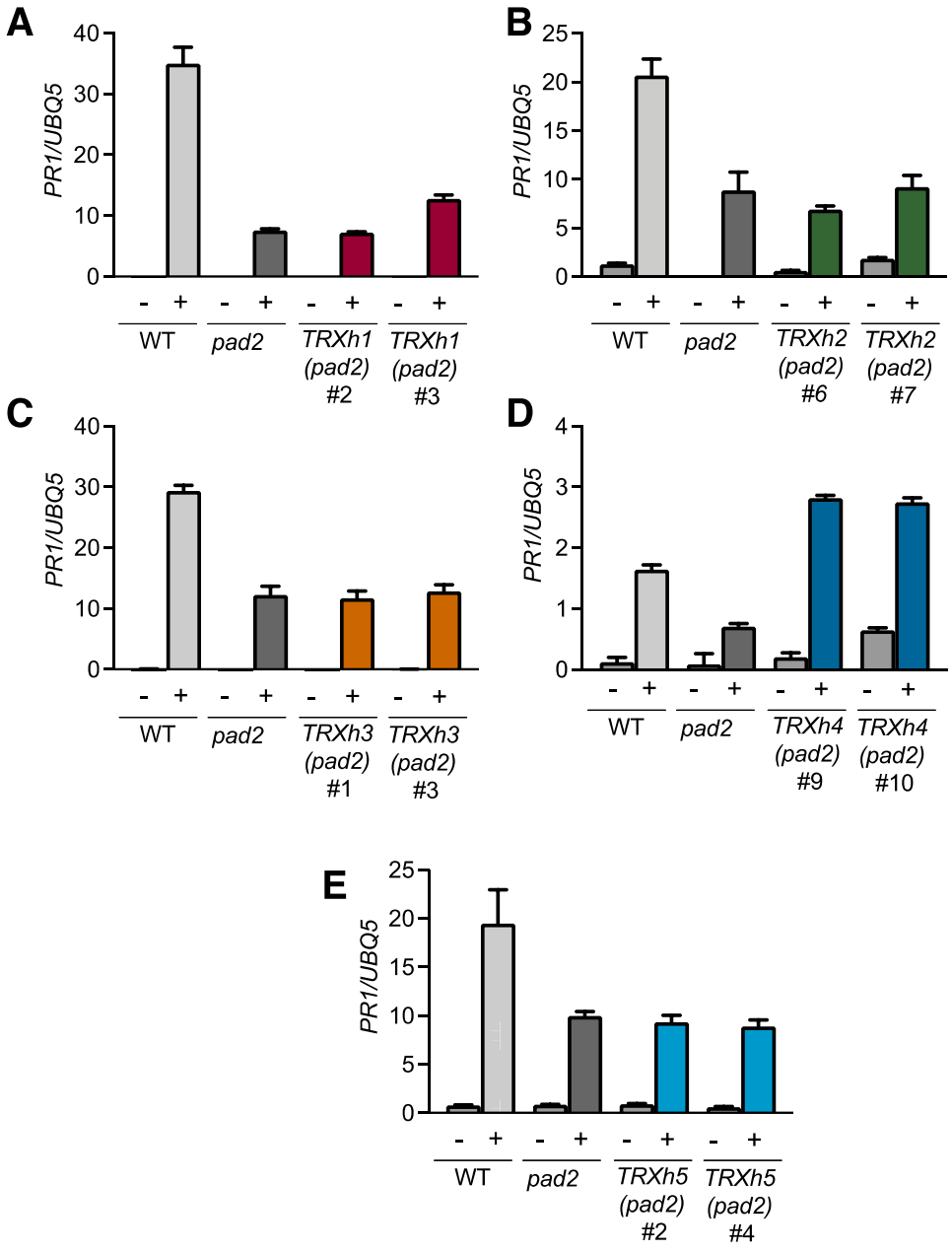

Figure 4. 17 *PR1* marker gene expression after *Psm* infection

Gene expression of *PR1* was analysed in Col-0 (WT), *pad2* and **(A)** *35S::Flag-TRXh1,* **(B)** *35S::Flag-TRXh2,* **(C)** *35S::Flag-TRXh3* **(D)** *35S::Flag-TRXh4*, and **(E)** *35S::Flag-TRXh5* expressed in *pad2* after *Psm* infection. Plants were infected with *Psm* ES4326 (OD_{600} = 0.002) (+) or infiltrated with $MgSO_4$ (-) for 24 hours. Error bars represent SEM of three technical replicates from a pool of leaves from 12 individually treated leaves

Experiment in panel D was conducted by Shi Rui Ong

4.3 Discussion

Redox modifications are essential in cellular signalling, but exactly how oxidative post-translational modifications are utilised as specific signalling switches remains poorly understood. While it is known that the TRX system can act redundantly for the GRX/GSH system (Marty et al., 2009), Chapter 3 identified for the first time that NRX1 protects plants from oxidative cell injury via the rescue of MV induced electrolyte leakage in absence of the antioxidant enzyme catalase. Moreover, this chapter demonstrates that TRXs may play different roles in *cat2* and *pad2* during different stress responses. For example, most members of the TRX-*h* family were able to rescue enhanced susceptibility to *Psm* observed in *pad2* mutants, whereas none conclusively rescued immunity in *cat2* mutants. Conversely, several were able to rescue MV-induced enhanced electrolyte leakage in *cat2* mutants, none of the TRX members tested were able to conclusively rescue the electrolyte leakage response observed in *pad2* mutants. This suggests that TRXs may have distinct oxidatively modified substrate repertoires under various stresses in different redox-perturbed mutants. Based on the findings of Kneeshaw et al. (2014), the authors hypothesised that NO and GSNO may have distinct protein targets that may or may not be reversed by TRX*h*5. The findings in this chapter show that specificity of the TRX-*h* family extends beyond TRX*h*5 and *S*-nitrosylation to other TRX-*h* enzymes and different oxidative protein modifications. This in turn suggests that ROS that accumulate in *cat2* and *pad2* may also have different targets. For example, the absence of CAT2 likely results in an accumulation of predominantly H_2O_2, which will result in initial *S*-sulphenation (S-OH) of target proteins, and under increasing oxidative conditions, lead to further reversible modifications such as disulphide bridges (S-S) and *S*-sulphination ($S\text{-}O_2H$). While the predominant absence of glutathione in *pad2* mutants

will also lead to accumulation of H_2O_2, these plants additionally experience decreased levels of *S*-glutathionylation (SSG), which can protect proteins from further oxidation, as well as reduced GSNO which is thought to *trans*-nitrosylate specific targets (Klatt and Lamas, 2000; Kovacs and Lindermayr, 2013). This difference in modified proteins between different redox-perturbed mutants may correspond to distinct target proteins of TRXs.

Almost all members of the TRX-*h* family tested were able to conclusively rescue enhanced susceptibility of *pad2* mutants upon infection with *Psm* (summarised in Table 4.1). The ability of the TRX system to provide GSH-like antioxidant activity has been highlighted in mouse cells lacking GSH, where the TRX/thioredoxin reductase system is able to take over the reduction of intracellular oxidised cysteine (Mandal et al., 2010). Furthermore, the lack of GSH in cells means that the GRX/GR system is inhibited, as GRXs require glutathione reductase and GSH for their reduction. While it is known that the TRX/NADPH-dependent TRX reductase system can substitute for reducing GSSG in the absence of glutathione reductase (Marty et al., 2009), it is not known what happens in the absence of GSH itself. It is possible that TRXs are either reducing oxidised targets that would otherwise have been reduced by GRXs or alternatively, are taking over the reduction of GRXs to maintain their activities.

Curiously, the TRX*h*-mediated broad rescue of immune phenotypes in *pad2* mutants appeared to require SA-dependent and SA-independent mechanisms. While TRX*h*4 rescued SA-responsive *PR1* gene expression, other TRX-*h* enzymes did not. As discussed in Chapter 3, *pad2* immune deficiencies are due to the inability of cells to accumulate SA and activate downstream responses (Dubreuil-Maurizi et al., 2011). This suggests that except for TRX*h*4, other TRXs are using alternative mechanisms to confer resistance. Indeed, the cotton homologue of NRX1 (GbNRX1) confers signalling by maintaining ROS homeostasis in the apoplast (Li et al., 2016), whereas

the atypical oxidoreductase NTRC suppresses chloroplast-induced ROS that enhances JA signalling (Ishiga et al., 2016). Thus, it is likely that other TRXs also use alternative mechanisms in the absence of SA.

While TRXs in general provided backup in *pad2* mutants during pathogen infection, this was not apparent for the oxidative cell death response. As mentioned above, glutathione-mediated protein *S*-glutathionylation protects Cys residues from further and potentially irreversible oxidation. *S*-glutathionylation can also change the conformation and structure of proteins and adds an additional negative charge to the modified protein (Kalinina and Novichkova, 2021). Therefore, protein oxidation induced by MV treatment could potentially render targets inactivated irreversibly or alter proteins in a way that makes them unrecognisable as TRX substrates.

While none of the TRX-*h* members tested conclusively rescued the immune phenotype of *cat2* mutants, specifically TRX*h*2, *h*4, and *h*5 were able to rescue enhanced electrolyte leakage in response to MV treatment (Figs. 4.6, 4.12, 4.15). The mitochondrial localisation of both MV-induced ROS (Ugalde et al., 2020) and TRX*h*2 may have contributed to the ability of TRX*h*2 to rescue enhanced cell death in *cat2* mutants. Furthermore, the additional two TRX-*h* members that were able to rescue the enhanced electrolyte leakage phenotype in *cat2* mutants, TRX*h*4 and TRX*h*5, are both members of the TRX-*h* subgroup I and contain the active site sequence WCPPC rather than WCGPC. It has been reported that the amino acids between the active site cysteines can determine the activities and the structure of TRXs (Behm and Jacquot, 2000; Bréhélin et al., 2000; Gelhaye et al., 2003), which may have contributed to ability of TRX*h*4 and TRX*h*5 to rescue enhanced the electrolyte leakage response in *cat2* mutants. Intriguingly, while NRX1 was able to rescue the expression of oxidative stress H_2O_2-responsive markers in response to high light in when expressed in *cat2* mutants, (Chapter 3), TRX*h*2, *h*4, and *h*5 did not all rescue the

expression of H_2O_2-induced markers in response to high light to the same extent (Fig. 4.7). This suggests that while TRX*h*2, *h*4, and *h*5 were able to rescue MV-induced electrolyte leakage, they may use alternative mechanisms to NRX1 in order to facilitate a rescue of oxidative signalling in response to increased light intensity.

In contrast to *pad2* mutants, TRX-*h* members were almost entirely unable to rescue the immune phenotype of *cat2* mutants (with the possible exception of TRX*h*5, but this remains unclear). There have been no reports of the TRX family acting redundantly in the absence of CAT2, but catalases have been identified as TRX enzyme substrates in both plants and algae (Balmer et al., 2004; Kneeshaw et al., 2017; Lemaire et al., 2004). Therefore, as mentioned in the discussion of chapter 3, TRX involvement in immune responses may be at least partly dependent on catalase enzymes.

Furthermore, the two assays used to survey the selectivity of the TRX-*h* family in this chapter result in ROS accumulation from different sources. Pathogen infection predominantly results in apoplast-induced ROS (Suzuki et al., 2011), while MV-induced ROS predominantly occurs in the chloroplast and mitochondria (Cui et al., 2019; Ugalde et al., 2020). This suggests that the different sources of ROS/RNS caused by different stresses result in the oxidation of different targets and may determine the difference between TRX-mediated rescue of the immune response and ROS-induced electrolyte leakage observed throughout this chapter.

In summary, this chapter has shown that specificity of the TRX family in redox signalling is extensive. Future large-scale efforts to identify the precise substrate repertoires of each TRX-*h* member in response to environmental stresses would provide further deep insight into the extent of redundancy/selectivity of the TRX family.

Chapter 5

Activity of the deubiquitinase UBP13 is maintained by NRX1-mediated reduction

5.1 Background

Post-translational modifications (PTMs) are vital chemical processes that regulate the activities and functions of proteins within signalling pathways. In eukaryotes, these include ubiquitination, the covalent attachment of the small regulatory protein ubiquitin to target proteins. In order to fine-tune signalling pathways, turnover of regulatory or dysfunctional proteins is essential, and this is largely conducted by the ubiquitin-proteasome system (UPS). Proteins are ubiquitinated via a cascade of E1 and E2 conjugating enzymes, and E3 ligases, which determine the fate of target proteins (Komander and Rape, 2012; Swatek and Komander, 2016). Ubiquitinated proteins are then degraded by the 26S proteasome, a multiprotein complex made up of the 20S core particle and the 19S regulatory particle (Bard et al., 2018) Like many PTMs, ubiquitination is reversible, with the removal of ubiquitin chains orchestrated by deubiquitinases (DUBs). DUBs are critical for maintaining appropriate levels of free ubiquitin in the cell by cleaving polyubiquitin chains, as well as for removing ubiquitin chains at the proteasome to enable entry, and for removing ubiquitin bound to proteins, which prevents the erroneous degradation of proteins in response to rapidly changing signalling events (Amerik and Hochstrasser, 2004; Mevissen and Komander, 2017).

While around 100 DUBs have been characterised in humans, only ~ 60 have been identified in *Arabidopsis*. Four Cys protease families have been reported in plants; Ubiquitin-Specific Proteases/ Ubiquitin Binding Protease (USP/UBP), Ubiquitin C-Terminal Hydrolase (UCH), Ovarian Tumor Protease (OTU), and Machado–Joseph Domain Protease (MJD) (Majumdar and Nath, 2020). Plant DUBs also include JAB1/MPN/MOV34 (JAMM) metalloproteases, as well as a relatively recently characterised sixth family found to be highly conserved across eukaryotes,

named Motif Interacting With Ub-Containing Novel DUB Family (MINDY) (Abdul Rehman et al., 2016; Majumdar and Nath, 2020). The largest group of DUBs in *Arabidopsis* and humans is the UBP family (Majumdar and Nath, 2020), which contain highly conserved Cys and His-boxes necessary for catalytic activity (Yan et al., 2000). Two well-studied plant DUBs are the homologues UBP12 and UBP13 that harbour a unique N-terminal Meprin and TRAF homology (MATH) domain (Ewan et al., 2011). Initially, UBP12 and UBP13 were found to be negative regulators of SA-mediated plant immunity, as silencing of UBP12/UBP13 resulted in enhanced resistance to *Pseudomonas syringae* (Ewan et al., 2011). More recently, however, UBP12/UBP13 have been described as positive regulators of JA signalling by counteracting polyubiquitination of the MYC2 transcription factor by the E3 ligase PUB10, thereby activating downstream JA responses (Jeong et al., 2017). Furthermore, it is now clear that UBP12 and UBP13 are involved in a wide range of critical biological processes, including flowering and the circadian clock (Cui et al., 2013; Lee et al., 2019), regulation of plant growth and development (Vanhaeren et al., 2020), regulation of gene expression via the deubiquitination of histones (Derkacheva et al., 2016), and most recently shade avoidance (Zhou et al., 2021). These wide-ranging roles of UBP12 and UBP13 in plant biology indicate that the maintenance of their activities is of high importance.

Reactive Cys residues are particularly sensitive to oxidative modification and this enables them to act as a regulatory switch defined by their redox state (Reddie and Carroll, 2008). Hyper-reactive Cys residues are especially prevalent in enzyme active sites (Weerapana et al., 2010) indicating that oxidation can determine levels of activity. Several human Cys protease DUBs are known to be at risk of oxidative inhibition, including the human homolog of UBP12/13, USP7 (Cotto-Rios et al., 2012; Kulathu et al., 2013; Lee et al., 2013). In cells, their oxidative inhibition in cells was

reversed over time or with the addition of the reducing agent DTT, which suggests these enzymes are subject to redox regulation. As UBP12 and UBP13 are Cys proteases, this could leave their catalytic Cys vulnerable to oxidation. Indeed, both UBP12 and UBP13 were identified as H_2O_2-modifed proteins (Waszczak et al., 2014). Moreover, in a previous proteomic study, UBP13 was identified as a potential target of NRX1 during *Psm* infection (Kneeshaw et al., 2017), suggesting that the activities of UBP12/13 are subject to reversible redox regulation. In this chapter, it is shown that the *Arabidopsis* DUB, UBP13, is subject to oxidative inhibition both *in vitro* and *in vivo*. Work presented in this chapter further shows that the TRX family member, NRX1, is responsible for reversing oxPTMs of UBP13. NRX1-mediated redox regulation of UBP13 activity may play a role in modulating UBP13-controlled responses to the plant developmental and stress hormone JA.

5.2 Results

5.2.1 Recombinant UBP13 cleaves different ubiquitin linkages

The addition of polyubiquitin chains of different linkage types to target proteins can result in divergent fates. For example, K48 linkages usually target proteins for proteasomal degradation, whereas K63 linkages are involved in non-degradative signalling roles such as endocytosis (Komander and Rape, 2012) Therefore, preference towards a particular ubiquitin linkage type can give an indication of what signalling pathways a DUB might regulate. The human homolog of Arabidopsis UBP13, USP7, appears to have no preference towards particular ubiquitin chain types (Faesen et al., 2011). While *Arabidopsis* UBP12 has been shown to cleave K48 di-ubiquitin (Ub_2) (Ewan et al., 2011) and UBP13 has been shown to cleave polyubiquitinated substrates (Jeong et al., 2017; Vanhaeren et al., 2020), the potential substrate preferences of UBP13 if any, are unknown. Recombinant GST-UBP13 and

the active site mutant GST-UBP13 (C207S) were expressed and purified from *E. coli* (Fig. S5) and tested for DUB activity on K48 polyubiquitin ($K48_{3-7}$) chains. Incubation of $K48_{3-7}$ chains with GST-UBP13 or GST-UBP13 (C207S) confirmed that GST-UBP13 was able to cleave these chains within 15 minutes, whereas GST-UBP13 (C207S) was inactive (Fig. 5.1). Incubation with different K48- and K63-linked diubiquitin (Ub_2) or polyubiquitin chains, showed that *in vitro* UBP13 was capable of cleaving both (Fig. 5.2). Although other chain types were not tested, these results suggest that like human USP7, Arabidopsis UBP13 can cleave multiple ubiquitin chain linkage types.

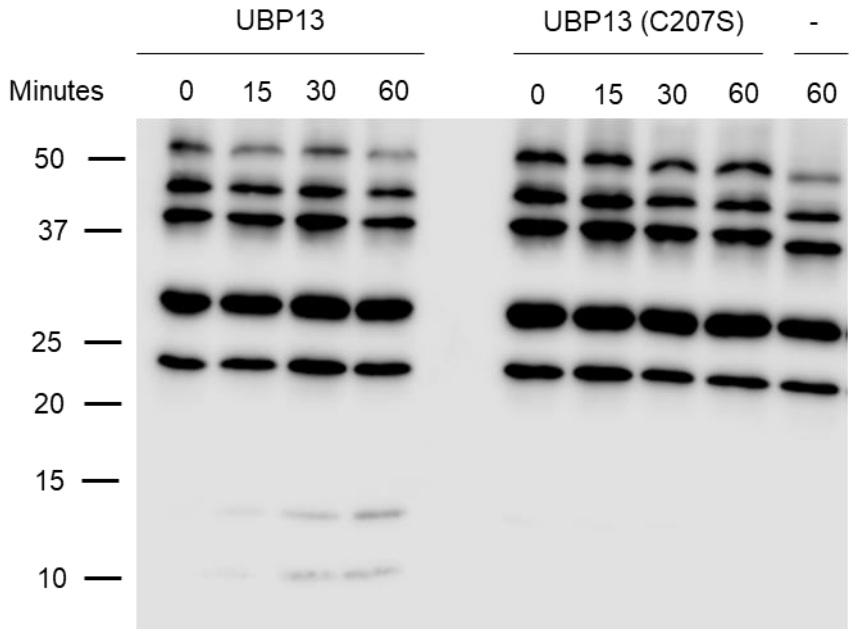

Figure 5. 1 Confirmation of Recombinant GST-UBP13 DUB activity

20nM GST-UBP13 and GST-UBP13 (C207S) were incubated with 300ng K48 Ub_{3-7} chains for the indicated time points at 30ºC. Proteins were separated by SDS-PAGE and analysed by western blot. Ubiquitin was detected using the P4D1 antibody. Markers indicate kDa

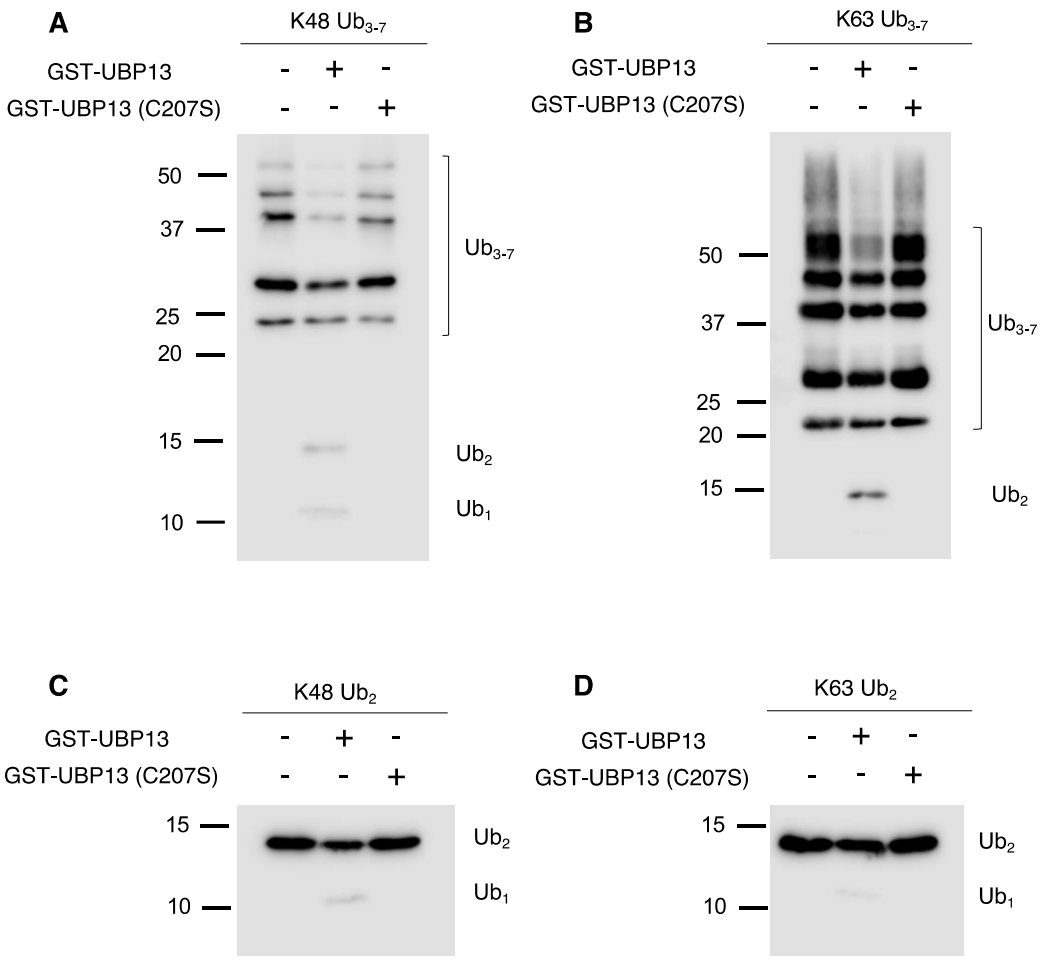

Figure 5. 2 UBP13 can cleave a variety of ubiquitin chain types

20nM recombinant GST-UBP13 or GST-UBP13 (C207S) was incubated with 300ng of **(A)** K48 Ub_{3-7}, **(B)** K63 Ub_{3-7}, **(C)** K48 Ub_2 or **(D)** K63 Ub_2 indicated ubiquitin chain for 1 hour at 30ºC. Ubiquitin chains were detected using the P4D1 antibody. Markers indicate kDa

5.2.2 Recombinant UBP13 activity is inhibited by H_2O_2

The identification of UBP13 as a H_2O_2-modified protein (Waszczak et al., 2014) suggests that it is susceptible to redox regulation. To determine if oxidation affects its activity, GST-UBP13 was treated with increasing concentrations of H_2O_2 and incubated with K63 Ub_2. At H_2O_2 concentrations of 10 µM and above, the ability of GST-UBP13 to cleave K63 Ub_2 chains was completely abolished (Fig. 5.3). Conversely, in the presence of increasing concentrations of the reducing agent DTT,

the ability of GST-UBP13 to cleave K63 Ub_2 was enhanced (Fig. 5.4), suggesting that UBP13 requires continuous reduction to maintain activity.

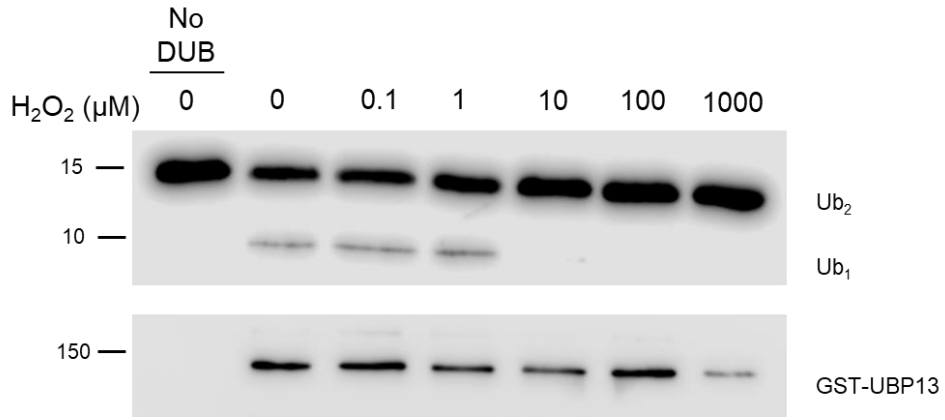

Figure 5. 3 UBP13 activity is inhibited by H_2O_2 *in vitro*

GST-tagged recombinant UBP13 was incubated with increasing concentrations of hydrogen peroxide (H_2O_2) for 15 minutes. The protein was desalted and incubated with K63 Ub_2 for 5 hours at 30ºC. Ubiquitin chains were detected using the P4D1 antibody. Total GST-UBP13 was detected using an anti-GST antibody. Markers indicate kDa

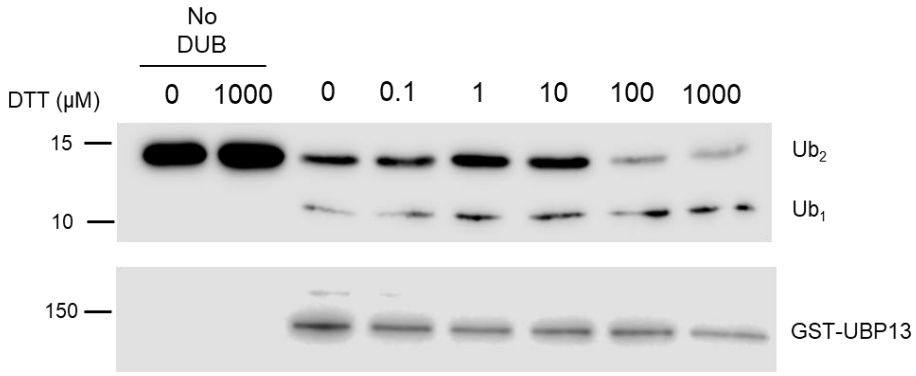

Figure 5. 4 UBP13 activity is enhanced with increasing concentrations of the reducing agent DTT *in vitro*

20nM GST-tagged recombinant UBP13 incubated with 300ng K63 di-ubiquitin (Ub_2) for 5 hours at 30ºC with increasing concentrations of DTT in the reaction buffer. Ubiquitin chains were detected using the P4D1 antibody. Total GST-UBP13 was detected using an anti-GST antibody. Markers indicate kDa

To confirm if H_2O_2-mediated inhibition of UBP13 was due to its oxidation, transgenic plants were generated expressing YFP-tagged UBP13 and UBP13 (C207S) driven by the *UBQ10* promoter (*pUBQ10:YFP-UBP13* or *UBP13 (C207S)*) (Fig. 5.5A), Total protein was extracted from these plants, treated with 5 mM H_2O_2 for 15 minutes and YFP-UBP13 oxidation determined using the reductive switch technique (Kneeshaw et al., 2017). Interestingly, some YFP-UBP13 was already oxidised in plant extracts. Upon H_2O_2 treatment, however, wild-type YFP-UBP13 exhibited an increase in oxidation compared to mock-treated extracts, while the active site mutant showed similar levels of oxidation in both H_2O_2- and mock-treated plants (Fig. 5.5B). These results indicate that although other Cys may also be oxidatively modified, C207 is the primary H_2O_2-responsive residue. Together, these findings show that H_2O_2-induced oxidation of the UBP13 active site inhibits its DUB activity.

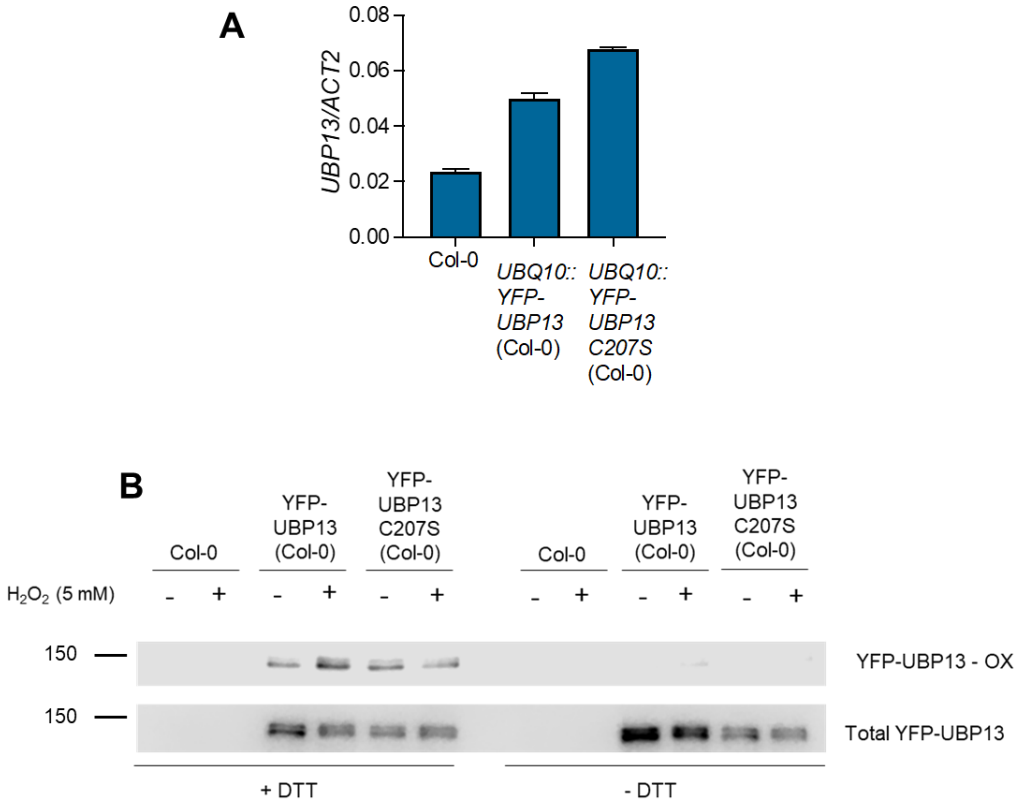

Figure 5. 5 UBP13 is oxidized by H_2O_2

(A) Expression of UBP13 in wild-type plants transformed with *pUBQ10::YFP-UBP13* or *pUBQ10::YFP-UBP13 (C207S).*

(B) Protein extracts of plants expressing UBQ10::YFP-UBP13 or UBQ10::YFP-UBP13 (C207S) were treated with water or 5mM H_2O_2 for 15 mins. Extracts were alkylated with NEM to irreversibly block free thiols before incubating with DTT (2 mM) to reduce *in vivo* oxidised proteins. Free thiols then were labelled with biotin and pulled down with Streptavidin. Oxidized UBP13 (YFP-UBP13-OX) was visualized by immunoblotting with an anti-GFP antibody and shown relative to total YFP-UBP13 and YFP-UBP13 (C207S). Markers indicate kDa

5.2.2 NRX1 maintains UBP13 activity

The data presented thus far suggest that UBP13 is 'redox-sensitive', and is vulnerable to oxidative inhibition, however the question of how this might be reversed remains. Activity of USP7 is also inhibited by H_2O_2 and can be reversed with the addition of the reducing agent DTT (Cotto-Rios et al., 2012). As UBP13 was identified by mass spectrometry as a potential substrate of NRX1 *in vitro*, it was hypothesised that NRX1 may be responsible for protecting UBP13 activity by keeping its active site reduced.

To assess if NRX1 and UBP13 interact *in vivo*, a co-immunoprecipitation assay was performed in *Nicotiana benthamiana* plants transiently expressing *35S::Flag-NRX1* and *35S::Myc-UBP13*. Indeed, Myc-UBP13 was specifically pulled down with Flag-NRX1 (Fig. 5.6), confirming that NRX1 and UBP13 interact *in planta*.

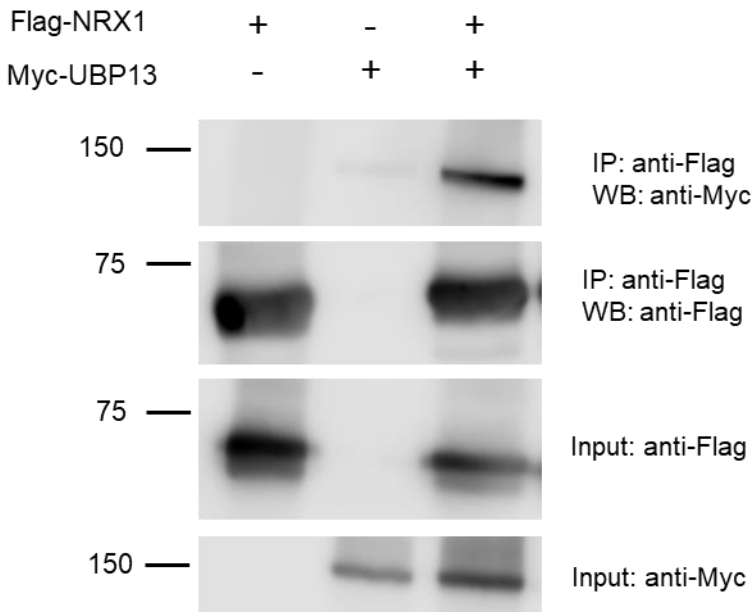

Figure 5. 6 NRX1 interacts with UBP13

3-week old *Nicotiana benthamiana* plants were infiltrated with Flag-NRX1 and/or Myc-UBP13. Leaf tissue was harvested 3 days post infiltration and a Flag-immunoprecipitation was conducted using Flag M2 beads. Myc-UBP13 and Flag-NRX1 was detected via Western Blot using a Myc and Flag antibodies, respectively. Markers indicate kDa

To test if NRX1 acts as a reducing agent for UBP13, recombinant GST-UBP13 was incubated with either DTT, recombinant His-tagged NRX1 or the NRX1 full active site mutant (C55,58,375,378S), and its ability to cleave the fluorescent ubiquitin substrate, ubiquitin-7-amino-4-trifluoromethylcoumarin (Ub-AFC), was measured. Whereas GST-UBP13 was inactive in absence of a reducing agent, addition of DTT strongly activated its DUB activity (Fig 5.7). Surprisingly, the addition of His-NRX1 also resulted in an increase in GST-UBP13 activity to the same level as addition of

DTT (Fig. 5.7). In contrast, incubation with His-NRX1(C55,58,375,378S) did not activate GST-UBP13 (Fig. 5.7). Taken together, the data suggests that UBP13 is indeed a substrate of NRX1 and that NRX1 may keep UBP13 in a reduced state to maintain its DUB activity.

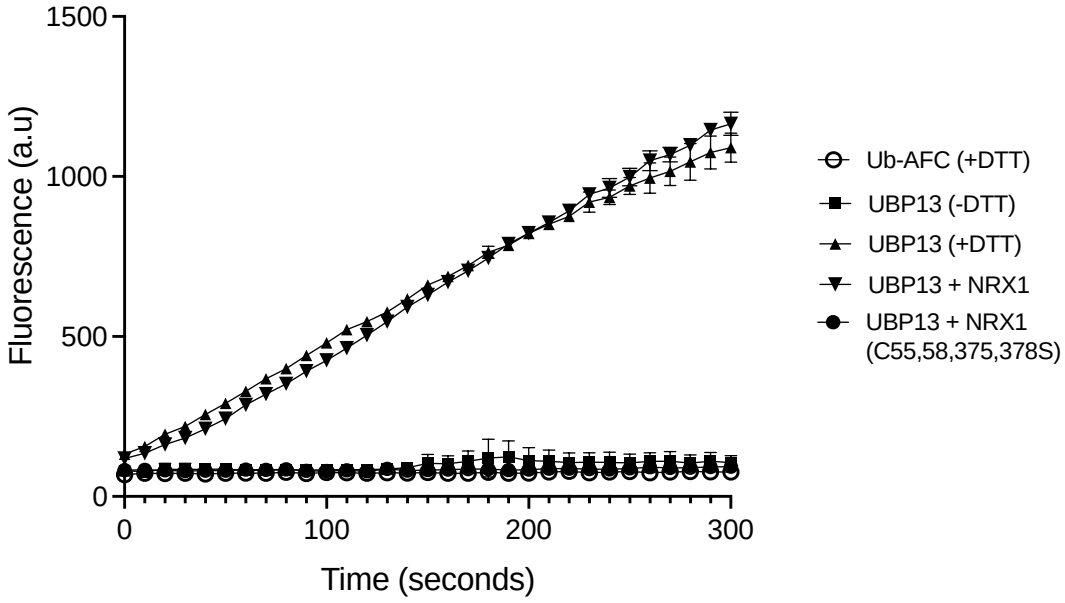

Figure 5. 7 NRX1 maintains UBP13 activity in the absence of DTT *in vitro*

20nM GST-tagged recombinant UBP13 was incubated with H_2O (-DTT), 1mM DTT, or 2µM His-NRX1 before adding Ub-AFC. The assay was conducted over 5 minutes at 30ºC. Fluorescence indicates cleavage of Ub-AFC by UBP13.

Research on human DUBs indicates that redox regulation of DUBs is not limited to the UBP/USP family, with UCH and out DUBs also showing oxidative inhibition (Kulathu et al., 2013; Lee et al., 2013). To establish if NRX1-mediated regulation of DUB activity is specific to UBP13 only, recombinant *Arabidopsis* His-tagged UCH3 was incubated with either DTT, His-NRX1 or His-NRX1(C55,58,375,378S), before testing its ability to cleave Ub-AFC. Similar to GST-UBP13, His-UCH3 activity was enhanced upon incubation with DTT. Although to a

somewhat lesser extent than DTT, the addition of His-NRX1 also strongly increased His-UCH3 activity (Fig. 5.8). Addition of NRX1(C55,58,375,378S) showed minimal effect on UCH3 activity, indicating the NRX1 active site was required for activation of UCH3 (Fig. 5.8). Together, these results suggest that NRX1 may have a general role in maintaining the activity of multiple DUBs.

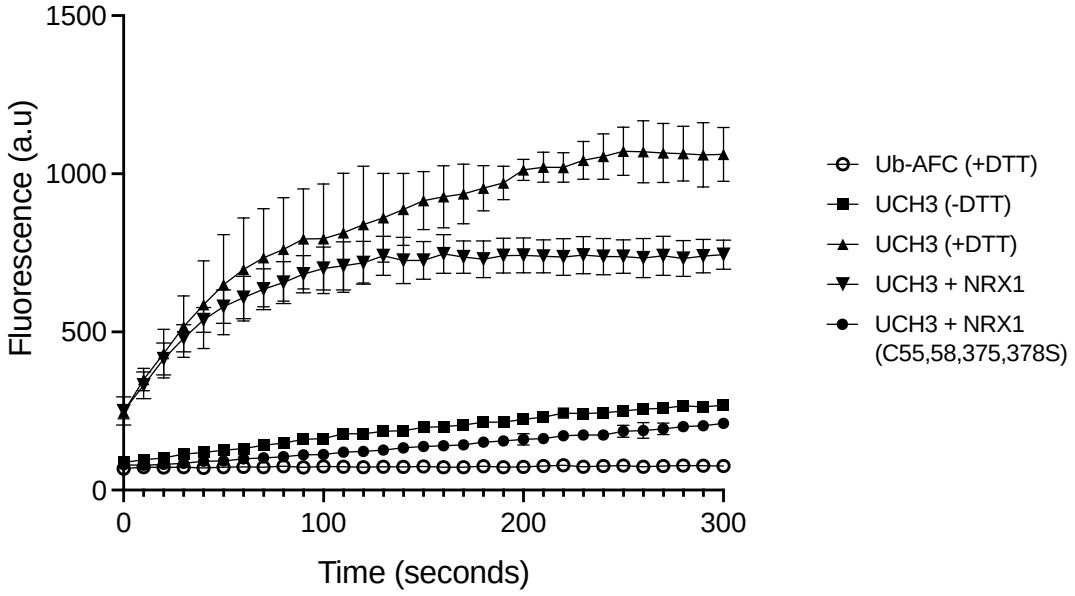

Figure 5. 8 NRX1 maintains UCH3 activity in the absence of DTT *in vitro*

20nM His-tagged recombinant UCH3 was incubated with H_2O (-DTT), 1mM DTT, or 2μM His-NRX1 before adding Ub-AFC. The assay was conducted over 5 minutes at 30ºC. Fluorescence indicates cleavage of Ub-AFC by UCH3.

5.2.3 NRX1 may play a role in regulating UBP13-mediated JA responses

Jeong et al. (2017) reported that UBP13 stabilises the transcriptional activator MYC2 during JA responses, thereby enabling downstream JA-responsive processes, including leaf senescence. Therefore, it was hypothesised that NRX1 might maintain UBP13 activity to promote JA signalling. Earlier in this chapter, UBP13 was shown to be subjected to oxidation in response to H_2O_2 (Fig 5.5B). As accumulation of JA also results in cellular oxidation and an increase in ROS (Ho et al., 2020; Spoel and Loake, 2011), transgenic lines were generated in which *pUBQ10::YFP-UBP13* introduced

into wild-type and mutant *nrx1-1* plants by transformation (Fig. 5.9A). UBP13 oxidation was then examined upon methyl jasmonate (MeJA) treatment in presence or absence of functional NRX1. As opposed to the previous oxidation experiment (Fig. 5.5B), in this assay oxidised UBP13 was not detected in *pUBQ10::YFP-UBP13* (Col-0) plants, in the presence or absence of MeJA (Fig. 5.10). This suggests that in the previous experiment some Cys residues of UBP13 were oxidised by air during the incubation with water or H_2O_2, therby causing background detection of oxidation. In this assay, however, adult plants were treated with MeJA and free Cys were immediately blocked upon protein extraction. Remarkably, oxidation of UBP13 was highly detectable in p*UBQ10::YFP-UBP13* (*nrx1-1*) plants and little change was observed between mock and MeJA treated plants (Fig. 5.9B). These findings demonstrate that NRX1 continuously maintains UBP13 in its reduced, enzymatically active state.

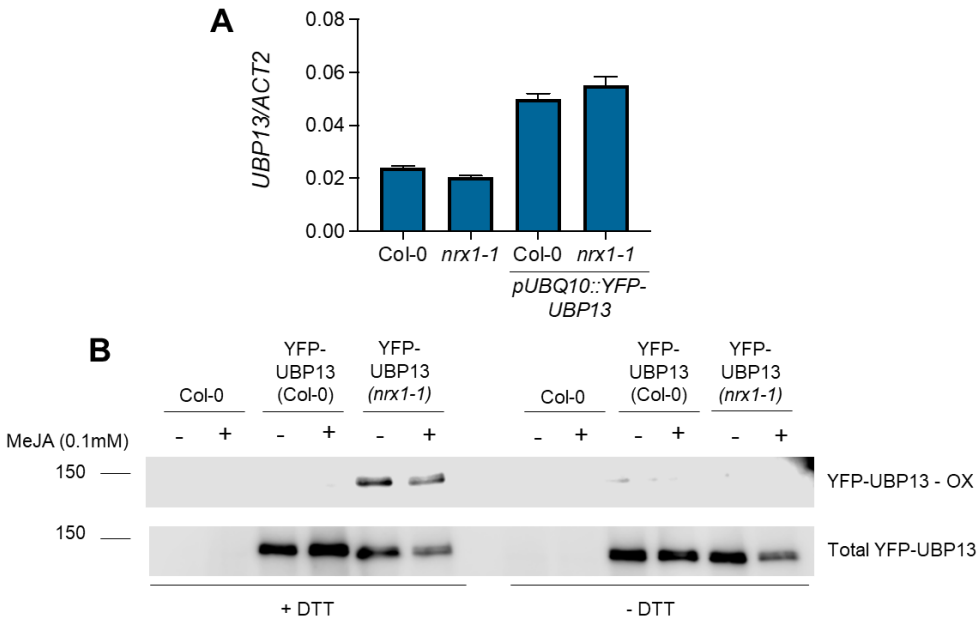

Figure 5. 9 UBP13 is oxidised in *nrx1* mutants

(A) Gene expression of plants wild-type (Col-0) and *nrx1-1* mutant plants transformed with *pUBQ10::YFP-UBP13*

(B) Plants expressing *pUBQ10::YFP-UBP13* in Col-0 and *nrx1-1* mock treated or treated with Methyl Jasmonate (MeJA) for 6hrs. Extracts were alkylated and incubated with or without DTT (2 mM). Free thiols were labelled with biotin and pulled down with Streptavidin. Oxidized UBP13 (YFP-UBP13-OX) was visualized by immunoblotting with an anti-GFP antibody and shown relative to total YFP-UBP13. Markers indicate kDa

To further investigate if NRX1 plays a role in UBP13-mediated JA responses, the transcriptional response of *nrx1* mutant plants to JA was assessed. Wild-type, *nrx1-1* and *35S::Flag-NRX1* in *nrx1-1* (Kneeshaw et al. 2017) plants were treated with MeJA and the expression of JA-responsive marker genes were tested. Interestingly, the *nrx1* mutant showed higher basal levels of expression of *PDF1.2* compared to wild-type and upon MeJA treatment, expression of *PDF1.2* was actually repressed, whereas expression was highly induced in wild-type plants (Fig. 5.10A). Induction of the marker genes *VSP2* and *LOX2* in response to MeJA was reduced in *nrx1* mutants compared to wild-type (Fig 5.10A). This response was partially rescued by the

35S::Flag-NRX1 (nrx1-1) complementation line (Fig. 5.10A). These data suggest that NRX1 may indeed play a role in JA responses. Jeong et al. (2017) found that overexpression of UBP13 in wild-type plants led to JA hypersensitivity. Therefore, to test the hypothesis that NRX1 might maintain UBP13-mediated JA responses, expression of JA-responsive and senescence marker genes were then tested in *pUBQ10::YFP-UBP13* in wild-type and *nrx1* mutants after treatment with MeJA. Induction of *SAG13* was not observed in wild-type or *nrx1* mutants in response to MeJA, but there was an induction of *TAT* in wild-type that was slightly reduced in *nrx1* mutants (Fig 5.10B). As reported previously by Jeong et al (2017), compared to the wild-type parent line, expression of *pUBQ10::YFP-UBP13* resulted in enhanced MeJA-induced expression of both genes. Importantly, enhancement of JA-induced gene expression by YFP-UBP13 was completely (*i.e. SAG13*) or partially (*i.e. TAT*) dependent on functional NRX1 (Fig 5.10B). Together, these data indicate that NRX1 plays a role in regulating UBP13-mediated JA responses.

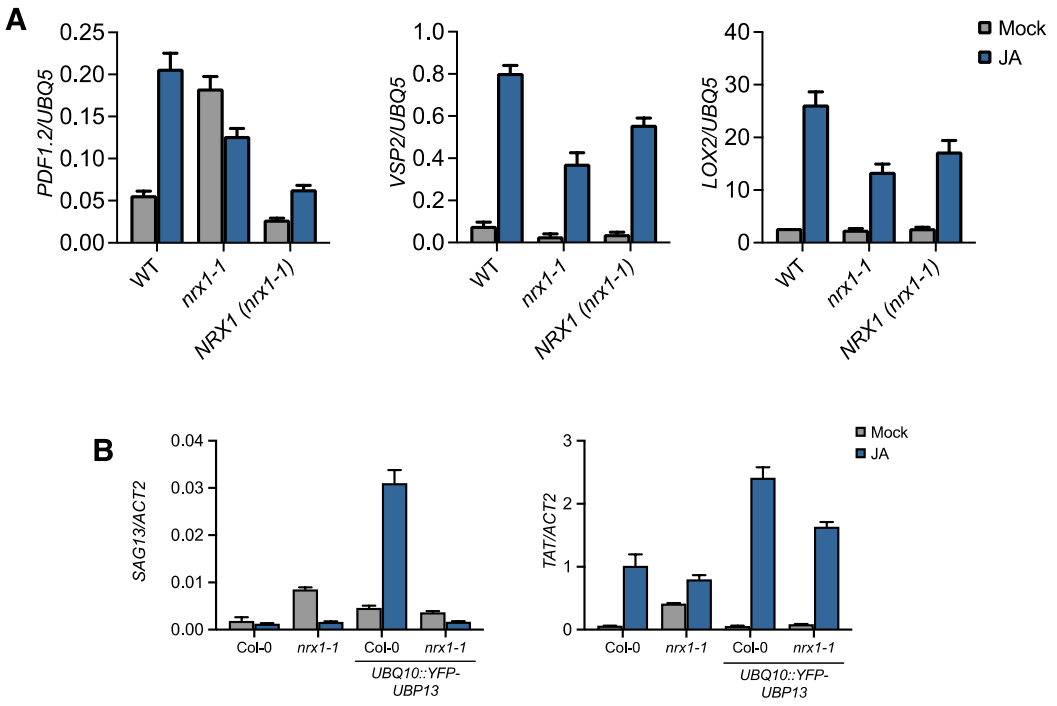

Figure 5. 10 NRX1 regulates UBP13-mediated JA responses

(A) Expression of JA marker genes were analysed in Col-0, *nrx1-1* and *35S::Flag-NRX1* expressed in the *nrx1-1* background. Plants were treated with Methyl Jasmonate for 6 hours. **(B)** Expression of JA and senescence markers from Jeong et al. (2017) were analysed in Col-0, *nrx1-1* and *UBQ10::YFP-UBP13* overexpressing lines. Plants were treated with Methyl Jasmonate for 6 hours.

5.3 Discussion

Many human DUBs are subject to oxidative inhibition via the oxidation of particularly their catalytic Cys residues (Cotto-Rios et al., 2012; Kulathu et al., 2013; Lee et al., 2013). Although inhibition is known to be reversible over time in cells, the mechanisms of how this occurs *in vivo* is in unknown. The plant DUB, UBP13 was identified as a H_2O_2 modified protein and a target of the TRX family member NRX1 (Kneeshaw et al., 2017; Waszczak et al., 2014), suggesting that the activity of UBP13 is subject to redox regulation. Therefore, this chapter set out to uncover if NRX1 is responsible for maintaining UBP13 activity. Here it was shown that NRX1 is responsible for reversing OxPTMs of UBP13, which is the first identification of a direct reducing agent for DUBs.

Ubiquitin chains of different linkage types have distinct cellular functions, and consequently, preference for specific linkages by DUBs may provide insight into the cellular functions they are involved in (Yau and Rape, 2016). The mechanisms behind human DUB specificity have been extensively studied (reviewed in Mevissen and Komander, 2017), while the knowledge of DUB specificity in plants still remains limited. While only K48 and K63 linkage types were tested in this chapter, the potential generalist nature of UBP13 could be linked to the wide range of developmental and stress-responsive signalling it has been implicated in. However, to fully understand UBP13 specificity different linkages must be tested.

After previously being identified as a sulphenated protein by Waszczak et al. (2014), this chapter confirmed that UBP13 is oxidised *in vivo* and further showed that the active site Cys is particularly redox-sensitive in response to H_2O_2 (Figs. 5.3 & 5.5). Generally, the function of DUBs is to counteract ubiquitination by E2 and E3 enzymes. Therefore, any shift in the abundance of active DUBs can have dramatic impacts on substrates that are important to relevant signalling pathways. For example, oxidation of the human DUBs, USP1 and USP7, correlated with increased ubiquitination of their substrates, proliferating cell nuclear antigen (PCNA) and the tumour suppresser protein p53, respectively (Cotto-Rios et al, 2012). Other studies have shown that the oxidative regulation of human DUBs is widespread across the Cys protease families (Kulathu et al., 2013; Lee et al., 2013), but this remains poorly studied in plants. Similarly, this chapter showed that H_2O_2-induced oxidation of the UBP13 active site Cys led to inhibition of its DUB activity (Fig. 5.3), showing that like many human DUBs, UBP13 and potentially other plant DUBs are subject to oxidative inhibition.

While there is evidence to suggest structural changes and formation of sulphenylamide protects the OTU DUB family from irreversible oxidation (Kulathu et al., 2013; Lee et al., 2013), how oxidation of DUBs is counteracted *in vivo* is unknown. Interestingly, oxidation of DUBs *in vivo* is reversed naturally over time and it has been postulated that antioxidants, along with TRXs and GRXs may play a role in the transient nature of oxidative DUB inhibition (Lee et al., 2013; Snyder and Silva, 2021). Indeed, the finding that NRX1 can act as a reducing agent to activate UBP13 activity *in vitro* (Fig. 5.7), supports this theory. Furthermore, NRX1 was also able to enhance UCH3 activity *in vitro* (Fig. 5.8), suggesting that maintenance of DUB activity might be a general role of NRX1. To further validate this, the activity of DUBs including UBP13 and UCH3 in *nrx1* mutant plants would require investigation. The two previous chapters have highlighted the specificity of the TRX family in rescuing oxidative stress, so determining if DUB regulation is NRX1 specific would give more insight into the specificity of the TRX family.

While TRXs have not been linked to reduction of DUBs specifically, they have been associated with maintaining the activity of the ubiquitin-proteasome system. For example, the TRX-like protein TRX LIKE 1 (TXNL1) was found to associate with the 26S proteasome in mammalian cells and *Schizosaccharomyces pombe* (Andersen et al., 2011, 2009). Similarly, in *Saccharomyces cerevisiae*, TRX1 and TRX2 are associated with the proteasome and are thought to function in the deglutathionylation of proteasome subunits (Demasi et al., 2003; Zmijewski et al., 2009). Furthermore, a human TRX reductase is thought to be the primary target of the anti-cancer drug, Auranofin, with inhibition of the proteasome-associated DUB, USP14, proposed to be an off-target effect (Zhang et al., 2019). While the authors did not make a direct link between TRXs and DUBs, this ‘off-target’ effect could be an indication that the inhibition of TRX activity subsequently leads to the inhibition of DUB activity.

In conjunction with NRX1 activation of UBP13 activity, the altered JA response phenotype of *nrx1* mutants (Fig. 5.9A) demonstrates that NRX1 is linked to UBP13-mediated JA signalling. UBP13 maintains MYC2 levels by acting antagonistically to the E3 ligase PUB10 (Jeong et al., 2017). The regulation of MYC2-dependent, JA-responsive genes has been linked to glutathione, antioxidants and H_2O_2 accumulation (Mhamdi et al., 2010a). Therefore, it is plausible that upon JA-induced ROS accumulation, NRX1 maintains UBP13 activity, enabling it to continue cleaving ubiquitin chains from MYC2. Although an increase in UBP13 oxidation was not observed in response to JA in the wild type, abundantly oxidised UBP13 was detected in *nrx1* mutants (Fig. 5.9). This suggests that while NRX1 removes JA-induced oxidative modifications of UBP13, it is also responsible for continuously maintaining UBP13 in a reduced state and by inference, its activity. Furthermore, while the active site Cys appears to be particularly sensitive to oxidation in wild-type plants, UBP13 contains 10 Cys residues, many of which may be susceptible to signal-induced oxidation, possibly resulting in changes to its conformation, function or activity. Therefore, determining if NRX1 also protects UBP13 via reduction of other important Cys residues would provide more insight into these processes.

The data presented in this chapter indicates that interaction between UBP13 and NRX1 may promote JA signalling (Fig 5.10), however further evidence will need to be collected to understand the full extent of the interplay between NRX1 and UBP13 For example, UBP13 has been reported as a negative regulator of SA-mediated plant immunity (Ewan et al., 2011), and mutant *nrx1* plants exhibit SA-dependent enhanced disease resistance (Kneeshaw et al., 2017), suggesting it is a negative regulator of SA-mediated plant immunity. This supports the hypothesis that NRX1 promotes UBP13 activity. Therefore, it would be interesting to see if the absence of NRX1

affects immune phenotypes associated with the overexpression of UBP13. Although UBP13 was identified as a substrate of NRX1 during pathogen infection, NRX1 could regulate UBP13 beyond immunity. For example, Jeong et al. (2017) also showed that UBP13 alters leaf senescence responses. Further questions that also remain unanswered include whether NRX1 might be a substrate of UBP13? This chapter does not address the possibility that while NRX1 may maintain UBP13 activity, NRX1 itself could be subject to ubiquitination and may require a DUB, such as UBP13, to protect it from degradation or altered signalling pathways.

In summary, the results of this chapter show the interplay between the regulation of two different PTM systems: ubiquitination and oxidation. The data indicates not only that plant DUBs are susceptible to oxidation, but they also demonstrate for the first time that members of the TRX family are responsible for reducing DUB active-site Cys residues to maintain their activities. Understanding if this is a general or specific role of TRX enzymes will provide future insights into the molecular and biological significance of this family.

Chapter 6

General discussion

6.1 Thioredoxins selectively restore redox signalling in antioxidant-deficient plants

Plants have widespread antioxidant networks responsible for scavenging ROS, with several systems that predominantly scavenge H_2O_2. While these systems are very much interlinked, the presence of multiple enzymes suggests there must be specificity in the signalling pathways they are involved in. By removing different parts of the H_2O_2 scavenging machinery, we can gain insights into specific signalling roles of ROS and associated antioxidants. Indeed, eliminating antioxidants greatly alters changes in transcription and different antioxidant knockout mutants exhibit distinct transcriptome footprints, demonstrating that each antioxidants functions at least in part in a separate signalling pathway (Gadjev et al., 2006). Members of the TRX family are important in maintaining antioxidant-mediated signalling during stress, as highlighted by the protective activities of NRX1 (Kneeshaw et al., 2017), but whether TRXs themselves provide a direct means to enable specific ROS signalling remains unclear. The data presented in chapters 3 and 4 highlight for the first time that TRXs selectively signal in absence of major cellular antioxidants, indicating TRXs functions in a specific ROS signalling pathway. Chapter 3 showed that while there are dramatic transcriptome changes between wild-type plants and *cat2* mutants during photo-oxidative stress, NRX1 partially restored the expression of a specific subset of genes back to wild-type levels (Fig. 3.6). This suggested that specific TRX family members have selective targets to enable them to mediate redox signalling. This is emphasised by identification of stress-inducible TRX*h*5 as a partially rescued gene (Fig 3.10, Table S1), which implies that nuclear or cytoplasmic NRX1-mediated signalling may regulate the activities of other TRXs. This prompted the surveying of the TRX-*h* family in chapter 4 to determine if other TRXs behave similarly to NRX1. The intriguing finding that expression of either NRX1 or TRX*h*5 in *cat2* both clearly rescued

electrolyte leakage in response to the light stress mimicking compound MV (Figs. 4.15 and 3.3A), adds weight to the notion that NRX1 may regulate other TRXs to protect proteins against oxidative stress. However, in response to photo-oxidative stress, TRX*h*5 in *cat2* mutants did not restore the expression of the oxidative stress markers to the same extent as NRX1 (Figs 3.4B and 4.16C), suggesting NRX1 also activates other TRXs or antioxidants systems. Indeed, TRX*h*2 and TRX*h*4 were also able to rescue MV-induced enhanced cell death in *cat2* mutants, but while TRX*h*2 restored the oxidative stress markers similarly to NRX1 in *cat2* mutants, TRX*h*4 did not (Figs. 3.4 and 4.16), further highlighting selectivity. It has been noted that due to the sensitivity of ROS signalling, minor changes in environment or stimuli can result in dramatic changes in results, so it is difficult to identify specific marker genes and looking for 'ROS signatures' would be an improved method of studying ROS signalling (Vaahtera et al., 2014). To fully uncover the specificity of TRX-mediated signalling in *cat2* mutants, the next logical steps would be to repeat the RNA-seq experiment performed in chapter 3 with TRX*h*2, *h*4, and *h*5 expressed in *cat2* mutants, as this may result in the full or partial rescue of different subsets of 'signature' genes. In Chapter 4 we expanded the observation of selective TRX signalling by using glutathione-deficient *pad2* mutants. The fact that most TRX-*h* members restored immunity in *pad2* mutants, but only TRX*h*4 restored SA-dependent immunity (Chapter 4), further implies that TRXs have distinct substrate repertoires. Using transcriptomic methods to identify specific clusters of genes altered by TRXs or identifying the direct targets of TRXs in *cat2* and *pad2* mutants by proteomics would help further uncover selectivity within the TRX family.

6.2 Potential mechanisms of TRX substrate selectivity

The striking differences in the TRXs that restored disrupted signalling in *cat2* and *pad2* in response to different oxidative stressors (summarised in Table 4.1) support the hypothesis that TRXs have distinct specific substrate repertoires. It is well-known that members of the H_2O_2 scavenging machinery are interlinked, however it is becoming apparent that they also display specific functions (Foyer and Noctor, 2011). As discussed in section 4.3, the different stresses used to survey the selectivity of the TRX family are likely to induce both ROS and RNS from different sources in the cell and different cellular signalling pathways, consequently resulting in different proteins being oxidatively modified (Fig. 6.1). Moreover, the absence of different antioxidants may result in different forms of oxidation on target proteins, which could subsequently determine specific TRXs recognising them as substrates. For example, it was shown that due to conformational restrictions imposed by disulphides on the substrate, TRXs recognise oxidised Cys residues with greater efficiency than their reduced counterparts (Palde and Carroll, 2015). However, if this is also true for oxidation states other than disulphide bonds remains to be explored. Another possibility is that specificity is determined through electrostatic complementarity between TRX and its substrate. Although the TRX active site is evolutionarily highly conserved, the electrostatic potential of the surrounding solution-exposed surfaces show variation. Gellert et al. (2019) assessed the primary and tertiary structure of human TRXs and GRXs, and found that primary and tertiary structure did not contribute to substrate specificity. Instead, they show that TRX/GRX could be grouped based on the positive or negative electrostatic potentials of their water-accessible surfaces, suggesting this may determine substrate specificity. Indeed, the *Chlamydomonas reinhardtii* TRX, CrTRXf1 was shown to have an electrostatic positive crown that corresponds to the electronegative surfaces surrounding the cysteines of its substrates FBPase and

SBPase (Lemaire et al., 2018), adding weight to this hypothesis. Hence, a combination of localisation, structural accessibility or flexibility, and electrostatic complementarity will likely determine specific TRX substrate repertoires.

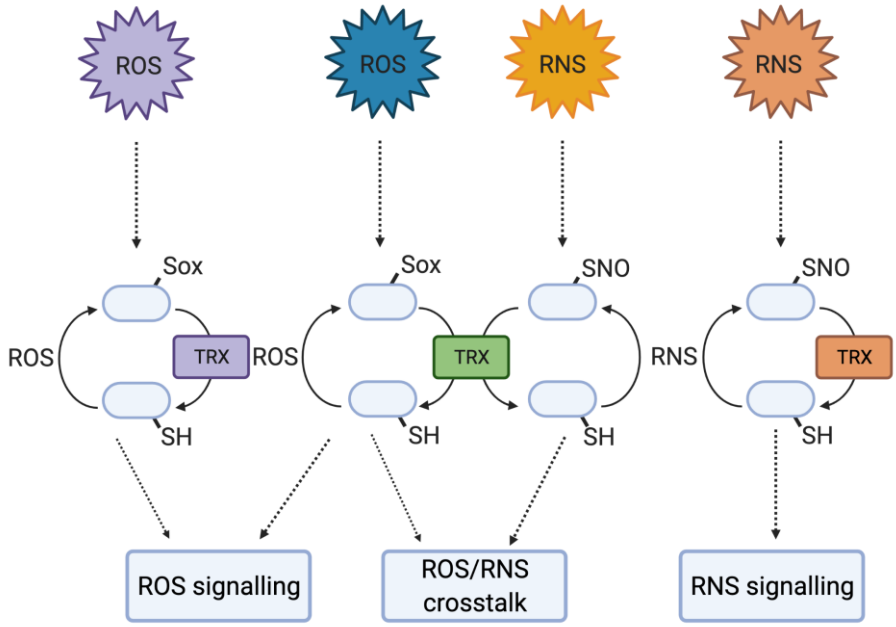

Figure 6. 1 Selective redox signalling shapes plant stress responses

Upon encountering different stresses different forms of ROS/RNS are generated, resulting in oxidative modifications of the reactive free thiols of 'redox sensitive' proteins. Modified proteins may be involved in specific ROS/RNS-mediated signalling pathways or overlap with different pathways. These modifications can be reversed by specific TRXs, adding an additional layer of selective regulation to ROS/RNS-mediated signalling. TRXs may also display selective tendencies for targets involved in specific pathways or display more general reductive activities. Created with BioRender.com, reproduced from Bleau & Spoel (2021)

As the selectivity of TRXs has been demonstrated in *cat2* and *pad2* in this thesis, it would be interesting to study how TRX specificity occurs in other antioxidant-deficient mutants, such as ascorbate-deficient *vtc* mutants (Conklin et al., 2000). Although glutathione and ascorbate are intricately connected in H_2O_2 scavenging, the ascorbate and glutathione pools are differentially altered in response to different

stimuli (Foyer and Noctor, 2011), as shown for example by the contrasting expression of SA- and JA-responsive markers in *vtc* and *pad2* mutants (Brosché and Kangasjärvi, 2012). Therefore, it is plausible that TRXs may also respond selectively in the absence of ascorbate. Given the work of Kneeshaw et al. (2017) and the work presented in chapters 3 and 4 of this thesis, it has now been clearly shown that the TRX family are important players in defining distinct antioxidant signalling pathways. Studying the roles of TRXs in different antioxidant mutants would provide a detailed overview of the specificities of TRX-mediated redox signalling. Emerging tools, such as the use of specific oxPTM probes coupled to mass spectrometry would enable characterisation of the full 'redoxome' (reviewed in Bleau and Spoel, 2021). The use of these probes in antioxidant mutants coupled to the TRX overexpression strategy used in Chapters 3 and 4 would also help to uncover the specific target substrates of TRXs and their oxidation sites.

6.3 NRX1 links redox and ubiquitin signalling during oxidative stress

Cross talk between redox and ubiquitin signalling is well established in yeast and mammalian systems (Kriegenburg et al., 2011), however research in this area in plants is lacking. Oxidised proteins are more likely to be targeted for ubiquitination (Dudek et al., 2005). In yeast cells there is a substantial overlap between oxidised proteins induced upon H_2O_2 stress and K48-linked ubiquitination, thereby selectively targeting oxidised proteins for degradation (Manohar et al., 2019). While some proteins will be irreversibly damaged by oxidation and will need to be degraded, many will have undergone small, reversible changes for which degradation of the protein would be unnecessary. Therefore, maintaining the balance of ubiquitinated vs non-ubiquitinated substrates is crucial in maintaining proteostasis, particularly during

stress. One of the ways in which this can occur is the cleavage of ubiquitin chains from proteins by DUBs. However, as shown in previous studies and in chapter 5, DUBs themselves are subject to oxidation (Cotto-Rios et al., 2012; Kulathu et al., 2013; Lee et al., 2013, Fig. 5.5). As evident from the DUB UBP13, active site cysteines can be particularly redox-sensitive, resulting in ROS-induced inhibition of activity (Figs. 5.3 and 5.5). Therefore, under oxidative conditions, DUB activity needs to be maintained to sustain target protein stability and preserve levels of free ubiquitin in the cell. In chapter 5 it was reported for the first time that in *Arabidopsis* the TRX family member, NRX1, is responsible for reversing oxPTMs of the DUB, UBP13. Furthermore, the absence of NRX1 disrupted UBP13-mediated JA signalling (Fig. 5.10), demonstrating that protection of oxidative inhibition of UBP13 by NRX1 is important for downstream hormonal signalling. Several *Arabidopsis* DUBs were identified as oxidised proteins, including UBP13 and UCH3 (Waszczak et al., 2014). As NRX1 was able to enhance the activities of both UBP13 and UCH3, two Cys proteases from different DUB families (Figs. 5.7 and 5.8), it is possible that the protection of DUBs could be a general function of NRX1. However, it is not known if this extends beyond DUBs to other UPS-associated proteins.

Although there is an increase in ubiquitin conjugates upon the onset of oxidative stress, persistent oxidative stress can result in inhibition of the proteasome (Caballero et al., 2003). As mentioned in section 5.3, the proteasome itself is subject to oxidative inhibition in yeast and requires proteasome-associated oxidoreductases to reduce oxidation of the core 20S particle (Silva et al., 2008). TRXs and GRXs in yeast have been found to enter the core proteolytic particle of dormant proteasomes that have been oxidatively inhibited, and restore proteasome activity (Silva et al., 2008). Additionally, the 19S subunit RPN7, which in yeast is important for structural integrity of the 26S proteasome (Isono et al., 2004), was also detected as a possible substrate for NRX1 (Kneeshaw et al., 2017), suggesting that the role of NRX1 in

protecting the UPS and associated proteins may not be limited to DUBs. TRXs could therefore be important in fine-tuning the activity of the UPS and its accessory proteins, by acting as an additional checkpoint before proteins are degraded. As a consistent theme of this thesis is the selectivity of TRX-mediated signalling, it would be interesting to determine how widespread TRX regulation of the UPS system is. For example, the proteasome subunit RPN10 is selectively ubiquitinated in NO-accumulating *nox1* mutants, but not in GSNO-accumulating *gsnor1* mutants (Kneeshaw, 2016). RPN10 is important for selective recognition of polyubiquitinated substrates at the proteasome and ubiquitination of RPN10 prevents it from interacting with ubiquitinated substrates (Isasa et al., 2010; Lipinszki et al., 2012). Overexpression of TRX*h*5 in *nox1* mutants was able to restore levels of ubiquitinated RPN10 back to WT (Kneeshaw, 2016), suggesting that the indirect reversal of RPN10 ubiquitination by TRXs may also be responsible for maintaining proteasome activity under oxidative stress.

Moreover, protein levels could be maintained during stress responses via the redox regulation of the ubiquitination machinery. Most E1, E2, and E3 enzymes contain active site cysteines (Kriegenburg et al., 2011) and so it is highly likely the UPS is at least in part regulated via the oxidised or reduced states of its enzymes. Indeed, oxidative conditions result in decreased ability of E1 and E2 enzymes to form thioesters, which is dependent on the ratio of oxidised to reduced glutathione (Jahngen-Hodge et al., 1997). Additionally, E3 ligases are also subject to redox regulation. For example, oxidation of the human E3 ligase adaptor Keap1 in humans prevents it from ubiquitinating the redox responsive TF, nuclear factor like 2 (Nrf2), allowing it to accumulate and activate downstream antioxidant genes in response to oxidative stress (Lefaki et al., 2017; Zhang and Hannink, 2003). Furthermore, *S*-nitrosylation of the *Arabidopsis* Skp-like 1 (ASK1) adaptor protein is required for assembly of the $SCF^{TIR1/AFB}$ E3 ligase complex and subsequent activation of auxin

signalling (Iglesias et al., 2018). Although no TRX enzymes have been associated with reversal of these modifications, based on detection of TRX and TRX-like enzymes throughout other aspects of the UPS, it is plausible that TRX members could also regulate the activity of E1, E2, and E3 enzymes as another mechanism to maintain proteostasis.

While oxidative inhibition of the UPS and its accessory proteins has been well-established in mammalian and yeast systems, there is still much to be uncovered. In most cases, it is unclear if oxidation is reversible and if so, the mechanisms behind the reversal of oxPTMs are often not described. Chapter 5 provided new insight into the role of the intersection between two key PTMs and how the TRX family could add an additional layer of regulation to prevent erroneous signalling or degradation of proteins by maintaining DUB activity. It is also very likely that the UPS regulates TRX-mediated signalling in a reciprocal manner, so understanding the interplay between these two PTM signalling pathways would increase our knowledge of the diverse ways in which the proteome is regulated.

6.3 Conclusions

The work in this thesis has highlighted the versatility and specificity of the TRX family. Data presented here has shown that TRXs can act both selectively and redundantly to tailor plant cell responses when challenged with different stresses. It has also shown how nucleocytoplasmic redox signalling via NRXs may be important for maintaining signal transduction during stress. The TRX system has been implicated in enabling plants to cope with potential climate change-induced environmental stress (de Pinto et al., 2015) and the prevention of crop loss (Ren et al., 2012), indicating that uncovering the mechanisms behind TRX signalling could be advantageous for biotechnological advancements in crops.

Understanding the selectivity of TRXs is likely critical for redox-based PTMs to be utilised as signalling tools in biotechnology. Additionally, it is highly unlikely that ubiquitination is the only PTM that is subject to redox regulation. Increasing our knowledge of how specific TRXs are recruited and recognise their substrates will be important for understanding how plant responses can be fine-tuned for optimal efficiency in combatting environmental stress. Furthermore, a question that still remains is how important is subcellular localisation for TRX signalling? While this thesis provided new insight into NRX1 signalling, the specific roles of nuclear vs cytoplasmic NRX signalling remain unknown. Understanding the specificities of compartmentalised TRX-mediated redox signalling will fill current gaps in our knowledge of how these compartmentalised signals are integrated throughout the cell when plants are faced with different oxidative stress-inducing stimuli.

While there are still many questions to answer regarding TRX-mediated signalling, the work in this thesis has demonstrated the TRX family are key players in regulating cellular responses. Future work identifying targets of TRX enzymes could mean that the TRX family are used as tools in the future to engineer tailored responses that confer stress tolerance in plants.

Bibliography

Abdul Rehman, S.A., Kristariyanto, Y.A., Choi, S.-Y., Nkosi, P.J., Weidlich, S., Labib, K., Hofmann, K., Kulathu, Y., 2016. MINDY-1 Is a Member of an Evolutionarily Conserved and Structurally Distinct New Family of Deubiquitinating Enzymes. Mol. Cell 63, 146–155. https://doi.org/10.1016/j.molcel.2016.05.009

Ahmad, P., Jaleel, C.A., Salem, M.A., Nabi, G., Sharma, S., 2010. Roles of enzymatic and nonenzymatic antioxidants in plants during abiotic stress. Crit. Rev. Biotechnol. 30, 161–175. https://doi.org/10.3109/07388550903524243

Amerik, A.Y., Hochstrasser, M., 2004. Mechanism and function of deubiquitinating enzymes. Biochim. Biophys. Acta BBA - Mol. Cell Res., The Ubiquitin-Proteasome System 1695, 189–207. https://doi.org/10.1016/j.bbamcr.2004.10.003

Andersen, K.M., Jensen, C., Kriegenburg, F., Lauridsen, A.-M.B., Gordon, C., Hartmann-Petersen, R., 2011. Txl1 and Txc1 Are Co-Factors of the 26S Proteasome in Fission Yeast. Antioxid. Redox Signal. 14, 1601–1608. https://doi.org/10.1089/ars.2010.3329

Andersen, K.M., Madsen, L., Prag, S., Johnsen, A.H., Semple, C.A., Hendil, K.B., Hartmann-Petersen, R., 2009. Thioredoxin Txnl1/TRP32 Is a Redox-active Cofactor of the 26 S Proteasome *. J. Biol. Chem. 284, 15246–15254. https://doi.org/10.1074/jbc.M900016200

Astier, Jéremy, Besson-Bard, A., Wawer, I., Parent, C., Rasul, S., Jeandroz, S., Dat, J., Wendehenne, D., 2018. Nitric oxide signalling in plants: cross-talk with Ca2+, protein kinases and reactive oxygen species. Annu. Plant Rev. Online 147–170.

Astier, Jeremy, Gross, I., Durner, J., 2018. Nitric oxide production in plants: an update. J. Exp. Bot. 69, 3401–3411. https://doi.org/10.1093/jxb/erx420

Balazadeh, S., Siddiqui, H., Allu, A.D., Matallana-Ramirez, L.P., Caldana, C., Mehrnia, M., Zanor, M.-I., Köhler, B., Mueller-Roeber, B., 2010. A gene regulatory network controlled by the NAC transcription factor ANAC092/AtNAC2/ORE1 during salt-promoted senescence. Plant J. 62, 250–264. https://doi.org/10.1111/j.1365-313X.2010.04151.x

Balmer, Y., Vensel, W.H., Tanaka, C.K., Hurkman, W.J., Gelhaye, E., Rouhier, N., Jacquot, J.-P., Manieri, W., Schürmann, P., Droux, M., Buchanan, B.B., 2004. Thioredoxin links redox to the regulation of fundamental processes of plant mitochondria. Proc. Natl. Acad. Sci. 101, 2642–2647. https://doi.org/10.1073/pnas.0308583101

Bard, J.A.M., Goodall, E.A., Greene, E.R., Jonsson, E., Dong, K.C., Martin, A., 2018. Structure and Function of the 26S Proteasome. Annu. Rev. Biochem. 87, 697–724. https://doi.org/10.1146/annurev-biochem-062917-011931

Begara-Morales, J.C., Sánchez-Calvo, B., Chaki, M., Valderrama, R., Mata-Pérez, C., López-Jaramillo, J., Padilla, M.N., Carreras, A., Corpas, F.J., Barroso, J.B., 2014a. Dual regulation of cytosolic ascorbate peroxidase (APX) by tyrosine nitration and S-nitrosylation. J. Exp. Bot. 65, 527–538. https://doi.org/10.1093/jxb/ert396

Begara-Morales, J.C., Sánchez-Calvo, B., Luque, F., Leyva-Pérez, M.O., Leterrier, M., Corpas, F.J., Barroso, J.B., 2014b. Differential Transcriptomic Analysis by RNA-Seq of GSNO-Responsive Genes Between Arabidopsis Roots and Leaves. Plant Cell Physiol. 55, 1080–1095. https://doi.org/10.1093/pcp/pcu044

Behm, M., Jacquot, J.-P., 2000. Isolation and characterization of thioredoxin h from poplar xylem. Plant Physiol. Biochem. 38, 363–369. https://doi.org/10.1016/S0981-9428(00)00760-9

Belin, C., Bashandy, T., Cela, J., Delorme-Hinoux, V., Riondet, C., Reichheld, J.P., 2015. A comprehensive study of thiol reduction gene expression under stress conditions in Arabidopsis thaliana. Plant Cell Environ. 38, 299–314. https://doi.org/10.1111/pce.12276

Benhar, M., Forrester, M.T., Hess, D.T., Stamler, J.S., 2008. Regulated Protein Denitrosylation by Cytosolic and Mitochondrial Thioredoxins. Science 320, 1050–1054. https://doi.org/10.1126/science.1158265

Bindschedler, L.V., Dewdney, J., Blee, K.A., Stone, J.M., Asai, T., Plotnikov, J., Denoux, C., Hayes, T., Gerrish, C., Davies, D.R., Ausubel, F.M., Paul Bolwell, G., 2006. Peroxidase-dependent apoplastic oxidative burst in Arabidopsis required for pathogen resistance. Plant J. 47, 851–863. https://doi.org/10.1111/j.1365-313X.2006.02837.x

Bleau, J.R., Spoel, S.H., 2021. Selective redox signaling shapes plant–pathogen interactions. Plant Physiol. 186, 53–65. https://doi.org/10.1093/plphys/kiaa088

Bréhélin, C., Mouaheb, N., Verdoucq, L., Lancelin, J.-M., Meyer, Y., 2000. Characterization of Determinants for the Specificity ofArabidopsis Thioredoxins h in Yeast Complementation*. J. Biol. Chem. 275, 31641–31647. https://doi.org/10.1074/jbc.M002916200

Broin, M., Cuiné, S., Eymery, F., Rey, P., 2002. The Plastidic 2-Cysteine Peroxiredoxin Is a Target for a Thioredoxin Involved in the Protection of the Photosynthetic Apparatus against Oxidative Damage. Plant Cell 14, 1417–1432. https://doi.org/10.1105/tpc.001644

Broin, M., Rey, P., 2003. Potato Plants Lacking the CDSP32 Plastidic Thioredoxin Exhibit Overoxidation of the BAS1 2-Cysteine Peroxiredoxin and Increased Lipid Peroxidation in Thylakoids under Photooxidative Stress. Plant Physiol. 132, 1335–1343. https://doi.org/10.1104/pp.103.021626

Brosché, M., Kangasjärvi, J., 2012. Low antioxidant concentrations impact on multiple signalling pathways in Arabidopsis thaliana partly through NPR1. J. Exp. Bot. 63, 1849–1861. https://doi.org/10.1093/jxb/err358

Caballero, M., Liton, P.B., Epstein, D.L., Gonzalez, P., 2003. Proteasome inhibition by chronic oxidative stress in human trabecular meshwork cells. Biochem. Biophys. Res. Commun. 308, 346–352. https://doi.org/10.1016/S0006-291X(03)01385-8

Caplan, J.L., Kumar, A.S., Park, E., Padmanabhan, M.S., Hoban, K., Modla, S., Czymmek, K., Dinesh-Kumar, S.P., 2015. Chloroplast Stromules Function during Innate Immunity. Dev. Cell 34, 45–57. https://doi.org/10.1016/j.devcel.2015.05.011

Chaouch, S., Queval, G., Vanderauwera, S., Mhamdi, A., Vandorpe, M., Langlois-Meurinne, M., Breusegem, F.V., Saindrenan, P., Noctor, G., 2010. Peroxisomal Hydrogen Peroxide Is Coupled to Biotic Defense Responses by ISOCHORISMATE SYNTHASE1 in a Daylength-Related Manner. Plant Physiol. 153, 1692–1705. https://doi.org/10.1104/pp.110.153957

Choi, H.W., Kim, Y.J., Lee, S.C., Hong, J.K., Hwang, B.K., 2007. Hydrogen Peroxide Generation by the Pepper Extracellular Peroxidase CaPO2 Activates Local and Systemic Cell Death and Defense Response to Bacterial Pathogens. Plant Physiol. 145, 890–904. https://doi.org/10.1104/pp.107.103325

Collet, J.-F., Messens, J., 2010. Structure, Function, and Mechanism of Thioredoxin Proteins. https://home.liebertpub.com/ars. https://doi.org/10.1089/ars.2010.3114

Collin, V., Issakidis-Bourguet, E., Marchand, C., Hirasawa, M., Lancelin, J.-M., Knaff, D.B., Miginiac-Maslow, M., 2003. The Arabidopsis Plastidial Thioredoxins: NEW FUNCTIONS AND NEW INSIGHTS INTO SPECIFICITY *. J. Biol. Chem. 278, 23747–23752. https://doi.org/10.1074/jbc.M302077200

Conklin, P.L., Saracco, S.A., Norris, S.R., Last, R.L., 2000. Identification of ascorbic acid-deficient Arabidopsis thaliana mutants. Genetics 154, 847–856.

Corpas, F.J., Barroso, J.B., González-Gordo, S., Muñoz-Vargas, M.A., Palma, J.M., 2019. Hydrogen sulfide: A novel component in Arabidopsis peroxisomes which triggers catalase inhibition. J. Integr. Plant Biol. 61, 871–883. https://doi.org/10.1111/jipb.12779

Cotto-Rios, X.M., Békés, M., Chapman, J., Ueberheide, B., Huang, T.T., 2012. Deubiquitinases as a signaling target of oxidative stress. Cell Rep. 2, 1475–1484. https://doi.org/10.1016/j.celrep.2012.11.011

Crisp, P.A., Ganguly, D.R., Smith, A.B., Murray, K.D., Estavillo, G.M., Searle, I., Ford, E., Bogdanović, O., Lister, R., Borevitz, J.O., Eichten, S.R., Pogson, B.J., 2017. Rapid Recovery Gene Downregulation during Excess-Light Stress and Recovery in Arabidopsis. Plant Cell 29, 1836–1863. https://doi.org/10.1105/tpc.16.00828

Cui, F., Brosché, M., Shapiguzov, A., He, X.-Q., Vainonen, J.P., Leppälä, J., Trotta, A., Kangasjärvi, S., Salojärvi, J., Kangasjärvi, J., Overmyer, K., 2019. Interaction of methyl viologen-induced chloroplast and mitochondrial signalling in Arabidopsis. Free Radic. Biol. Med. 134, 555–566. https://doi.org/10.1016/j.freeradbiomed.2019.02.006

Cui, Xia, Lu, F., Li, Y., Xue, Y., Kang, Y., Zhang, S., Qiu, Q., Cui, Xiekui, Zheng, S., Liu, B., Xu, X., Cao, X., 2013. Ubiquitin-Specific Proteases UBP12 and UBP13 Act in Circadian Clock and Photoperiodic Flowering Regulation in Arabidopsis. Plant Physiol. 162, 897–906. https://doi.org/10.1104/pp.112.213009

da Fonseca-Pereira, P., Souza, P.V.L., Hou, L.-Y., Schwab, S., Geigenberger, P., Nunes-Nesi, A., Timm, S., Fernie, A.R., Thormählen, I., Araújo, W.L., Daloso, D.M., 2020. Thioredoxin h2 contributes to the redox regulation of

mitochondrial photorespiratory metabolism. Plant Cell Environ. 43, 188–208. https://doi.org/10.1111/pce.13640

Daloso, D.M., Müller, K., Obata, T., Florian, A., Tohge, T., Bottcher, A., Riondet, C., Bariat, L., Carrari, F., Nunes-Nesi, A., Buchanan, B.B., Reichheld, J.-P., Araújo, W.L., Fernie, A.R., 2015. Thioredoxin, a master regulator of the tricarboxylic acid cycle in plant mitochondria. Proc. Natl. Acad. Sci. 112, E1392–E1400. https://doi.org/10.1073/pnas.1424840112

Daudi, A., Cheng, Z., O'Brien, J.A., Mammarella, N., Khan, S., Ausubel, F.M., Bolwell, G.P., 2012. The Apoplastic Oxidative Burst Peroxidase in Arabidopsis Is a Major Component of Pattern-Triggered Immunity. Plant Cell tpc.111.093039. https://doi.org/10.1105/tpc.111.093039

D'Autréaux, B., Toledano, M.B., 2007. ROS as signalling molecules: mechanisms that generate specificity in ROS homeostasis. Nat. Rev. Mol. Cell Biol. 8, 813–824. https://doi.org/10.1038/nrm2256

De Clercq, I., Van de Velde, J., Luo, X., Liu, L., Storme, V., Van Bel, M., Pottie, R., Vaneechoutte, D., Van Breusegem, F., Vandepoele, K., 2021. Integrative inference of transcriptional networks in Arabidopsis yields novel ROS signalling regulators. Nat. Plants 7, 500–513. https://doi.org/10.1038/s41477-021-00894-1

De Clercq, I., Vermeirssen, V., Van Aken, O., Vandepoele, K., Murcha, M.W., Law, S.R., Inzé, A., Ng, S., Ivanova, A., Rombaut, D., van de Cotte, B., Jaspers, P., Van de Peer, Y., Kangasjärvi, J., Whelan, J., Van Breusegem, F., 2013. The Membrane-Bound NAC Transcription Factor ANAC013 Functions in Mitochondrial Retrograde Regulation of the Oxidative Stress Response in Arabidopsis. Plant Cell 25, 3472–3490. https://doi.org/10.1105/tpc.113.117168

de Pinto, M.C., Locato, V., Paradiso, A., De Gara, L., 2015. Role of redox homeostasis in thermo-tolerance under a climate change scenario. Ann. Bot. 116, 487–496. https://doi.org/10.1093/aob/mcv071

de Pinto, M.C., Locato, V., Sgobba, A., Romero-Puertas, M. del C., Gadaleta, C., Delledonne, M., Gara, L.D., 2013. S-Nitrosylation of Ascorbate Peroxidase Is Part of Programmed Cell Death Signaling in Tobacco Bright Yellow-2 Cells. Plant Physiol. 163, 1766–1775. https://doi.org/10.1104/pp.113.222703

de Torres Zabala, M., Littlejohn, G., Jayaraman, S., Studholme, D., Bailey, T., Lawson, T., Tillich, M., Licht, D., Bölter, B., Delfino, L., Truman, W., Mansfield, J., Smirnoff, N., Grant, M., 2015. Chloroplasts play a central role in plant defence and are targeted by pathogen effectors. Nat. Plants 1, 1–10. https://doi.org/10.1038/nplants.2015.74

Delannoy, E., Jalloul, A., Assigbetsé, K., Marmey, P., Geiger, J.P., Lherminier, J., Daniel, J.F., Martinez, C., Nicole, M., 2003. Activity of Class III Peroxidases in the Defense of Cotton to Bacterial Blight. Mol. Plant. Microbe Interact. 16, 1030–1038. https://doi.org/10.1094/MPMI.2003.16.11.1030

Demasi, M., Silva, G.M., Netto, L.E.S., 2003. 20 S Proteasome from Saccharomyces cerevisiae Is Responsive to Redox Modifications and IsS-Glutathionylated *. J. Biol. Chem. 278, 679–685. https://doi.org/10.1074/jbc.M209282200

Derkacheva, M., Liu, S., Figueiredo, D.D., Gentry, M., Mozgova, I., Nanni, P., Tang, M., Mannervik, M., Köhler, C., Hennig, L., 2016. H2A deubiquitinases UBP12/13 are part of the Arabidopsis polycomb group protein system. Nat. Plants 2, 1–10. https://doi.org/10.1038/nplants.2016.126

Dietz, K.-J., 2014. Redox Regulation of Transcription Factors in Plant Stress Acclimation and Development. Antioxid. Redox Signal. 21, 1356–1372. https://doi.org/10.1089/ars.2013.5672

Ding, X., Jimenez-Gongora, T., Krenz, B., Lozano-Duran, R., 2019. Chloroplast clustering around the nucleus is a general response to pathogen perception in Nicotiana benthamiana. Mol. Plant Pathol. 20, 1298–1306. https://doi.org/10.1111/mpp.12840

Doll, J., Muth, M., Riester, L., Nebel, S., Bresson, J., Lee, H.-C., Zentgraf, U., 2020. Arabidopsis thaliana WRKY25 Transcription Factor Mediates Oxidative Stress Tolerance and Regulates Senescence in a Redox-Dependent Manner. Front. Plant Sci. 10. https://doi.org/10.3389/fpls.2019.01734

Dubiella, U., Seybold, H., Durian, G., Komander, E., Lassig, R., Witte, C.-P., Schulze, W.X., Romeis, T., 2013. Calcium-dependent protein kinase/NADPH oxidase activation circuit is required for rapid defense signal propagation. Proc. Natl. Acad. Sci. 110, 8744–8749. https://doi.org/10.1073/pnas.1221294110

Dubreuil-Maurizi, C., Vitecek, J., Marty, L., Branciard, L., Frettinger, P., Wendehenne, D., Meyer, A.J., Mauch, F., Poinssot, B., 2011. Glutathione deficiency of the Arabidopsis mutant pad2-1 affects oxidative stress-related events, defense gene expression, and the hypersensitive response. Plant Physiol. 157, 2000–2012. https://doi.org/10.1104/pp.111.182667

Dudek, E.J., Shang, F., Liu, Q., Valverde, P., Hobbs, M., Taylor, A., 2005. Selectivity of the ubiquitin pathway for oxidatively modified proteins: relevance to protein precipitation diseases. FASEB J. 19, 1707–1709. https://doi.org/10.1096/fj.05-4049fje

Ewan, R., Pangestuti, R., Thornber, S., Craig, A., Carr, C., O'Donnell, L., Zhang, C., Sadanandom, A., 2011. Deubiquitinating enzymes AtUBP12 and AtUBP13 and their tobacco homologue NtUBP12 are negative regulators of plant immunity. New Phytol. 191, 92–106. https://doi.org/10.1111/j.1469-8137.2011.03672.x

Exposito-Rodriguez, M., Laissue, P.P., Yvon-Durocher, G., Smirnoff, N., Mullineaux, P.M., 2017. Photosynthesis-dependent H2O2 transfer from chloroplasts to nuclei provides a high-light signalling mechanism. Nat. Commun. 8, 49. https://doi.org/10.1038/s41467-017-00074-w

Faesen, A.C., Luna-Vargas, M.P.A., Geurink, P.P., Clerici, M., Merkx, R., van Dijk, W.J., Hameed, D.S., El Oualid, F., Ovaa, H., Sixma, T.K., 2011. The Differential Modulation of USP Activity by Internal Regulatory Domains, Interactors and Eight Ubiquitin Chain Types. Chem. Biol. 18, 1550–1561. https://doi.org/10.1016/j.chembiol.2011.10.017

Feechan, A., Kwon, E., Yun, B.-W., Wang, Y., Pallas, J.A., Loake, G.J., 2005. A central role for S-nitrosothiols in plant disease resistance. Proc. Natl. Acad. Sci. 102, 8054–8059. https://doi.org/10.1073/pnas.0501456102

Fichman, Y., Mittler, R., 2020. Rapid systemic signaling during abiotic and biotic stresses: is the ROS wave master of all trades? Plant J. 102, 887–896. https://doi.org/10.1111/tpj.14685

Fichman, Y., MyersJr, R.J., Grant, D.G., Mittler, R., 2021. Plasmodesmata-localized proteins and ROS orchestrate light-induced rapid systemic signaling in Arabidopsis. Sci. Signal. https://doi.org/10.1126/scisignal.abf0322

Foyer, C.H., Kyndt, T., Hancock, R.D., 2019. Vitamin C in Plants: Novel Concepts, New Perspectives, and Outstanding Issues. Antioxid. Redox Signal. 32, 463–485. https://doi.org/10.1089/ars.2019.7819

Foyer, C.H., Noctor, G., 2011. Ascorbate and Glutathione: The Heart of the Redox Hub. Plant Physiol. 155, 2–18. https://doi.org/10.1104/pp.110.167569

Foyer, C.H., Noctor, G., 2009. Redox Regulation in Photosynthetic Organisms: Signaling, Acclimation, and Practical Implications. Antioxid. Redox Signal. 11, 861–905. https://doi.org/10.1089/ars.2008.2177

Frungillo, L., Skelly, M.J., Loake, G.J., Spoel, S.H., Salgado, I., 2014. S -nitrosothiols regulate nitric oxide production and storage in plants through the nitrogen assimilation pathway. Nat. Commun. 5, 5401. https://doi.org/10.1038/ncomms6401

Gadjev, I., Vanderauwera, S., Gechev, T.S., Laloi, C., Minkov, I.N., Shulaev, V., Apel, K., Inzé, D., Mittler, R., Van Breusegem, F., 2006. Transcriptomic Footprints Disclose Specificity of Reactive Oxygen Species Signaling in Arabidopsis. Plant Physiol. 141, 436–445. https://doi.org/10.1104/pp.106.078717

Gelhaye, E., Rouhier, N., Jacquot, J.-P., 2004. The thioredoxin h system of higher plants. Plant Physiol. Biochem. PPB 42, 265–271. https://doi.org/10.1016/j.plaphy.2004.03.002

Gelhaye, E., Rouhier, N., Navrot, N., Jacquot, J.P., 2005. The plant thioredoxin system. Cell. Mol. Life Sci. CMLS 62, 24–35. https://doi.org/10.1007/s00018-004-4296-4

Gelhaye, E., Rouhier, N., Vlamis-Gardikas, A., Girardet, J.-M., Sautière, P.-E., Sayzet, M., Martin, F., Jacquot, J.-P., 2003. Identification and characterization of a third thioredoxin h in poplar. Plant Physiol. Biochem. 41, 629–635. https://doi.org/10.1016/S0981-9428(03)00063-9

Gellert, M., Hossain, M.F., Berens, F.J.F., Bruhn, L.W., Urbainsky, C., Liebscher, V., Lillig, C.H., 2019. Substrate specificity of thioredoxins and glutaredoxins – towards a functional classification. Heliyon 5, e02943. https://doi.org/10.1016/j.heliyon.2019.e02943

Gill, S.S., Tuteja, N., 2010. Reactive oxygen species and antioxidant machinery in abiotic stress tolerance in crop plants. Plant Physiol. Biochem. 48, 909–930. https://doi.org/10.1016/j.plaphy.2010.08.016

Glazebrook, J., Ausubel, F.M., 1994. Isolation of phytoalexin-deficient mutants of Arabidopsis thaliana and characterization of their interactions with bacterial

pathogens. Proc. Natl. Acad. Sci. 91, 8955–8959. https://doi.org/10.1073/pnas.91.19.8955

Gutscher, M., Pauleau, A.-L., Marty, L., Brach, T., Wabnitz, G.H., Samstag, Y., Meyer, A.J., Dick, T.P., 2008. Real-time imaging of the intracellular glutathione redox potential. Nat. Methods 5, 553–559. https://doi.org/10.1038/nmeth.1212

Hancock, J.T., Henson, D., Nyirenda, M., Desikan, R., Harrison, J., Lewis, M., Hughes, J., Neill, S.J., 2005. Proteomic identification of glyceraldehyde 3-phosphate dehydrogenase as an inhibitory target of hydrogen peroxide in Arabidopsis. Plant Physiol. Biochem. 43, 828–835. https://doi.org/10.1016/j.plaphy.2005.07.012

Henne, M., König, N., Triulzi, T., Baroni, S., Forlani, F., Scheibe, R., Papenbrock, J., 2015. Sulfurtransferase and thioredoxin specifically interact as demonstrated by bimolecular fluorescence complementation analysis and biochemical tests. FEBS Open Bio 5, 832–843. https://doi.org/10.1016/j.fob.2015.10.001

Ho, T.-T., Murthy, H.N., Park, S.-Y., 2020. Methyl Jasmonate Induced Oxidative Stress and Accumulation of Secondary Metabolites in Plant Cell and Organ Cultures. Int. J. Mol. Sci. 21, 716. https://doi.org/10.3390/ijms21030716

Huang, J., Niazi, A.K., Young, D., Rosado, L.A., Vertommen, D., Bodra, N., Abdelgawwad, M.R., Vignols, F., Wei, B., Wahni, K., Bashandy, T., Bariat, L., Van Breusegem, F., Messens, J., Reichheld, J.-P., 2018. Self-protection of cytosolic malate dehydrogenase against oxidative stress in Arabidopsis. J. Exp. Bot. 69, 3491–3505. https://doi.org/10.1093/jxb/erx396

Huang, J., Zhao, X., Chory, J., 2019. The Arabidopsis Transcriptome Responds Specifically and Dynamically to High Light Stress. Cell Rep. 29, 4186-4199.e3. https://doi.org/10.1016/j.celrep.2019.11.051

Iglesias, M.J., Terrile, M.C., Correa-Aragunde, N., Colman, S.L., Izquierdo-Álvarez, A., Fiol, D.F., París, R., Sánchez-López, N., Marina, A., Calderón Villalobos,

L.I.A., Estelle, M., Lamattina, L., Martínez-Ruiz, A., Casalongué, C.A., 2018. Regulation of SCFTIR1/AFBs E3 ligase assembly by S-nitrosylation of Arabidopsis SKP1-like1 impacts on auxin signaling. Redox Biol. 18, 200–210. https://doi.org/10.1016/j.redox.2018.07.003

Imran, Q.M., Hussain, A., Mun, B.-G., Lee, S.U., Asaf, S., Ali, M.A., Lee, I.-J., Yun, B.-W., 2018. Transcriptome wide identification and characterization of NO-responsive WRKY transcription factors in Arabidopsis thaliana L. Environ. Exp. Bot. 148, 128–143. https://doi.org/10.1016/j.envexpbot.2018.01.010

Isasa, M., Katz, E.J., Kim, W., Yugo, V., González, S., Kirkpatrick, D.S., Thomson, T.M., Finley, D., Gygi, S.P., Crosas, B., 2010. Monoubiquitination of RPN10 Regulates Substrate Recruitment to the Proteasome. Mol. Cell 38, 733–745. https://doi.org/10.1016/j.molcel.2010.05.001

Ishiga, Y., Ishiga, T., Ikeda, Y., Matsuura, T., Mysore, K.S., 2016. NADPH-dependent thioredoxin reductase C plays a role in nonhost disease resistance against Pseudomonas syringae pathogens by regulating chloroplast-generated reactive oxygen species. PeerJ 4, e1938. https://doi.org/10.7717/peerj.1938

Isono, E., Saeki, Y., Yokosawa, H., Toh-e, A., 2004. Rpn7 Is Required for the Structural Integrity of the 26 S Proteasome of Saccharomyces cerevisiae. J. Biol. Chem. 279, 27168–27176. https://doi.org/10.1074/jbc.M314231200

Jahngen-Hodge, J., Obin, M.S., Gong, X., Shang, F., Nowell, T.R., Gong, J., Abasi, H., Blumberg, J., Taylor, A., 1997. Regulation of ubiquitin-conjugating enzymes by glutathione following oxidative stress. J. Biol. Chem. 272, 28218–28226. https://doi.org/10.1074/jbc.272.45.28218

Jeong, J.S., Jung, C., Seo, J.S., Kim, J.-K., Chua, N.-H., 2017. The Deubiquitinating Enzymes UBP12 and UBP13 Positively Regulate MYC2 Levels in Jasmonate Responses. Plant Cell tpc.00216.2017. https://doi.org/10.1105/tpc.17.00216

Jian, W., Zhang, D., Zhu, F., Wang, S., Zhu, T., Pu, X., Zheng, T., Feng, H., Lin, H., 2015. Nitrate reductase-dependent nitric oxide production is required for regulation alternative oxidase pathway involved in the resistance to Cucumber mosaic virus infection in Arabidopsis. Plant Growth Regul. 77, 99–107. https://doi.org/10.1007/s10725-015-0040-3

Jiang, G., Yan, H., Wu, F., Zhang, D., Zeng, W., Qu, H., Chen, F., Tan, L., Duan, X., Jiang, Y., 2017. Litchi Fruit LcNAC1 is a Target of LcMYC2 and Regulator of Fruit Senescence Through its Interaction with LcWRKY1. Plant Cell Physiol. 58, 1075–1089. https://doi.org/10.1093/pcp/pcx054

Jiang, G., Zeng, J., Li, Z., Song, Y., Yan, H., He, J., Jiang, Y., Duan, X., 2020. Redox Regulation of the NOR Transcription Factor Is Involved in the Regulation of Fruit Ripening in Tomato1. Plant Physiol. 183, 671–685. https://doi.org/10.1104/pp.20.00070

Kadota, Y., Sklenar, J., Derbyshire, P., Stransfeld, L., Asai, S., Ntoukakis, V., Jones, J.D., Shirasu, K., Menke, F., Jones, A., Zipfel, C., 2014. Direct regulation of the NADPH oxidase RBOHD by the PRR-associated kinase BIK1 during plant immunity. Mol. Cell 54, 43–55. https://doi.org/10.1016/j.molcel.2014.02.021

Kalinina, E., Novichkova, M., 2021. Glutathione in Protein Redox Modulation through S-Glutathionylation and S-Nitrosylation. Molecules 26, 435. https://doi.org/10.3390/molecules26020435

Kang, C.H., Park, J.H., Lee, E.S., Paeng, S.K., Chae, H.B., Hong, J.C., Lee, S.Y., 2020. Redox-Dependent Structural Modification of Nucleoredoxin Triggers Defense Responses against Alternaria brassicicola in Arabidopsis. Int. J. Mol. Sci. 21, 9196. https://doi.org/10.3390/ijms21239196

Karpinska, B., Zhang, K., Rasool, B., Pastok, D., Morris, J., Verrall, S.R., Hedley, P.E., Hancock, R.D., Foyer, C.H., 2018. The redox state of the apoplast influences

the acclimation of photosynthesis and leaf metabolism to changing irradiance. Plant Cell Environ. 41, 1083–1097. https://doi.org/10.1111/pce.12960

Kaur, S., Prakash, P., Bak, D.-H., Hong, S.H., Cho, C., Chung, M.-S., Kim, J.-H., Lee, S., Bai, H.-W., Lee, S.Y., Chung, B.Y., Lee, S.S., 2021. Regulation of Dual Activity of Ascorbate Peroxidase 1 From Arabidopsis thaliana by Conformational Changes and Posttranslational Modifications. Front. Plant Sci. 12, 678111. https://doi.org/10.3389/fpls.2021.678111

Kidwai, M., Ahmad, I.Z., Chakrabarty, D., 2020. Class III peroxidase: an indispensable enzyme for biotic/abiotic stress tolerance and a potent candidate for crop improvement. Plant Cell Rep. 39, 1381–1393. https://doi.org/10.1007/s00299-020-02588-y

Kim, G., Weiss, S.J., Levine, R.L., 2014. Methionine Oxidation and Reduction in Proteins. Biochim. Biophys. Acta 1840. https://doi.org/10.1016/j.bbagen.2013.04.038

Kimura, S., Hunter, K., Vaahtera, L., Tran, H.C., Citterico, M., Vaattovaara, A., Rokka, A., Stolze, S.C., Harzen, A., Meißner, L., Wilkens, M.M.T., Hamann, T., Toyota, M., Nakagami, H., Wrzaczek, M., 2020. CRK2 and C-terminal Phosphorylation of NADPH Oxidase RBOHD Regulate Reactive Oxygen Species Production in Arabidopsis. Plant Cell 32, 1063–1080. https://doi.org/10.1105/tpc.19.00525

Kimura, S., Waszczak, C., Hunter, K., Wrzaczek, M., 2017. Bound by Fate: The Role of Reactive Oxygen Species in Receptor-Like Kinase Signaling. Plant Cell 29, 638–654. https://doi.org/10.1105/tpc.16.00947

Kinkema, M., Fan, W., Dong, X., 2000. Nuclear localization of NPR1 is required for activation of PR gene expression. Plant Cell 12, 2339–2350.

Klatt, P., Lamas, S., 2000. Regulation of protein function by S-glutathiolation in response to oxidative and nitrosative stress. Eur. J. Biochem. 267, 4928–4944. https://doi.org/10.1046/j.1432-1327.2000.01601.x

Kneeshaw, S., 2016. Molecular mechanisms of redoxin-mediated signalling in plant immunity (PhD). University of Edinburgh.

Kneeshaw, S., Gelineau, S., Tada, Y., Loake, G.J., Spoel, S.H., 2014. Selective Protein Denitrosylation Activity of Thioredoxin-h5 Modulates Plant Immunity. Mol. Cell 56, 153–162. https://doi.org/10.1016/j.molcel.2014.08.003

Kneeshaw, S., Keyani, R., Delorme-Hinoux, V., Imrie, L., Loake, G.J., Le Bihan, T., Reichheld, J.-P., Spoel, S.H., 2017. Nucleoredoxin guards against oxidative stress by protecting antioxidant enzymes. Proc. Natl. Acad. Sci. U. S. A. 114, 8414–8419. https://doi.org/10.1073/pnas.1703344114

Komander, D., Rape, M., 2012. The Ubiquitin Code. Annu. Rev. Biochem. 81, 203–229. https://doi.org/10.1146/annurev-biochem-060310-170328

Kovacs, I., Lindermayr, C., 2013. Nitric oxide-based protein modification: formation and site-specificity of protein S-nitrosylation. Front. Plant Sci. 4.

Kriegenburg, F., Poulsen, E.G., Koch, A., Krüger, E., Hartmann-Petersen, R., 2011. Redox Control of the Ubiquitin-Proteasome System: From Molecular Mechanisms to Functional Significance. Antioxid. Redox Signal. 15, 2265–2299. https://doi.org/10.1089/ars.2010.3590

Kulathu, Y., Garcia, F.J., Mevissen, T.E.T., Busch, M., Arnaudo, N., Carroll, K.S., Barford, D., Komander, D., 2013. Regulation of A20 and other OTU deubiquitinases by reversible oxidation. Nat. Commun. 4, 1569. https://doi.org/10.1038/ncomms2567

Kumar, A.S., Park, E., Nedo, A., Alqarni, A., Ren, L., Hoban, K., Modla, S., McDonald, J.H., Kambhamettu, C., Dinesh-Kumar, S.P., Caplan, J.L., 2018. Stromule extension along microtubules coordinated with actin-mediated anchoring

guides perinuclear chloroplast movement during innate immunity. eLife 7, e23625. https://doi.org/10.7554/eLife.23625

Kwak, J.M., Mori, I.C., Pei, Z.-M., Leonhardt, N., Torres, M.A., Dangl, J.L., Bloom, R.E., Bodde, S., Jones, J.D., Schroeder, J.I., 2003. NADPH oxidase AtrbohD and AtrbohF genes function in ROS-dependent ABA signaling in Arabidopsis. EMBO J. 22, 2623–2633. https://doi.org/10.1093/emboj/cdg277

Laloi, C., Mestres-Ortega, D., Marco, Y., Meyer, Y., Reichheld, J.-P., 2004. The Arabidopsis Cytosolic Thioredoxin h5 Gene Induction by Oxidative Stress and Its W-Box-Mediated Response to Pathogen Elicitor. Plant Physiol. 134, 1006–1016. https://doi.org/10.1104/pp.103.035782

Laugier, E., Tarrago, L., Courteille, A., Innocenti, G., Eymery, F., Rumeau, D., Issakidis-Bourguet, E., Rey, P., 2013. Involvement of thioredoxin y2 in the preservation of leaf methionine sulfoxide reductase capacity and growth under high light. Plant Cell Environ. 36, 670–682. https://doi.org/10.1111/pce.12005

Lechward, K., Sugajska, E., de Baere, I., Goris, J., Hemmings, B.A., Zolnierowicz, S., 2006. Interaction of nucleoredoxin with protein phosphatase 2A. FEBS Lett. 580, 3631–3637. https://doi.org/10.1016/j.febslet.2006.04.101

Lee, C.-M., Li, M.-W., Feke, A., Liu, W., Saffer, A.M., Gendron, J.M., 2019. GIGANTEA recruits the UBP12 and UBP13 deubiquitylases to regulate accumulation of the ZTL photoreceptor complex. Nat. Commun. 10, 3750. https://doi.org/10.1038/s41467-019-11769-7

Lee, D.S., Kim, Y.C., Kwon, S.J., Ryu, C.-M., Park, O.K., 2017. The Arabidopsis Cysteine-Rich Receptor-Like Kinase CRK36 Regulates Immunity through Interaction with the Cytoplasmic Kinase BIK1. Front. Plant Sci. 8. https://doi.org/10.3389/fpls.2017.01856

Lee, J.-G., Baek, K., Soetandyo, N., Ye, Y., 2013. Reversible inactivation of deubiquitinases by reactive oxygen species in vitro and in cells. Nat. Commun. 4, 1568. https://doi.org/10.1038/ncomms2532

Lee, K.P., Kim, C., Landgraf, F., Apel, K., 2007. EXECUTER1- and EXECUTER2-dependent transfer of stress-related signals from the plastid to the nucleus of Arabidopsis thaliana. Proc. Natl. Acad. Sci. 104, 10270–10275. https://doi.org/10.1073/pnas.0702061104

Lefaki, M., Papaevgeniou, N., Chondrogianni, N., 2017. Redox regulation of proteasome function. Redox Biol. 13, 452–458. https://doi.org/10.1016/j.redox.2017.07.005

Lemaire, S.D., Guillon, B., Le Maréchal, P., Keryer, E., Miginiac-Maslow, M., Decottignies, P., 2004. New thioredoxin targets in the unicellular photosynthetic eukaryote Chlamydomonas reinhardtii. Proc. Natl. Acad. Sci. 101, 7475–7480. https://doi.org/10.1073/pnas.0402221101

Lemaire, S.D., Tedesco, D., Crozet, P., Michelet, L., Fermani, S., Zaffagnini, M., Henri, J., 2018. Crystal Structure of Chloroplastic Thioredoxin f2 from Chlamydomonas reinhardtii Reveals Distinct Surface Properties. Antioxidants 7, 171. https://doi.org/10.3390/antiox7120171

Levine, R.L., Moskovitz, J., Stadtman, E.R., 2000. Oxidation of Methionine in Proteins: Roles in Antioxidant Defense and Cellular Regulation. IUBMB Life 50, 301–307. https://doi.org/10.1080/713803735

Li, S., Lauri, A., Ziemann, M., Busch, A., Bhave, M., Zachgo, S., 2009. Nuclear Activity of ROXY1, a Glutaredoxin Interacting with TGA Factors, Is Required for Petal Development in Arabidopsis thaliana. Plant Cell 21, 429–441. https://doi.org/10.1105/tpc.108.064477

Li, Y.-B., Han, L.-B., Wang, H.-Y., Zhang, J., Sun, S.-T., Feng, D.-Q., Yang, C.-L., Sun, Y.-D., Zhong, N.-Q., Xia, G.-X., 2016. The Thioredoxin GbNRX1 Plays a

Crucial Role in Homeostasis of Apoplastic Reactive Oxygen Species in Response to Verticillium dahliae Infection in Cotton. Plant Physiol. 170, 2392–2406. https://doi.org/10.1104/pp.15.01930

Lin, A., Wang, Y., Tang, J., Xue, P., Li, C., Liu, L., Hu, B., Yang, F., Loake, G.J., Chu, C., 2012. Nitric Oxide and Protein S-Nitrosylation Are Integral to Hydrogen Peroxide-Induced Leaf Cell Death in Rice. Plant Physiol. 158, 451–464. https://doi.org/10.1104/pp.111.184531

Lindermayr, C., Saalbach, G., Durner, J., 2005. Proteomic Identification of S-Nitrosylated Proteins in Arabidopsis. Plant Physiol. 137, 921–930. https://doi.org/10.1104/pp.104.058719

Lipinszki, Z., Kovács, L., Deák, P., Udvardy, A., 2012. Ubiquitylation of Drosophila p54/Rpn10/S5a Regulates Its Interaction with the UBA–UBL Polyubiquitin Receptors. Biochemistry 51, 2461–2470. https://doi.org/10.1021/bi3001006

Liu, B., Sun, L., Ma, L., Hao, F.-S., 2017. Both AtrbohD and AtrbohF are essential for mediating responses to oxygen deficiency in Arabidopsis. Plant Cell Rep. 36, 947–957. https://doi.org/10.1007/s00299-017-2128-x

Liu, R.-N., Jiao, T.-Q., Li, J., Wang, A.-Y., Li, Y.-X., Wu, S.-J., Du, L.-Q., Dijkwel, P.P., Zhu, J.-B., 2021. Drought-induced increase in catalase activity improves cotton yield when grown under water-limiting field conditions. J. Agron. Crop Sci. https://doi.org/10.1111/jac.12533

Lledías, F., Rangel, P., Hansberg, W., 1998. Oxidation of Catalase by Singlet Oxygen *. J. Biol. Chem. 273, 10630–10637. https://doi.org/10.1074/jbc.273.17.10630

Lu, Y., Yao, J., 2018. Chloroplasts at the Crossroad of Photosynthesis, Pathogen Infection and Plant Defense. Int. J. Mol. Sci. 19, 3900. https://doi.org/10.3390/ijms19123900

Majumdar, P., Nath, U., 2020. De-ubiquitinases on the move: an emerging field in plant biology. Plant Biol. 22, 563–572. https://doi.org/10.1111/plb.13118

Mandal, P.K., Seiler, A., Perisic, T., Kölle, P., Canak, A.B., Förster, H., Weiss, N., Kremmer, E., Lieberman, M.W., Bannai, S., Kuhlencordt, P., Sato, H., Bornkamm, G.W., Conrad, M., 2010. System xc− and Thioredoxin Reductase 1 Cooperatively Rescue Glutathione Deficiency *. J. Biol. Chem. 285, 22244–22253. https://doi.org/10.1074/jbc.M110.121327

Manohar, S., Jacob, S., Wang, J., Wiechecki, K.A., Koh, H.W.L., Simões, V., Choi, H., Vogel, C., Silva, G.M., 2019. Polyubiquitin Chains Linked by Lysine Residue 48 (K48) Selectively Target Oxidized Proteins In Vivo. Antioxid. Redox Signal. 31, 1133–1149. https://doi.org/10.1089/ars.2019.7826

Marchal, C., Delorme-Hinoux, V., Bariat, L., Siala, W., Belin, C., Saez-Vasquez, J., Riondet, C., Reichheld, J.-P., 2014. NTR/NRX define a new thioredoxin system in the nucleus of Arabidopsis thaliana cells. Mol. Plant 7, 30–44. https://doi.org/10.1093/mp/sst162

Marty, L., Siala, W., Schwarzländer, M., Fricker, M.D., Wirtz, M., Sweetlove, L.J., Meyer, Y., Meyer, A.J., Reichheld, J.-P., Hell, R., 2009. The NADPH-dependent thioredoxin system constitutes a functional backup for cytosolic glutathione reductase in Arabidopsis. Proc. Natl. Acad. Sci. 106, 9109–9114. https://doi.org/10.1073/pnas.0900206106

Maruta, T., Noshi, M., Tanouchi, A., Tamoi, M., Yabuta, Y., Yoshimura, K., Ishikawa, T., Shigeoka, S., 2012. H2O2-triggered Retrograde Signaling from Chloroplasts to Nucleus Plays Specific Role in Response to Stress. J. Biol. Chem. 287, 11717–11729. https://doi.org/10.1074/jbc.M111.292847

Mata-Pérez, C., Spoel, S.H., 2019. Thioredoxin-mediated redox signalling in plant immunity. Plant Sci. Int. J. Exp. Plant Biol. 279, 27–33. https://doi.org/10.1016/j.plantsci.2018.05.001

Meng, L., Wong, J.H., Feldman, L.J., Lemaux, P.G., Buchanan, B.B., 2010. A membrane-associated thioredoxin required for plant growth moves from cell

to cell, suggestive of a role in intercellular communication. Proc. Natl. Acad. Sci. U. S. A. 107, 3900–3905. https://doi.org/10.1073/pnas.0913759107

Menges, M., Hennig, L., Gruissem, W., Murray, J.A.H., 2002. Cell Cycle-regulated Gene Expression in Arabidopsis. J. Biol. Chem. 277, 41987–42002. https://doi.org/10.1074/jbc.M207570200

Mevissen, T.E.T., Komander, D., 2017. Mechanisms of Deubiquitinase Specificity and Regulation. Annu. Rev. Biochem. 86, 159–192. https://doi.org/10.1146/annurev-biochem-061516-044916

Meyer, Y., Belin, C., Delorme-Hinoux, V., Reichheld, J.-P., Riondet, C., 2012. Thioredoxin and Glutaredoxin Systems in Plants: Molecular Mechanisms, Crosstalks, and Functional Significance. Antioxid. Redox Signal. 17, 1124–1160. https://doi.org/10.1089/ars.2011.4327

Meyer, Y., Siala, W., Bashandy, T., Riondet, C., Vignols, F., Reichheld, J.P., 2008. Glutaredoxins and thioredoxins in plants. Biochim. Biophys. Acta 1783, 589–600. https://doi.org/10.1016/j.bbamcr.2007.10.017

Mhamdi, A., Hager, J., Chaouch, S., Queval, G., Han, Y., Taconnat, L., Saindrenan, P., Gouia, H., Issakidis-Bourguet, E., Renou, J.-P., Noctor, G., 2010a. Arabidopsis GLUTATHIONE REDUCTASE1 plays a crucial role in leaf responses to intracellular hydrogen peroxide and in ensuring appropriate gene expression through both salicylic acid and jasmonic acid signaling pathways. Plant Physiol. 153, 1144–1160. https://doi.org/10.1104/pp.110.153767

Mhamdi, A., Queval, G., Chaouch, S., Vanderauwera, S., Van Breusegem, F., Noctor, G., 2010b. Catalase function in plants: a focus on Arabidopsis mutants as stress-mimic models. J. Exp. Bot. 61, 4197–4220. https://doi.org/10.1093/jxb/erq282

Miao, Y., Lv, D., Wang, P., Wang, X.-C., Chen, J., Miao, C., Song, C.-P., 2006. An Arabidopsis Glutathione Peroxidase Functions as Both a Redox Transducer

and a Scavenger in Abscisic Acid and Drought Stress Responses. Plant Cell 18, 2749–2766. https://doi.org/10.1105/tpc.106.044230

Miller, G., Schlauch, K., Tam, R., Cortes, D., Torres, M.A., Shulaev, V., Dangl, J.L., Mittler, R., 2009. The plant NADPH oxidase RBOHD mediates rapid systemic signaling in response to diverse stimuli. Sci. Signal. 2, ra45. https://doi.org/10.1126/scisignal.2000448

Mou, Z., Fan, W., Dong, X., 2003. Inducers of Plant Systemic Acquired Resistance Regulate NPR1 Function through Redox Changes. Cell 113, 935–944. https://doi.org/10.1016/S0092-8674(03)00429-X

Mubarakshina, M.M., Ivanov, B.N., Naydov, I.A., Hillier, W., Badger, M.R., Krieger-Liszkay, A., 2010. Production and diffusion of chloroplastic H2O2 and its implication to signalling. J. Exp. Bot. 61, 3577–3587. https://doi.org/10.1093/jxb/erq171

Nietzel, T., Elsässer, M., Ruberti, C., Steinbeck, J., Ugalde, J.M., Fuchs, P., Wagner, S., Ostermann, L., Moseler, A., Lemke, P., Fricker, M.D., Müller-Schüssele, S.J., Moerschbacher, B.M., Costa, A., Meyer, A.J., Schwarzländer, M., 2019. The fluorescent protein sensor roGFP2-Orp1 monitors in vivo H2 O2 and thiol redox integration and elucidates intracellular H2 O2 dynamics during elicitor-induced oxidative burst in Arabidopsis. New Phytol. 221, 1649–1664. https://doi.org/10.1111/nph.15550

Noctor, G., 2006. Metabolic signalling in defence and stress: the central roles of soluble redox couples. Plant Cell Environ. 29, 409–425. https://doi.org/10.1111/j.1365-3040.2005.01476.x

O'Brien, J.A., Daudi, A., Finch, P., Butt, V.S., Whitelegge, J.P., Souda, P., Ausubel, F.M., Bolwell, G.P., 2012. A peroxidase-dependent apoplastic oxidative burst in cultured Arabidopsis cells functions in MAMP-elicited defense. Plant Physiol. 158, 2013–2027. https://doi.org/10.1104/pp.111.190140

Oikawa, K., Matsunaga, S., Mano, S., Kondo, M., Yamada, K., Hayashi, M., Kagawa, T., Kadota, A., Sakamoto, W., Higashi, S., Watanabe, M., Mitsui, T., Shigemasa, A., Iino, T., Hosokawa, Y., Nishimura, M., 2015. Physical interaction between peroxisomes and chloroplasts elucidated by in situ laser analysis. Nat. Plants 1, 1–12. https://doi.org/10.1038/nplants.2015.35

Okegawa, Y., Motohashi, K., 2015. Chloroplastic thioredoxin m functions as a major regulator of Calvin cycle enzymes during photosynthesis in vivo. Plant J. 84, 900–913. https://doi.org/10.1111/tpj.13049

op den Camp, R.G.L., Przybyla, D., Ochsenbein, C., Laloi, C., Kim, C., Danon, A., Wagner, D., Hideg, É., Göbel, C., Feussner, I., Nater, M., Apel, K., 2003. Rapid Induction of Distinct Stress Responses after the Release of Singlet Oxygen in Arabidopsis[W]. Plant Cell 15, 2320–2332. https://doi.org/10.1105/tpc.014662

Palde, P.B., Carroll, K.S., 2015. A universal entropy-driven mechanism for thioredoxin–target recognition. Proc. Natl. Acad. Sci. 112, 7960–7965. https://doi.org/10.1073/pnas.1504376112

Park, S.-C., Jung, Y.J., Kim, I.R., Lee, Y., Kim, Y.-M., Jang, M.-K., Lee, J.R., 2017. Functional characterization of thioredoxin h type 5 with antimicrobial activity from Arabidopsis thaliana. Biotechnol. Bioprocess Eng. 22, 129–135. https://doi.org/10.1007/s12257-017-0074-7

Park, S.-C., Kim, I.R., Hwang, J.E., Kim, J.-Y., Jung, Y.J., Choi, W., Lee, Y., Jang, M.-K., Lee, J.R., 2019a. Functional Mechanisms Underlying the Antimicrobial Activity of the Oryza sativa Trx-like Protein. Int. J. Mol. Sci. 20. https://doi.org/10.3390/ijms20061413

Park, S.-C., Kim, I.R., Kim, J.-Y., Lee, Y., Yoo, S.-H., Jung, J.H., Cheong, G.-W., Lee, S.Y., Jang, M.-K., Lee, J.R., 2019b. Functional Characterization of a Rice

Thioredoxin Protein OsTrxm and Its Cysteine Mutant Variant with Antifungal Activity. Antioxidants 8. https://doi.org/10.3390/antiox8120598

Peskin, A.V., Winterbourn, C.C., 2001. Kinetics of the reactions of hypochlorous acid and amino acid chloramines with thiols, methionine, and ascorbate. Free Radic. Biol. Med. 30, 572–579. https://doi.org/10.1016/S0891-5849(00)00506-2

Pignocchi, C., Kiddle, G., Hernández, I., Foster, S.J., Asensi, A., Taybi, T., Barnes, J., Foyer, C.H., 2006. Ascorbate Oxidase-Dependent Changes in the Redox State of the Apoplast Modulate Gene Transcript Accumulation Leading to Modified Hormone Signaling and Orchestration of Defense Processes in Tobacco. Plant Physiol. 141, 423–435. https://doi.org/10.1104/pp.106.078469

Queval, G., Issakidis-Bourguet, E., Hoeberichts, F.A., Vandorpe, M., Gakière, B., Vanacker, H., Miginiac-Maslow, M., Van Breusegem, F., Noctor, G., 2007. Conditional oxidative stress responses in the Arabidopsis photorespiratory mutant cat2 demonstrate that redox state is a key modulator of daylength-dependent gene expression, and define photoperiod as a crucial factor in the regulation of H2O2-induced cell death. Plant J. 52, 640–657. https://doi.org/10.1111/j.1365-313X.2007.03263.x

Queval, G., Jaillard, D., Zechmann, B., Noctor, G., 2011. Increased intracellular H2O2 availability preferentially drives glutathione accumulation in vacuoles and chloroplasts. Plant Cell Environ. 34, 21–32. https://doi.org/10.1111/j.1365-3040.2010.02222.x

Ramel, F., Birtic, S., Ginies, C., Soubigou-Taconnat, L., Triantaphylidès, C., Havaux, M., 2012. Carotenoid oxidation products are stress signals that mediate gene responses to singlet oxygen in plants. Proc. Natl. Acad. Sci. 109, 5535–5540. https://doi.org/10.1073/pnas.1115982109

Ran, X., Zhao, F., Wang, Y., Liu, J., Zhuang, Y., Ye, L., Qi, M., Cheng, J., Zhang, Y., 2019. Plant Regulomics: a data-driven interface for retrieving upstream regulators from plant multi-omics data. Plant J. 101, 237–248. https://doi.org/10.1111/tpj.14526

Rasul, S., Dubreuil-Maurizi, C., Lamotte, O., Koen, E., Poinssot, B., Alcaraz, G., Wendehenne, D., Jeandroz, S., 2012. Nitric oxide production mediates oligogalacturonide-triggered immunity and resistance to Botrytis cinerea in Arabidopsis thaliana. Plant Cell Environ. 35, 1483–1499. https://doi.org/10.1111/j.1365-3040.2012.02505.x

Reddie, K.G., Carroll, K.S., 2008. Expanding the functional diversity of proteins through cysteine oxidation. Curr. Opin. Chem. Biol., Biopolymers/Model Systems 12, 746–754. https://doi.org/10.1016/j.cbpa.2008.07.028

Reichheld, J.-P., Bashandy, T., Siala, W., Riondet, C., Delorme, V., Meyer, A., Meyer, Y., 2009. Chapter 9 Redundancy and Crosstalk Within the Thioredoxin and Glutathione Pathways: A New Development in Plants, in: Advances in Botanical Research, Advances in Botanical Research. Academic Press, pp. 253–276. https://doi.org/10.1016/S0065-2296(10)52009-3

Ren, J.-P., Li, Y., Wong, J.H., Meng, L., Cho, M.-J., Buchanan, B.B., Yin, J., Lemaux, P.G., 2012. Modifying thioredoxin expression in cereals leads to improved pre-harvest sprouting resistance and changes in other grain properties. Seed Sci. Res. 22, S30–S35. https://doi.org/10.1017/S0960258511000353

Rey, P., Cuiné, S., Eymery, F., Garin, J., Court, M., Jacquot, J.-P., Rouhier, N., Broin, M., 2005. Analysis of the proteins targeted by CDSP32, a plastidic thioredoxin participating in oxidative stress responses. Plant J. 41, 31–42. https://doi.org/10.1111/j.1365-313X.2004.02271.x

Rey, P., Sanz-Barrio, R., Innocenti, G., Ksas, B., Courteille, A., Rumeau, D., Issakidis-Bourguet, E., Fra, I., 2013. Overexpression of plastidial thioredoxins f and m

differentially alters photosynthetic activity and response to oxidative stress in tobacco plants. Front. Plant Sci. 4. https://doi.org/10.3389/fpls.2013.00390

Scarpeci, T.E., Zanor, M.I., Carrillo, N., Mueller-Roeber, B., Valle, E.M., 2008. Generation of superoxide anion in chloroplasts of Arabidopsis thaliana during active photosynthesis: a focus on rapidly induced genes. Plant Mol. Biol. 66, 361–378. https://doi.org/10.1007/s11103-007-9274-4

Schneider, M., Knuesting, J., Birkholz, O., Heinisch, J.J., Scheibe, R., 2018. Cytosolic GAPDH as a redox-dependent regulator of energy metabolism. BMC Plant Biol. 18, 184. https://doi.org/10.1186/s12870-018-1390-6

Sharma, P., Jha, A.B., Dubey, R.S., Pessarakli, M., 2012. Reactive Oxygen Species, Oxidative Damage, and Antioxidative Defense Mechanism in Plants under Stressful Conditions. J. Bot. 2012, e217037. https://doi.org/10.1155/2012/217037

Shigeto, J., Tsutsumi, Y., 2016. Diverse functions and reactions of class III peroxidases. New Phytol. 209, 1395–1402. https://doi.org/10.1111/nph.13738

Silva, G.M., Netto, L.E.S., Discola, K.F., Piassa-Filho, G.M., Pimenta, D.C., Bárcena, J.A., Demasi, M., 2008. Role of glutaredoxin 2 and cytosolic thioredoxins in cysteinyl-based redox modification of the 20S proteasome. FEBS J. 275, 2942–2955. https://doi.org/10.1111/j.1742-4658.2008.06441.x

Snyder, N.A., Silva, G.M., 2021. Deubiquitinating enzymes (DUBs): Regulation, homeostasis, and oxidative stress response. J. Biol. Chem. 297. https://doi.org/10.1016/j.jbc.2021.101077

Spadaro, D., Yun, B.-W., Spoel, S.H., Chu, C., Wang, Y.-Q., Loake, G.J., 2010. The redox switch: dynamic regulation of protein function by cysteine modifications. Physiol. Plant. 138, 360–371. https://doi.org/10.1111/j.1399-3054.2009.01307.x

Spoel, S.H., Loake, G.J., 2011. Redox-based protein modifications: the missing link in plant immune signalling. Curr. Opin. Plant Biol., Biotic interactions 14, 358–364. https://doi.org/10.1016/j.pbi.2011.03.007

Straus, M.R., Rietz, S., Themaat, E.V.L. van, Bartsch, M., Parker, J.E., 2010. Salicylic acid antagonism of EDS1-driven cell death is important for immune and oxidative stress responses in Arabidopsis. Plant J. 62, 628–640. https://doi.org/10.1111/j.1365-313X.2010.04178.x

Survila, M., Davidsson, P.R., Pennanen, V., Kariola, T., Broberg, M., Sipari, N., Heino, P., Palva, E.T., 2016. Peroxidase-Generated Apoplastic ROS Impair Cuticle Integrity and Contribute to DAMP-Elicited Defenses. Front. Plant Sci. 7. https://doi.org/10.3389/fpls.2016.01945

Suzuki, N., Miller, G., Morales, J., Shulaev, V., Torres, M.A., Mittler, R., 2011. Respiratory burst oxidases: the engines of ROS signaling. Curr. Opin. Plant Biol., 14/6 Cell biology 14, 691–699. https://doi.org/10.1016/j.pbi.2011.07.014

Swatek, K.N., Komander, D., 2016. Ubiquitin modifications. Cell Res. 26, 399–422. https://doi.org/10.1038/cr.2016.39

Tada, Y., Spoel, S.H., Pajerowska-Mukhtar, K., Mou, Z., Song, J., Wang, C., Zuo, J., Dong, X., 2008. Plant Immunity Requires Conformational Charges of NPR1 via S-Nitrosylation and Thioredoxins. Science 321. https://doi.org/10.1126/science.1156970

Tan, S.-X., Greetham, D., Raeth, S., Grant, C.M., Dawes, I.W., Perrone, G.G., 2010. The Thioredoxin-Thioredoxin Reductase System Can Function in Vivo as an Alternative System to Reduce Oxidized Glutathione in Saccharomyces cerevisiae. J. Biol. Chem. 285, 6118–6126. https://doi.org/10.1074/jbc.M109.062844

Tarrago, L., Laugier, E., Zaffagnini, M., Marchand, C.H., Le Maréchal, P., Lemaire, S.D., Rey, P., 2010. Plant thioredoxin CDSP32 regenerates 1-cys methionine

sulfoxide reductase B activity through the direct reduction of sulfenic acid. J. Biol. Chem. 285, 14964–14972. https://doi.org/10.1074/jbc.M110.108373

Tian, Y., Fan, M., Qin, Z., Lv, H., Wang, M., Zhang, Z., Zhou, W., Zhao, N., Li, X., Han, C., Ding, Z., Wang, W., Wang, Z.-Y., Bai, M.-Y., 2018. Hydrogen peroxide positively regulates brassinosteroid signaling through oxidation of the BRASSINAZOLE-RESISTANT1 transcription factor. Nat. Commun. 9, 1063. https://doi.org/10.1038/s41467-018-03463-x

Torres, M.A., Dangl, J.L., Jones, J.D.G., 2002. Arabidopsis gp91phox homologues AtrbohD and AtrbohF are required for accumulation of reactive oxygen intermediates in the plant defense response. Proc. Natl. Acad. Sci. 99, 517–522. https://doi.org/10.1073/pnas.012452499

Torres, M.A., Jones, J.D.G., Dangl, J.L., 2006. Reactive Oxygen Species Signaling in Response to Pathogens. Plant Physiol. 141, 373–378. https://doi.org/10.1104/pp.106.079467

Traverso, J.A., Micalella, C., Martinez, A., Brown, S.C., Satiat-Jeunemaître, B., Meinnel, T., Giglione, C., 2013. Roles of N-Terminal Fatty Acid Acylations in Membrane Compartment Partitioning: Arabidopsis h-Type Thioredoxins as a Case Study. Plant Cell 25, 1056–1077. https://doi.org/10.1105/tpc.112.106849

Triantaphylidès, C., Krischke, M., Hoeberichts, F.A., Ksas, B., Gresser, G., Havaux, M., Van Breusegem, F., Mueller, M.J., 2008. Singlet Oxygen Is the Major Reactive Oxygen Species Involved in Photooxidative Damage to Plants. Plant Physiol. 148, 960–968. https://doi.org/10.1104/pp.108.125690

Ugalde, J.M., Fuchs, P., Nietzel, T., Cutolo, E.A., Homagk, M., Vothknecht, U.C., Holuigue, L., Schwarzländer, M., Müller-Schüssele, S.J., Meyer, A.J., 2021. Chloroplast-derived photo-oxidative stress causes changes in H2O2 and

EGSH in other subcellular compartments. Plant Physiol. 186, 125–141. https://doi.org/10.1093/plphys/kiaa095

Ugalde, J.M., Fuchs, P., Nietzel, T., Cutolo, E.A., Vothknecht, U.C., Holuigue, L., Schwarzländer, M., Müller-Schüssele, S.J., Meyer, A.J., 2020. Chloroplast-derived photo-oxidative stress causes changes in H2O2 and EGSH in other subcellular compartments. bioRxiv 2020.07.20.212670. https://doi.org/10.1101/2020.07.20.212670

Umbreen, S., Lubega, J., Cui, B., Pan, Q., Jiang, J., Loake, G.J., 2018. Specificity in nitric oxide signalling. J. Exp. Bot. 69, 3439–3448. https://doi.org/10.1093/jxb/ery184

Vaahtera, L., Brosché, M., Wrzaczek, M., Kangasjärvi, J., 2014. Specificity in ROS Signaling and Transcript Signatures. Antioxid. Redox Signal. 21, 1422–1441. https://doi.org/10.1089/ars.2013.5662

Vandenabeele, S., Vanderauwera, S., Vuylsteke, M., Rombauts, S., Langebartels, C., Seidlitz, H.K., Zabeau, M., Van Montagu, M., Inzé, D., Van Breusegem, F., 2004. Catalase deficiency drastically affects gene expression induced by high light in Arabidopsis thaliana. Plant J. Cell Mol. Biol. 39, 45–58. https://doi.org/10.1111/j.1365-313X.2004.02105.x

Vanhaeren, H., Chen, Y., Vermeersch, M., De Milde, L., De Vleeschhauwer, V., Natran, A., Persiau, G., Eeckhout, D., De Jaeger, G., Gevaert, K., Inzé, D., 2020. UBP12 and UBP13 negatively regulate the activity of the ubiquitin-dependent peptidases DA1, DAR1 and DAR2. eLife 9, e52276. https://doi.org/10.7554/eLife.52276

Wagner, D., Przybyla, D., op den Camp, R., Kim, C., Landgraf, F., Lee, K.P., Würsch, M., Laloi, C., Nater, M., Hideg, E., Apel, K., 2004. The Genetic Basis of Singlet Oxygen Induced Stress Responses of Arabidopsis thaliana. Science 306, 1183–1185. https://doi.org/10.1126/science.1103178

Wang, C., El-Shetehy, M., Shine, M.B., Yu, K., Navarre, D., Wendehenne, D., Kachroo, A., Kachroo, P., 2014. Free Radicals Mediate Systemic Acquired Resistance. Cell Rep. 7, 348–355. https://doi.org/10.1016/j.celrep.2014.03.032

Wang, D., Amornsiripanitch, N., Dong, X., 2006. A Genomic Approach to Identify Regulatory Nodes in the Transcriptional Network of Systemic Acquired Resistance in Plants. PLOS Pathog. 2, e123. https://doi.org/10.1371/journal.ppat.0020123

Wang, L., Kim, C., Xu, X., Piskurewicz, U., Dogra, V., Singh, S., Mahler, H., Apel, K., 2016. Singlet oxygen- and EXECUTER1-mediated signaling is initiated in grana margins and depends on the protease FtsH2. Proc. Natl. Acad. Sci. 113, E3792–E3800. https://doi.org/10.1073/pnas.1603562113

Wang, Y., Cui, X., Yang, B., Xu, S., Wei, X., Zhao, P., Niu, F., Sun, M., Wang, C., Cheng, H., Jiang, Y.-Q., 2020. WRKY55 transcription factor positively regulates leaf senescence and the defense response by modulating the transcription of genes implicated in the biosynthesis of reactive oxygen species and salicylic acid in Arabidopsis. Development 147, dev189647. https://doi.org/10.1242/dev.189647

Waszczak, C., Akter, S., Eeckhout, D., Persiau, G., Wahni, K., Bodra, N., Molle, I.V., Smet, B.D., Vertommen, D., Gevaert, K., Jaeger, G.D., Montagu, M.V., Messens, J., Breusegem, F.V., 2014. Sulfenome mining in Arabidopsis thaliana. Proc. Natl. Acad. Sci. 111, 11545–11550. https://doi.org/10.1073/pnas.1411607111

Waszczak, C., Akter, S., Jacques, S., Huang, J., Messens, J., Van Breusegem, F., 2015. Oxidative post-translational modifications of cysteine residues in plant signal transduction. J. Exp. Bot. 66, 2923–2934. https://doi.org/10.1093/jxb/erv084

Weerapana, E., Wang, C., Simon, G.M., Richter, F., Khare, S., Dillon, M.B.D., Bachovchin, D.A., Mowen, K., Baker, D., Cravatt, B.F., 2010. Quantitative reactivity profiling predicts functional cysteines in proteomes. Nature 468, 790–795. https://doi.org/10.1038/nature09472

Weigel, D., Glazebrook, J., 2002. Arabidopsis: A Laboratory Manual. CSHL Press.

Wu, F., Chi, Y., Jiang, Z., Xu, Y., Xie, L., Huang, F., Wan, D., Ni, J., Yuan, F., Wu, X., Zhang, Y., Wang, L., Ye, R., Byeon, B., Wang, W., Zhang, S., Sima, M., Chen, S., Zhu, M., Pei, J., Johnson, D.M., Zhu, S., Cao, X., Pei, C., Zai, Z., Liu, Y., Liu, T., Swift, G.B., Zhang, W., Yu, M., Hu, Z., Siedow, J.N., Chen, X., Pei, Z.-M., 2020. Hydrogen peroxide sensor HPCA1 is an LRR receptor kinase in Arabidopsis. Nature 578, 577–581. https://doi.org/10.1038/s41586-020-2032-3

Yan, N., Doelling, J.H., Falbel, T.G., Durski, A.M., Vierstra, R.D., 2000. The Ubiquitin-Specific Protease Family from Arabidopsis.AtUBP1 and 2 Are Required for the Resistance to the Amino Acid Analog Canavanine1. Plant Physiol. 124, 1828–1843. https://doi.org/10.1104/pp.124.4.1828

Yang, H., Mu, J., Chen, L., Feng, J., Hu, J., Li, L., Zhou, J.-M., Zuo, J., 2015. S-Nitrosylation Positively Regulates Ascorbate Peroxidase Activity during Plant Stress Responses1. Plant Physiol. 167, 1604–1615. https://doi.org/10.1104/pp.114.255216

Yau, R., Rape, M., 2016. The increasing complexity of the ubiquitin code. Nat. Cell Biol. 18, 579–586. https://doi.org/10.1038/ncb3358

Yoshida, K., Hara, S., Hisabori, T., 2015. Thioredoxin selectivity for thiol-based redox regulation of target proteins in chloroplasts. J. Biol. Chem. 290, 19540. https://doi.org/10.1074/jbc.A115.647545

Yuan, H.-M., Liu, W.-C., Lu, Y.-T., 2017. CATALASE2 Coordinates SA-Mediated Repression of Both Auxin Accumulation and JA Biosynthesis in Plant

Defenses. Cell Host Microbe 21, 143–155. https://doi.org/10.1016/j.chom.2017.01.007

Yun, B.-W., Feechan, A., Yin, M., Saidi, N.B.B., Bihan, T.L., Yu, M., Moore, J.W., Kang, J.-G., Kwon, E., Spoel, S.H., Pallas, J.A., Loake, G.J., 2011. S-nitrosylation of NADPH oxidase regulates cell death in plant immunity. Nature 478, 264–268. https://doi.org/10.1038/nature10427

Yun, B.-W., Skelly, M.J., Yin, M., Yu, M., Mun, B.-G., Lee, S.-U., Hussain, A., Spoel, S.H., Loake, G.J., 2016. Nitric oxide and S-nitrosoglutathione function additively during plant immunity. New Phytol. 211, 516–526. https://doi.org/10.1111/nph.13903

Zaffagnini, M., Morisse, S., Bedhomme, M., Marchand, C.H., Festa, M., Rouhier, N., Lemaire, S.D., Trost, P., 2013. Mechanisms of Nitrosylation and Denitrosylation of Cytoplasmic Glyceraldehyde-3-phosphate Dehydrogenase from Arabidopsis thaliana*. J. Biol. Chem. 288, 22777–22789. https://doi.org/10.1074/jbc.M113.475467

Zandalinas, S.I., Sengupta, S., Burks, D., Azad, R.K., Mittler, R., 2019. Identification and characterization of a core set of ROS wave-associated transcripts involved in the systemic acquired acclimation response of Arabidopsis to excess light. Plant J. 98, 126–141. https://doi.org/10.1111/tpj.14205

Zhang, D.D., Hannink, M., 2003. Distinct Cysteine Residues in Keap1 Are Required for Keap1-Dependent Ubiquitination of Nrf2 and for Stabilization of Nrf2 by Chemopreventive Agents and Oxidative Stress. Mol. Cell. Biol. https://doi.org/10.1128/MCB.23.22.8137-8151.2003

Zhang, X., Selvaraju, K., Saei, A.A., D'Arcy, P., Zubarev, R.A., Arnér, E.SJ., Linder, S., 2019. Repurposing of auranofin: Thioredoxin reductase remains a primary target of the drug. Biochimie 162, 46–54. https://doi.org/10.1016/j.biochi.2019.03.015

Zhou, Y., Park, S.-H., Soh, M.Y., Chua, N.-H., 2021. Ubiquitin-specific proteases UBP12 and UBP13 promote shade avoidance response by enhancing PIF7 stability. Proc. Natl. Acad. Sci. 118. https://doi.org/10.1073/pnas.2103633118

Zmijewski, J.W., Banerjee, S., Abraham, E., 2009. S-Glutathionylation of the Rpn2 Regulatory Subunit Inhibits 26 S Proteasomal Function *. J. Biol. Chem. 284, 22213–22221. https://doi.org/10.1074/jbc.M109.028902

Zurbriggen, M.D., Carrillo, N., Tognetti, V.B., Melzer, M., Peisker, M., Hause, B., Hajirezaei, M.-R., 2009. Chloroplast-generated reactive oxygen species play a major role in localized cell death during the non-host interaction between tobacco and Xanthomonas campestris pv. vesicatoria. Plant J. 60, 962–973. https://doi.org/10.1111/j.1365-313X.2009.04010.x

Supplementary figures

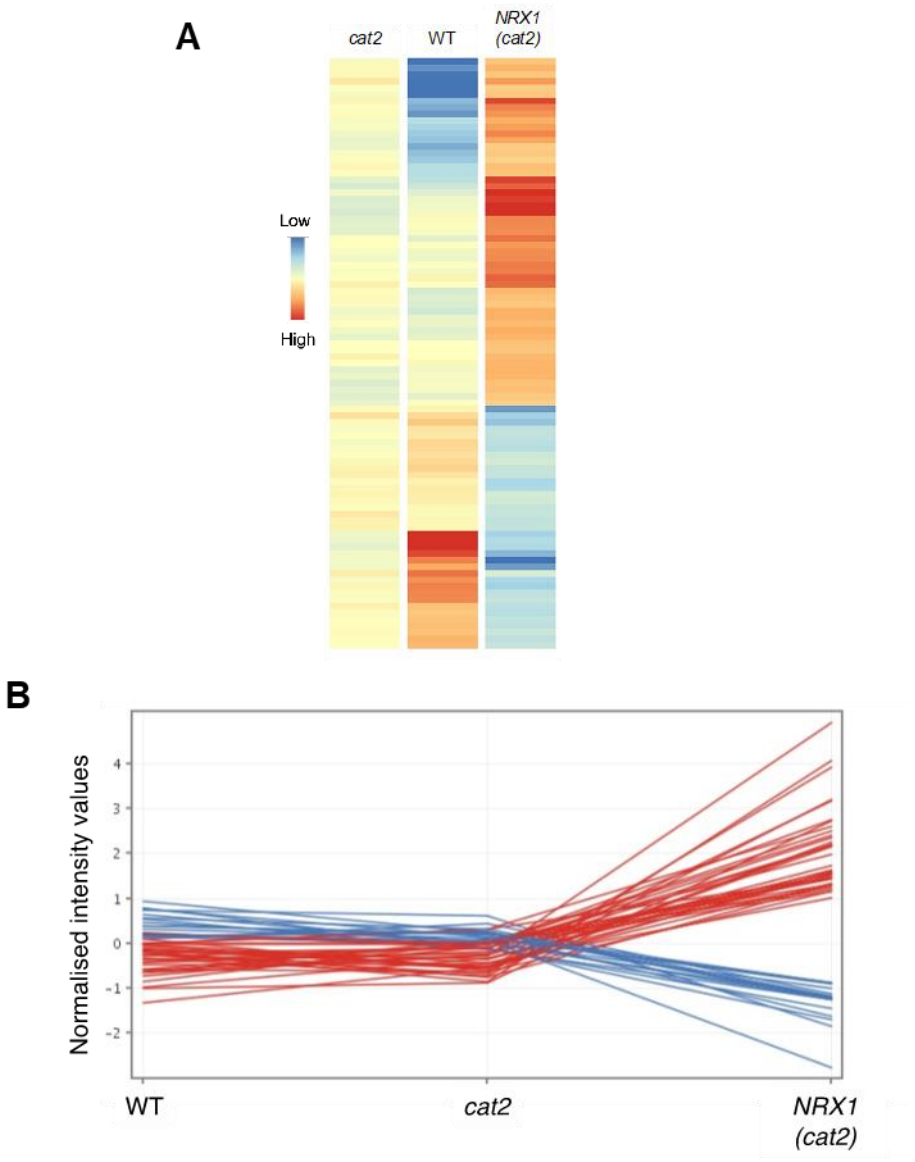

Figure S 1 Genes that are only differentially expressed in *35S::Flag-NRX1 (cat2)*

(A) Heatmap and **(B)** profile plot of genes that were not differentially expressed between wild-type plants and *cat2* mutants but were differentially expressed in *35S::Flag-NRX1* expressed in *cat2* mutants compared to *cat2* and wild-type in placed under light-stress conditions for 3 days (FC >2, $p < 0.05$).

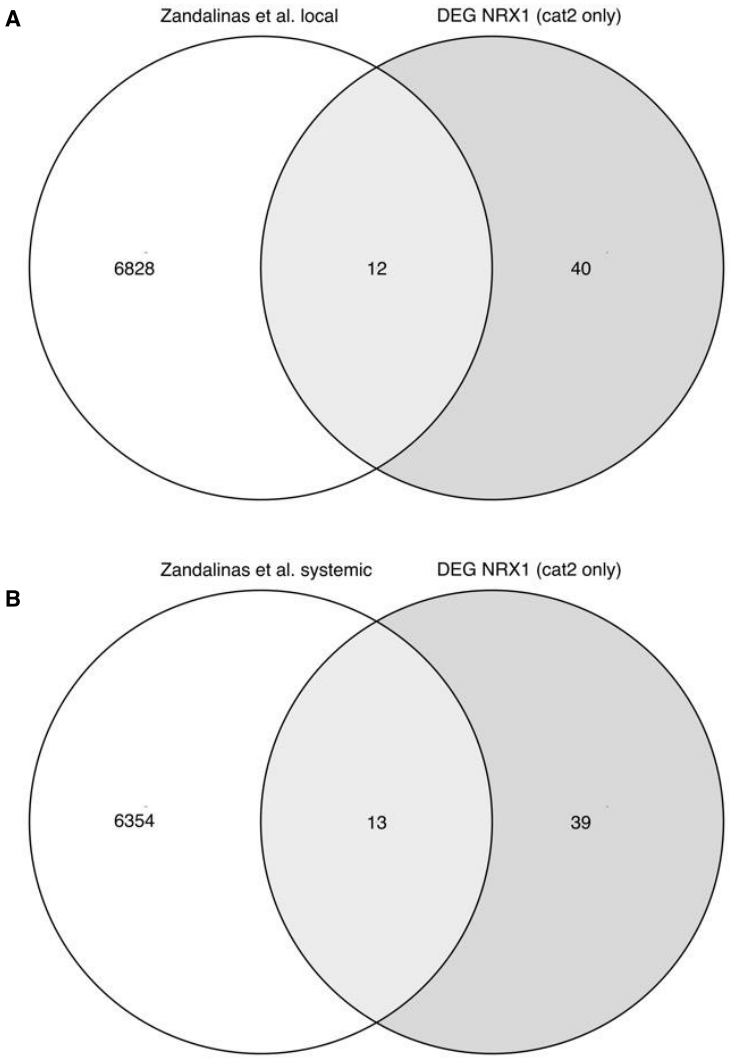

Figure S 2 Genes identified as only differentially expressed in *35S::Flag-NRX1 (cat2)* correspond to published RNA-seq datasets of plants in 'high light' conditions

Comparisons were made between genes identified as only differentially expressed in *35S::Flag-NRX (cat2)* (Fig. S1) and genes that were differentially expressed in response to local light stress **(A)** and systemic stress in untreated leaves **(B)** from Zandalinas et al. (2019)

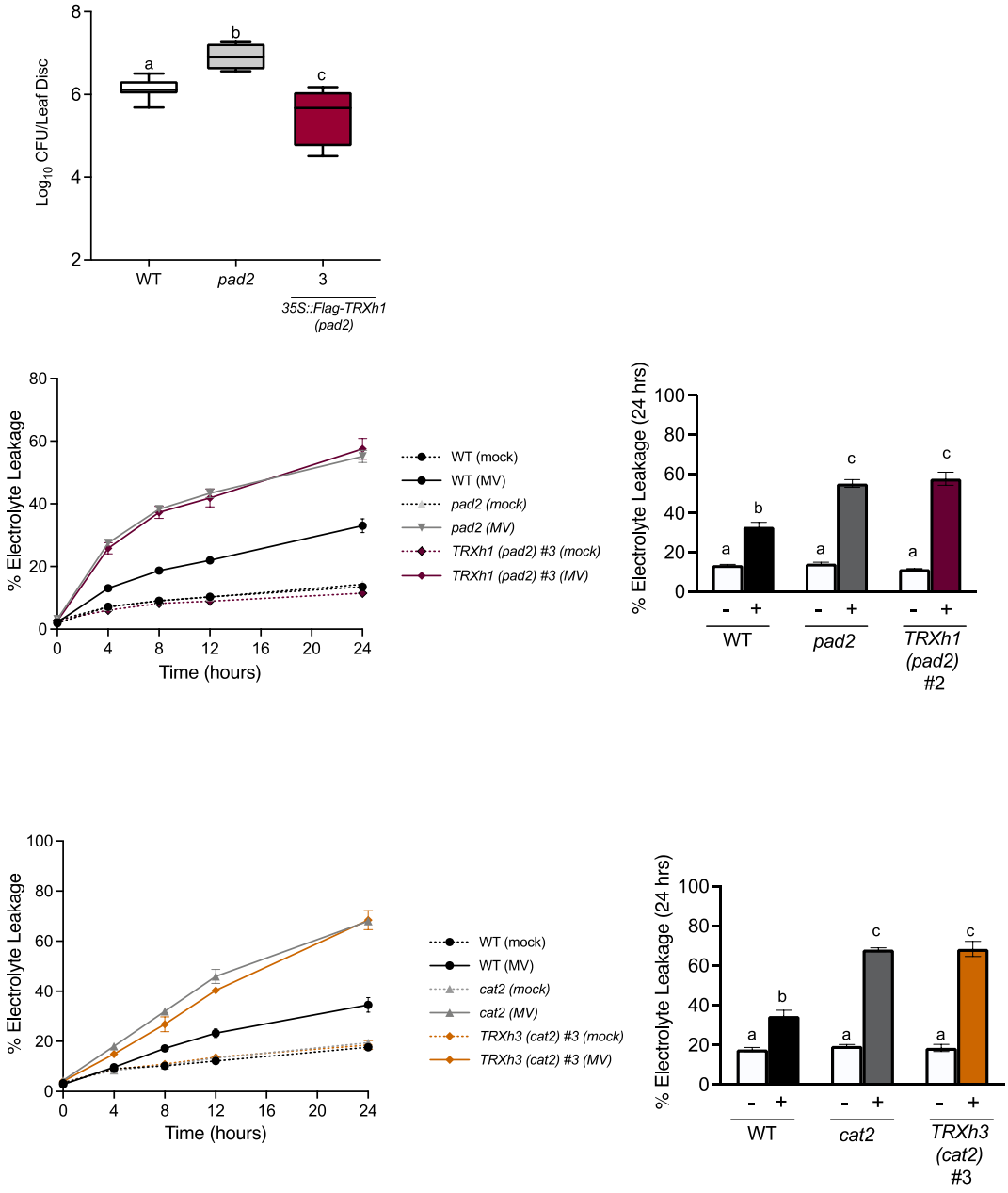

Figure S 3 Second independent lines for TRX-*h* survey

(A) Plants were infected with *Psm* ES4326 (OD_{600} = 0.002) and pathogen grown was assessed after 3 days. Different letters indicate statistical significance (ANOVA, Tukey p <0.05) CFU, colony forming units (n=8)

(B) and **(C)** Plants were infiltrated with 10µM of the oxidative stressor methyl viologen (MV) or water (mock). Electrolyte leakage was measured at indicated timepoints over a period of 24 hours and are presented as a percentage of the total electrolytes. Error bars indicate standard error (n=3)

Figure S 4 Expression of Flag-tagged TRXh8 in *cat2* mutant plants

Mutant *cat2* plants were transformed with *35S::Flag-TRXh8*. Expression of the transgene was detected by Western blot against the Flag tag. Markers indicate kDa

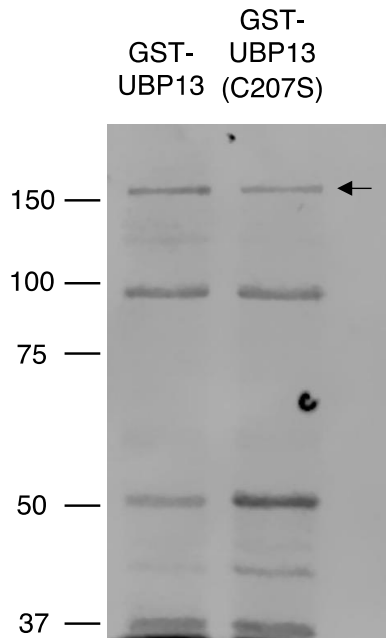

Figure S 5 Purification of GST-tagged recombinant UBP13 wild-type and mutant proteins

Escherichia coli expressing GST-UBP13 or the active site mutant GST-UBP13 (C207S) proteins were treated with IPTG and total protein extracted. Protein extracts were incubated with GST-binding Glutathione Sepharose 4B resin and the proteins eluted with reduced glutathione. Purified proteins were visualised with Instant Blue staining following separation with SDS-PAGE. Arrow indicates expected size of UBP13 with a GST tag. Markers indicate kDa